Type of article: Review

Designing of Gradient Scaffolds and their Applications in Tissue Regeneration

Ananya Pattnaik[1#], A.Swaroop Sanket[1#], Sanghamitra Pradhan[2], Rajashree Sahoo[1], Sudiptee Das[1], Swarnaprbha Pany[1], Timothy E.L. Douglas[3,4], Rambabu Dandela[5], Qiang Liu[6], Jaykumar Rajadas[6,7], Sanghamitra Pati[1], Stefaan C. De Smedt[8]*, Kevin Braeckmans[8], Sangram Keshari Samal[1]*

[1]Laboratory of Biomaterials and Regenerative Medicine for Advanced Therapies, ICMR-Regional Medical Research Centre, Bhubaneswar-751023, Odisha, India.

[2]Department of Chemistry, Institute of Technical Education and Research, Siksha 'O' Anusandhan University, Bhubaneswar-751030, Odisha, India.

[3]Engineering Department, Lancaster University, Lancaster, United Kingdom.

[4]Materials Science Institute, Lancaster University, Lancaster, United Kingdom.

[5]Department of Industrial and Engineering Chemistry, Institute of Chemical Technology, Indian Oil Odisha Campus, Bhubaneswar, Odisha, India.

[6]Advanced Drug delivery and Regenerative Biomaterials laboratory, Cardiovascular Institute, Stanford University School of Medicine, Department of Medicine, Stanford University, California-94304, USA.

[7]Department of Bioengineering and Therapeutic Sciences, University of California San Francusco (UCSF) School of Parmacy, California, USA.

[8]Laboratory of General Biochemistry and Physical Pharmacy, University of Ghent, Ghent, 9000, Belgium.

#: Both the authors contributed equally

Corresponding author: Stefaan.desmedt@Ugent.be, sksamalrec@gmail.com

Graphical Abstract:

Gradient scaffolds are isotropic/anisotropic three-dimensional structures with gradual transitions in geometry, density, porosity, stiffness, etc., that mimic the biological extracellular matrix. The designing of gradient scaffolds can overcome the current challenges in the clinic. The recent advanced techniques play a significant role in designing gradient scaffolds with the utmost biomimetic properties for bone, cartilage, neuron, cardiovascular, and skin tissue regeneration. The insights from such advances using gradient-based scaffolds can widen the horizon for using gradient biomaterials in tissue regeneration applications.

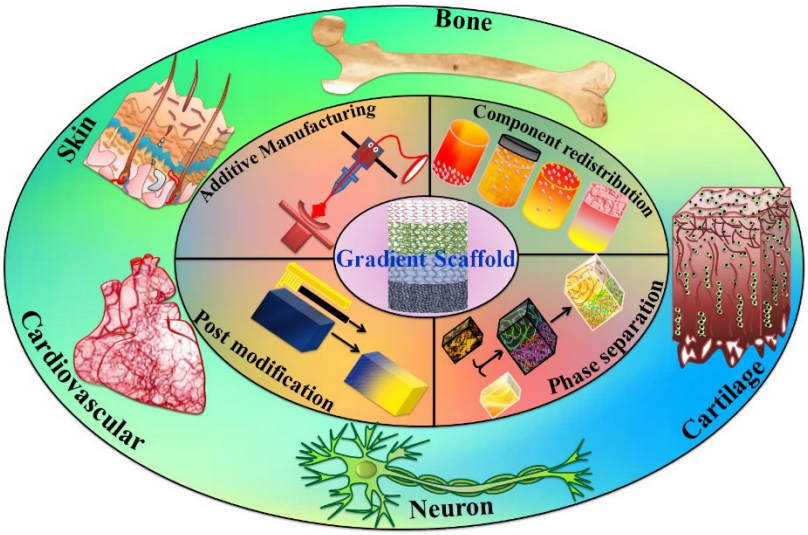

Abstract:

Gradient scaffolds are isotropic/anisotropic three-dimensional structures with gradual transitions in geometry, density, porosity, stiffness, etc., that mimic the biological extracellular matrix. The gradient structures in biological tissues play a major role in various functional and metabolic activities in the body. The designing of gradients in the scaffold can overcome the current challenges in the clinic compared to conventional scaffolds by exhibiting excellent penetration capacity for nutrients & cells, increased cellular adhesion, cell viability & differentiation, improved mechanical stability, and biocompatibility. In this review, the recent advancements in designing gradient scaffolds with desired biomimetic properties, and their implication in tissue regeneration applications have been briefly explained. Furthermore, the gradients in native tissues such as bone, cartilage, neuron, cardiovascular, skin and their specific utility in tissue regeneration have been discussed in detail. The insights from such advances using gradient-based scaffolds can widen the horizon for using gradient biomaterials in tissue regeneration applications.

Keywords: gradient, scaffolds, biocompatibility, extracellular matrix, tissue regeneration

1. Introduction:

The gradient structures in biological tissues play a major role in tissue physiological development and maturation guided by variations in physical and chemical cues [1–3]. The gradients nature of the tissues can be broadly classified into cellular, compositional, structural, mechanical, and morphogenic, whose importance can be seen at different developmental stages of the organism [4–7]. Natural gradients vary in different tissues from the polarization of the neural tube to the structural arrangement in the osteochondral interface. The cellular gradients are observed in tissues such as osteochondral, dental, cartilage, muscular, epithelial, neural, etc. The epithelial tissue of skin has gradients in porosity whereas muscular fibers present in the cardiovascular system form structural gradients [8–11]. The interface between cartilage & bone, bone & tendon also presents structural & molecular gradients along the longitudinal axis [12]. The presence of different minerals in varying amounts in the bone tissue, and the concentration of ionic components like sodium, potassium, calcium, etc. in the Extracellular Matrix (ECM) create a compositional gradient in the human body [13–15]. Moreover, the morphogenic gradient observed in the biological system is created during the early developmental stages of the organism; this can also be attributed to the accumulative presence of other gradients which elicits different cellular responses such as the signaling system [15,16]. Implementing the idea, of integrating naturally occurring gradients into clinically designed scaffolds have shown potential functionality for biological tissue regeneration [17]. Owing to the rapid utilization of implantable biomaterials, various scaffolds in combination with tissue engineering technology have been provided by several companies to address the existing clinical limitations [4,18,19]. This strategy is well accepted in the existing clinical setup, but several challenges restrict the use of these scaffolds in recapitulating the natural

gradient present in cells or tissues of the human body. Therefore, natural/synthetic scaffolds with gradual transition gradients in geometry, stiffness, porosity, density, or combinations that mimic the ECM can help enhance the therapeutic potential which is favorable for tissue regeneration [20–24]. Designing compositional and structural gradient scaffolds using various techniques such as additive manufacturing, component redistribution, controlled phase changes, and post-modification has maximized the efficiency observed against conventional non-gradient scaffolds [25,26]. The gradual transitions in the gradient scaffolds create differential patterns in physical or chemical composition, which induces the spatial and temporal behavior of the 3D structure [27]. These also regulate the cellular micro environment for tissue regeneration, show better biocompatibility by improving the diffusion of nutrients and cells, which provides better cellular adhesion, improve cell viability, differentiation, increase the ductility, mechanical strength, and stability in comparison to the conventional scaffolds [28].

In the last decade, there has been considerable progress in gradient scaffold designing techniques to accelerate tissue regeneration. There are several reviews focusing on the fabrication of gradient scaffolds for tissue regeneration and reviewing fabrication techniques. But none of them have explained both the designing of gradient scaffolds by various advanced techniques and their specific application in tissue regeneration. In this review, the recent advancements in designing gradient scaffolds with desired biomimetic properties, and their implication in tissue regeneration have been briefly explained. Furthermore, the gradients in native tissues such as bone, cartilage, neuron, cardiovascular, skin and their specific utility in tissue regeneration have been discussed in detail. The insights from such advances using gradient-based scaffolds can widen the horizon for using gradient biomaterials in tissue regeneration applications.

2. Designing of gradient scaffolds:

The natural tissues are made up of complex structures with various physical, chemical, and cellular gradients which is an ideal platform for supporting biological activities such as cellular integration, migration, and differentiation [1]. In case of injury, accident, or any medical complication, the regeneration of these tissues sometimes becomes difficult which further deteriorates the quality of life [19]. To address these clinical challenges various conventional 3D scaffolds are being used from different companies like Amvisc®, ACUFEX™, HemoFoam®, Hemosponge®, Corning® Matrigel®, MaxGel™, Alvetex®, Celox™, SteriGraft®, OSSIX™, and SmartBone® etc by the clinicians [29]. Conventional manufacturing techniques like solvent casting, particle leaching, freeze-drying, gas foaming, and electrospinning are well-advanced to manufacture identical scaffolds. The conventional top-down approach techniques were able to create scaffold structures for tissue formation; however, due to irregular pore shape, insufficient connectivity and lack of natural gradient in these systems, fail to mimic the native gradient environment for specific tissue attachment, migration, and regeneration of cells. Hence, there is an urgent need to design ideal gradient scaffolds for manifesting their potential use in successful integration & complete functional restoration of the native tissues [30,31]. In recent years, new advanced techniques have been developed such as Additive Manufacturing, Component Redistribution, Controlled Phase Changes, and Post Modification to fabricate 3D gradient scaffolds that have shown tremendous potential for tissue regeneration [32–36]. These techniques have been illustrated in the subsequent sections with a detailed description by citing relevant examples for the implementation of gradient scaffolds in the biological system.

2.1. Additive manufacturing/3D printing-based designing of gradient scaffolds

Additive Manufacturing (AM) is a 3D technology that allows the direct production of customized functional scaffolds having intricate architecture. To accelerate tissue regeneration, the scaffolds need to be designed such as to offer an appropriate cellular microenvironment with the help of computer-aided tools [37]. These strategies for manufacturing gradient scaffolds gained a lot of attention in the field of regenerative medicine. Sometimes this process can also help to create more complex 3D gradient structure scaffolds with tunable properties such as desired pore size, optimized mechanical strength, biodegradation kinetics, high flexibility in the internal/external architecture, and increased tissue regeneration ability [38]. The global healthcare market size value of AM was USD 1.6 billion in 2021 which is expected to increase at a CAGR of 22.6% from 2022 to 2030 [39].

The design and 3D printing process in AM allow a variety of geometrical features and functional gradients to be fabricated in the scaffolds, which enhances the modularity for addressing specific treatment problems in tissue regeneration. Mohseni et al., utilized additive bio manufacturing to design gradient scaffolds for the reconstruction of patient-specific breast tissues. The authors entrapped adipose tissue and channelized the mobility within the designed gradient scaffold to reduce the chances of leaking the fat tissues to the external environment (Figure 1). With the advancements in technology, the diversity and spatial resolution of the designed gradient scaffolds could be controlled and optimized to improve end-use production [32].

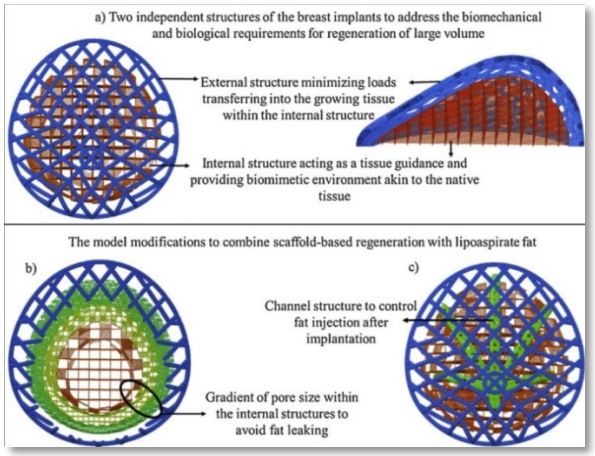

Figure 1: CAD based model for printing of (a) breast implants with biocompatibility (b) porous gradients within the scaffold model (c) incorporated channels to control fat tissue. Adapted with permission from Ref. [32] © 2019 Published by Elsevier B.V.

This advanced technique also allows the engineering of hydrogel-based gradient scaffolds for personalized therapy by overcoming the weak mechanical strength and uncontrollable swelling of conventional hydrogel gradient scaffolds. In a study, the authors have synthesized a hydrogel gradient scaffold by one-step copolymerization of dual hydrogen bonding monomers, *N*-acryloyl glycinamide, and *N*-[tris(hydroxymethyl)methyl] acrylamide (PNT hydrogel) for individualized therapy. The obtained hydrogel shows excellent mechanical properties (Figure 2) and rapid thermoreversible gel ⇔ sol transition behavior that makes it a suitable ink for direct 3D printing. The gradient hydrogel scaffold thus produced had a controlled 3D structure due to its sheer thinning property. The gradient scaffold facilitated attachment, spreading, and chondrogenic & osteogenic differentiation of human bone marrow stem cells (hBMSCs) in vitro when printed with transforming growth factor β-1 and β-tricalcium phosphate (β-TCP) on distinct layers. This scaffold also accelerates cartilage regeneration in a mouse model in vivo [40].

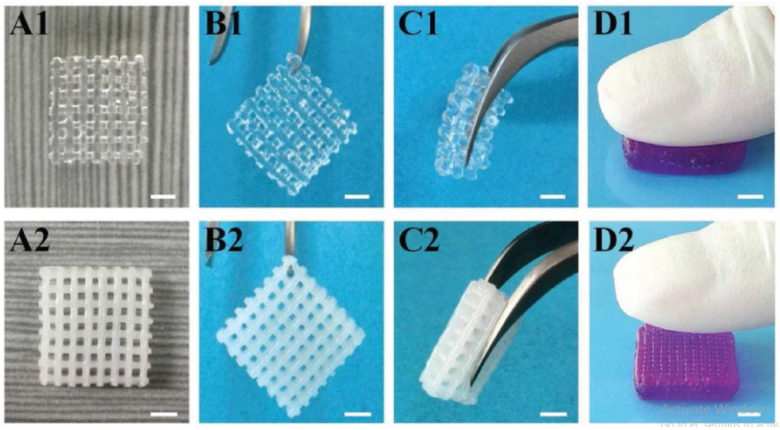

Figure 2: Macroscopic appearance and mechanical performance of the printed porous PNT-35%-6 hydrogel scaffolds A1–D1) and PNT-35%-6-β-TCP-22% hydrogel scaffolds A2–D2). The 3D printed scaffolds showing excellent mechanical performances: supporting its own weight B1, B2); twisting C1,C2); and compression D1,D2). The top and bottom layers of the scaffold were stained with rhodamine and gentian violet, respectively (Scale bar = 2 mm). Adapted with permission from Ref. [40] © 2018 WILEY-VCH Verlag GmbH & Co. KGaA, Weinheim.

Although, AM has shown potential in fabricating appropriate gradient scaffolds, however, it is limited to a handful of printing materials available in the market. Rapid prototyping was first attempted by Hideo Kodama in the year 1981, following which Stereolithography, Selective Laser Sintering (SLS), and Fused Deposition Modeling (FDM) technology were patented in the year 1983, 1988, and 1989 respectively. After the invention of all these techniques, recently bioplotter printing is highly in demand and was first developed in the early 21st century [41]. However, photochemistry being an age-old process has recently been utilized in combination with the advanced fabrication techniques for designing various gradient scaffolds. This technique involves the basic mechanism of photo-crosslinking that serves several advantages over physical and chemical crosslinking such as spatiotemporal control, nano-features with better resolution and control over the mechanical properties. Photochemistry offers a great

opportunity and an alternative to the physical deposition for scaffold designing by in situ chemical alteration in the fabrication process [42]. All the techniques that utilize ultraviolet (UV), visible light or infrared radiation (IR) comes under photochemistry based designing methods [43].

AM is majorly divided into seven different techniques such as Vat polymerization (Stereolithography, Digital Light Processing, 2-Photon Polymerization and Digital Light Synthesis), Powder bed fusion (Selective Laser Sintering, Selective Laser Melting, Direct Metal Laser Sintering, Electron Beam Melting), Material extrusion (Fused Deposition Modeling, Fused Filament Fabrication), Sheet lamination, Direct energy deposition, Material binder jetting and Bioplotter printing (Figure 3) [44]. The following sections have described these advanced technologies in detailed.

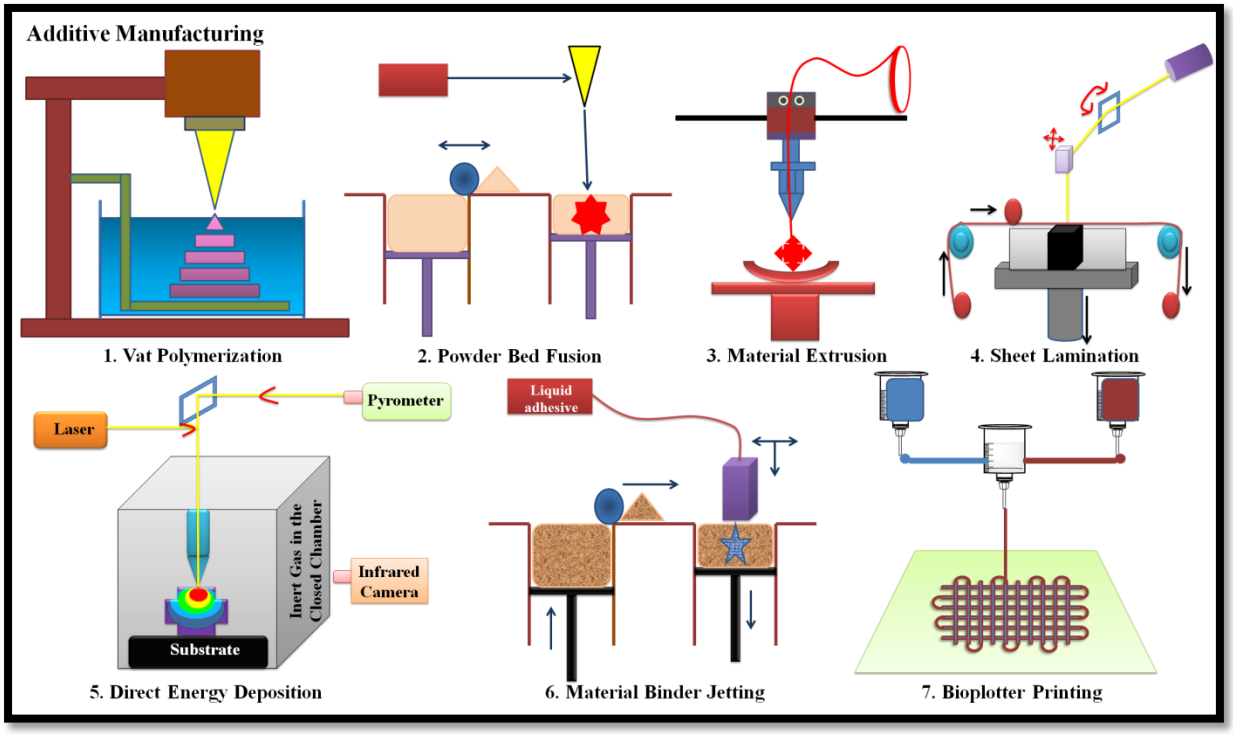

Figure 3: Different techniques of additive manufacturing for designing of gradient scaffolds.

2.1.1. Vat polymerization:

Vat polymerization is one type of AM process that is the first-ever introduced 3D printing technology using UV, IR, and visible light waves. This process selectively cures or hardens a vat of liquid photopolymer resin to form highly accurate 3D scaffolds with smooth surface. The layer by layer formation of the scaffold is controlled by mirrors that direct light across the photo curable resin. Limited photopolymerization-compatible materials and generation of brittle structures restrict the use of this technique to form gradient scaffolds [45]. However, nowadays due to the availability of various photocurable materials in the market, single and multi-material functional gradient scaffold fabrication is possible using this technique. Stereolithography (SL) was the first technique of vat polymerization introduced and patented by Chuck Hull in 1983 [46]. Furthermore, vat polymerization includes 2-Photon Polymerization (2PP), Digital Light Processing (DLP), and Digital Light Synthesis (DLS) those of which differ in the light source and mechanism used for polymerization [47].

SL is a high-resolution computer aided 3D printing technique that utilizes UV light source which crosslinks the structural units of monomers and oligomers in a layer-by-layer pattern in the presence of photo initiators [48]. However this technique is limited to photo-crosslinkable scaffolds with single directional gradients. This has been widely used in the patient-specific dental implants; Invisalign® is the most well-known commercially available products of SL technique [49]. It is capable of generating gradient scaffold with controlled architecture and micrometer-level resolution. In a recent study, SL has been used to design a porosity gradient Hydroxyapatite (HA) scaffold, where the porosity varied from 9.2% to 94.6% from edge to center of the scaffold which resembled the gradient structural property and functional performance of the natural bone. The horizontal cross-section of the porosity distribution within the HA gradient scaffold is shown in Figure 4. Furthermore, the porosity influenced the compressive strength and effective elastic modulus; however, the horizontal pores impart a

negative impact on the compressive strength of the scaffold which co-relates to the Volkmann canal that is narrower than the Haversian canal [50].

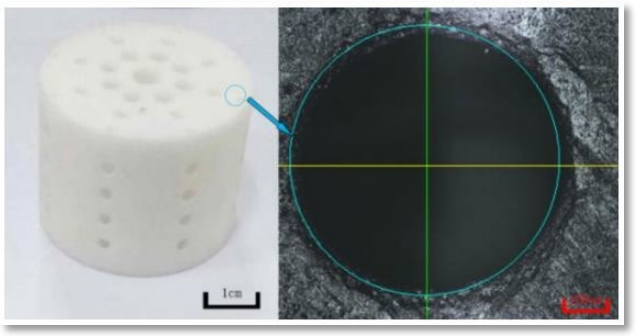

Figure 4: Microarchitecture for porous gradient scaffolds using stereolithography. Adapted with permission from Ref. [50] © 2020 The Authors. Published by Elsevier B.V.

Applying the knowledge of gradient parameters that influence various cell signaling, researchers' are able to generate optimal gradient scaffolds for tissue regeneration. In a study Grijpma group added a linear term to the mathematical equation to design poly (D, L-lactide)-based porous gradient scaffold by using SL technology. In Figure 5 μCT-visualisation demonstrates that the pores in the upper half of the scaffold are more open than the lower part. The gradient in pore size and porosity is observed, while porosity gradually decreases from the middle (70%) of the structure to lower end (30%). This gradient imparts a stiffness and permeability gradient, which is needed for proper bone tissue regeneration [51].

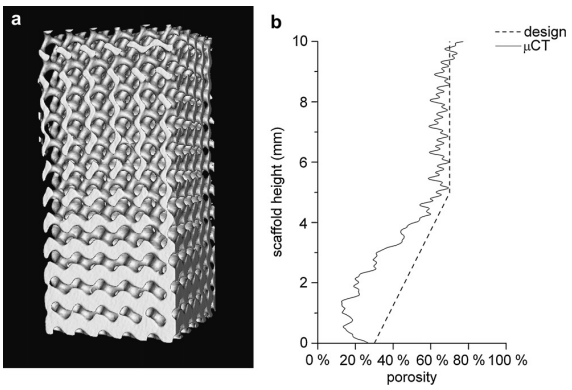

Figure 5: Mathematical modeling based SL PDLLA scaffold with gyroid architecture showing a gradient in porosity and pore size. a: μCT visualization. b: Change in the average porosity with scaffold height (solid line) in comparison with the designed porosity (dotted line). Adapted with permission from Ref. [51] © 2010 Elsevier Ltd.

Furthermore, SL is divided into three techniques based on the light patterning system: vector scanning, mask projection and 2-photon polymerization. In case of vector scanning approach a very fine laser beam solidify the vat photo-resin in point-by-point pattern. Highly precised layers are formed in this technique; however point-by-point patterning system increases the fabrication time for which the mask projection has been developed [52].

Mask projection SL also known as DLP can cure an entire part of the scaffold at once, where digital micro mirror device chip is being used to project the entire image of the layer onto the LCD screen within a short period of time. This approach is a unique technique to design gradient scaffolds using multiple materials in a single component [53]. Wu et al., had developed a bottom-up mask projection SL method to fabricate multi-material osteochondral gradient scaffold using photo curable poly(ethylene glycol) diacrylate (PEGDA) hydrogel and beta-tricalcium phosphate (b -TCP) ceramic suspension. The biphasic interface was formed using variable-power light source to harden the materials with different curing capacities that can be highly potential for developing functional gradient scaffolds for osteochondral tissue regeneration [54].

Another well-known stereolithographic technique includes 2PP technology that relies on absorption of 2-photons of Near-IR region focused on a light-sensitive material which quenches to initiate the polymerization of the structural components to form a gradient scaffold. The rapid technical development of this approach is able to create exciting possibilities for precise localization of the light energy to produce novel gradient scaffolds with high resolution architecture [55]. Greiner et al, have used 2PP based sandwich model of Direct Laser Writing

(DLW) technique to fabricate adjustable mesh of varying sizes (2 µm, 5 µm and 10 µm) (Figure 6 A) on glass/microporous polymer membrane substrates for easy diffusion of bio agents. However, migration of epithelial cancer cells needs to be directed by prior spatial chemokines and growth factors gradients. In addition the A549 cells were also unable to proliferate within the larger pore sizes of the scaffold. Therefore, the porous scaffold was coated with fibronectin and given a gradient of fetal calf serum to enhance cell invasion in presence of chemoattractant. It was observed that both the cell types invaded at a similar degree at a respective pore size as shown in (Figure 6 B). Therefore, this technique of engineering 3D scaffolds provides a multifaceted tool to study the cell migration within chemical gradient porous scaffold [56].

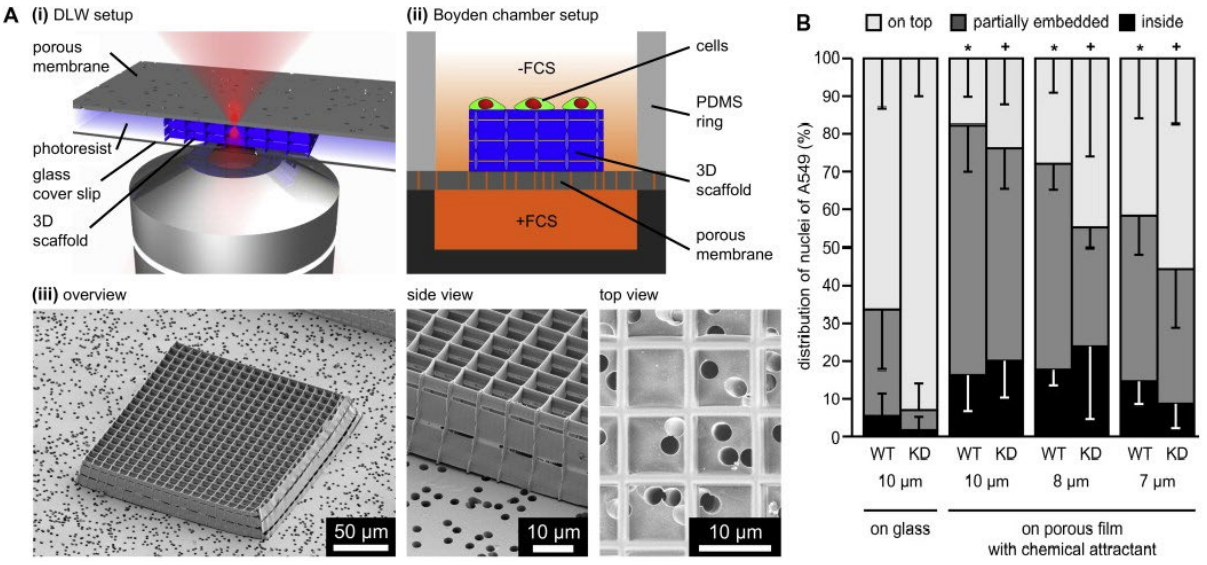

Figure 6: 3D setup for chemically controlled cell invasion. (A) (i) Direct laser writing (DLW) was applied to fabricate non-cytotoxic 3D scaffolds on porous membranes. Briefly, the porous polymeric membrane was mounted in a photoresist and placed between two glass cover slips. A femto-second laser beam was focused onto the photosensitive liquid material, excited photoinitiator molecules by two photon absorption and causing a highly localized chemical polymerization reaction strictly confined to the focal volume of the laser. (ii) Side view of the experimental setup. The porous membrane equipped with the 3D scaffold is placed over a reservoir containing medium supplemented with fetal calf serum (FCS). The 3D scaffold is

surrounded by a ring made of polydimethylsiloxane (PDMS) and covered with media containing no FCS. Cells are seeded onto the 3D scaffold and cell invasion into the 3D scaffold is studied (iii) SEM overview, side view and top view images of a 3D scaffold with a mesh size of 10 mm resting on a membrane with a pore diameter of 3 mm. (B) The majority of A549 wildtype (WT) and lamin A/C knockdown (KD) cells did not invade 3D woodpile scaffold written on glass (no chemoattractant). Instead, cell invasion into the scaffold was achieved by using 3D structures fabricated on a porous membrane and exposure of this setup to a soluble chemical gradient (Boyden chamber approach). Adapted with permission from Ref. [56] © 2013 Elsevier Ltd.

Another variant of vat polymerization is Continuous Liquid Interface Production (CLIP) or DLS which involves manufacturing of gradient scaffolds as a whole rather than the layering fashion. The scaffolds are prepared utilizing UV light, oxygen that creates a dead zone, and liquid resin with the help of computer-aided programmable design which are shown to exhibit excellent mechanical properties [57]. However, in a recent study, authors have modified the conventional CLIP by introducing a pressurized source of microfluidic ducts that injects continuous flow of resin to create a growing pressure gradient within the dead zone of the printed scaffold as described in Figure 7. In this system, the rapid printing of gradient scaffolds was possible by increasing the printing speeds to 5- to 10-fold as compared to the traditional CLIP technique. The complex models formed using simulation-driven control strategy displayed the speculated gradients that were desired. Further works on injection CLIP will be able to surpass the advanced techniques and can have a better opportunity to broaden its applicability in the field of regenerative medicine (4D printing) and other medical fields [58].

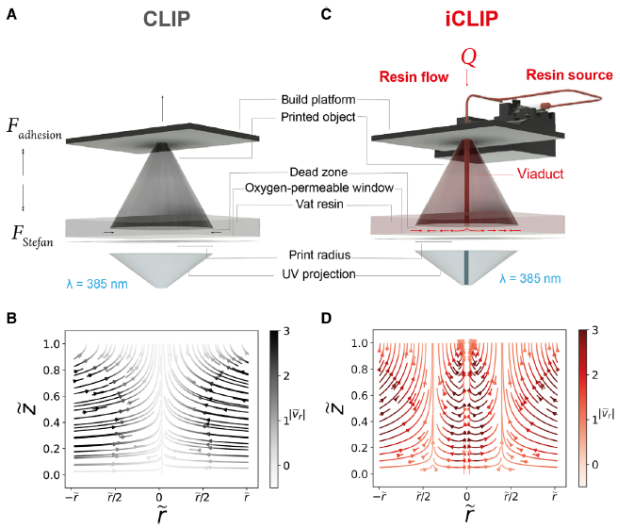

Figure 7: Injection continuous liquid interface production. (A) Traditional CLIP process, with force diagram for the printed object and resin flows indicated. (B) Analytically derived dead zone velocity fields and pressure gradients from the lubrication theory while printing a cylindrical geometry by CLIP, where ź and ŕ are the vertical and radial distances in the dead zone, respectively, and v_r is the radial velocity. Darker hues indicate higher-magnitude velocity vectors, and, conversely, lighter hues indicate stagnation zones of low-fluid velocity. (C) iCLIP process indicating the flow of the injected resin from a pressurized source through microfluidic ducts engineered within the growing part into the dead zone. (D) Analytically derived dead zone velocity fields and pressure gradients from the lubrication theory while printing a cylindrical geometry by CLIP, with continuous injection through a central viaduct. Adapted with permission from Ref. [58] © 2022 The Authors.

2.1.2. Powder Bed Fusion:

Powder Bed Fusion (PBF) is a 3D printing technology in combination of computer aided design uses a high power source (laser or electron beam) to melt and fuse the powder present inside a container. The technique allows the fabrication of wide range of materials to form geometrically complex scaffold architectures with high precision. The powder bed acts as the support and medium of heat transfer for the scaffold making reducing the thermal gradients in

326 the print whereas subsequent heating and cooling may affect the physical parameters of the
327 part architecture [59]. The Selective Laser Sintering (SLS) is type of PBF technique that was
328 invented and patented by Carl R. Deckard, which relies on high power laser source like carbon-
329 dioxide or neodymium-doped yttrium aluminum garnet to sinter small particles of polymer
330 powder into 2D base layer of the scaffolds. Furthermore, a new layer is deposited on the pre-
331 built base by a piston to sinter on the next layer which continues until the desired complex
332 vertical gradient scaffold is obtained. However fabrication of horizontal gradient scaffolds in
333 this technique is difficult [60–62].

334

335 Although this process is suitable for visual prototypes, and relatively inexpensive. However, it
336 uses high power, which may alter the structural properties of newly designed gradient scaffolds.
337 The finishing and porosity of the gradient scaffold depends on the particle size and type of the
338 polymeric powder. In a study, authors have used SLS technique to investigate the influence of
339 high density polyethylene powder particle size (range 106-125, 150-212 and 212-380 μm) to
340 achieve porosity gradient scaffold. The obtained result showed that larger sized particles with
341 high degree sintering yielded compact structures, whereas smaller size particles yielded more
342 open pores with low degree sintering as shown in microscopic images (Figure 8). The part of
343 the gradient scaffold prepared using larger particle size had poor mechanical properties due to
344 the limited number of union points [63].

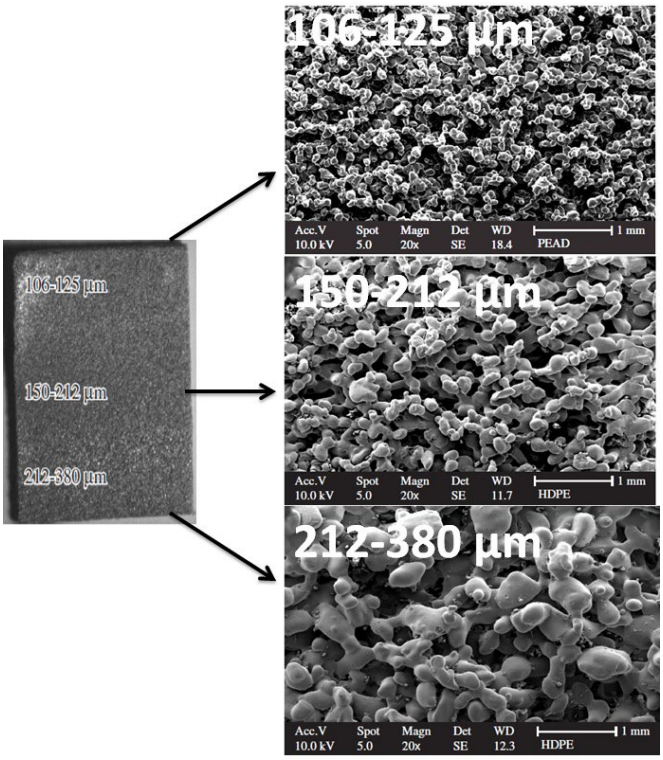

Figure 8: Images of the scaffold with controlled pore size gradients using SLS different particles size (106-125, 150-212 and 212-380 µm) of high density polyethylene. Adapted with permission from Ref. [63] © 2007.

The complex hierarchical architecture, the lack of blood supply and incapability of self-repair in osteochondral defects causes major obstacle in designing of gradient scaffold that meets the desired properties of osteochondral gradients. Over the recent years the SLS technology has shown remarkable advancements in various tissue regeneration, specifically to address one of the major problems of designing osteochondral scaffolds. Du et al., have used SLS to designed Poly(e-caprolactone) (PCL) and HA microspheres based gradient scaffold to address the problem associated with designing scaffolds for osteochondral defects. The prepared scaffolds was implanted into osteochondral defects of a rabbit model and evaluate the rpaire potential. The obtaine result demonstrated that the newly designed scaffold has ability to accelerate early subchondral bone regeneration, which well integrate with the native tissues for inducing

articular cartilage formation. Hence, this SLS strategy is a promising approach for the designing of biomimitic gradient scaffolds and repair osteochondral defects [64]. Therefore, the SLS technique suggests a better prospective to engineer bio-inspire multilayer scaffolds with well-designed architecture for tissue regeneration.

A variant of SLS is Selective Laser Melting (SLM) technique whose mechanism is same as that of SLS but is restricted to metal and alloys sintering. The technique uses high energy power source to fully melt and fuse the fine metal powder to liquid to form solid 3D gradient scaffolds [64]. The metals used in SLM are of biomedical importance (stainless steel, tool steel, titanium, cobalt chrome, and aluminum), because they are ideal for treating bone defects. The biomedical metal materials are biocompatible and show high resistance for corrosion and excellent physical properties but due to its higher modulus may lead to stress shielding of the bone tissue implant [65]. To overcome this limitation, Lv. Et al., utilized SLM technique to fabricate Ni46.5Ti44.5Nb9 alloy porous scaffold with continuous gradient based on triply periodic minimal surface (TPMS) structure design. The increase in pore size leads to decrease in specific surfaces which improves the permeability of the designed scaffold [66].

However, in case of Direct Metal Laser Sintering (DMLS) technique, the laser is used to sinter the metal powder based thin layer upon which additional layers are then applied to generate a 3D scaffold through a series of layers. As compared to SLS, DMLS has an advantage of using a low power laser as it has to melt and fuse the layers rather than melting the whole powder bed. It is possible to adjust the porosity level, interconnectivity and overall architecture of the scaffold by altering the processing parameters [67]. In a study, DSLM technique was used to sinter titanium alloy powder to fabricate porous gradient from center to outside of the scaffold for dental implants. The study concluded that DSLM is an efficient method to design gradient scaffolds with better elasticity as that of the bone which can improve the longevity of the implant [68].

In another technique of PBD that uses tungsten electron beam instead of laser light to fuse metal powder particles in layer-by-layer fashion under vacuum condition is called Electron Beam Melting (EBM). However, the process requires a base material that is conductive in nature [69]. In a study, the authors have taken the advantage of EBM combined with computational biology to interconnect the foamed structure inside the scaffold. The 3D porous gradient scaffold with pore sizes (700, 1000, and 1500 μm) were favorable for osteoblastic activities [70]. This technique is relatively faster than SLM however; SLM has higher resolution and accuracy with smooth accurate parts. However, impurity or contamination is restrained due to the vacuum chamber which leads to high quality architecture [71].

2.1.3. Material extrusion:

Material extrusion works on the principle of extruding material through a heated nozzle applying pressure to form 3D printed scaffolds. This technique follows two different basic approaches to design the gradient scaffolds. The most widely used approach is Fused Deposition Modeling (FDM) that is used to produce gradient 3D scaffolds with fully interconnected channel network, controllable porosity and honeycomb-like pattern. This technique is highly dependent on temperature induced melting of thermoplastic that is extruded through a small orifice to form the base, and the layer is fused with the base layer to produce layer-by-layer architecture of the scaffold [72]. The temperature of system can vary from100-140°C depending on the types of polymers for proper flow and layer diffusion throughout the scaffold designing. However, incorporating & printing of bioactive molecules within the 3D scaffold structure is difficult due to high heat, and weak bonding between the interlayers [73–75]. It is proved that altering the process parameters of FDM and printing angles of scaffolds

410 can greatly influence the mechanical properties of the designed gradient [76]. In a study authors
411 have used PCL which is a FDA approved polymer to design porous FDM scaffolds with the
412 help of two different lay-down patterns of 0/90° (Figure 9a) and 0/60/120° (Figure 9c) that
413 resulted in the honeycomb patterns of square (Figure 9b) and triangular pores (Figure 9d)
414 within the 3D scaffolds. The stress-strain curves of the 0/90° scaffolds increases in the initial
415 linear gradient and plateau height when compressed in-layer than out-of-layer, however there
416 was no such pattern observed in the 0/60/120° scaffolds. The anisotropicity of these scaffolds
417 depends on the mechanical behaviour of the scaffolds. The obtained results support the further
418 in vitro and in vivo studies for tissue regeneration [74,77,78].

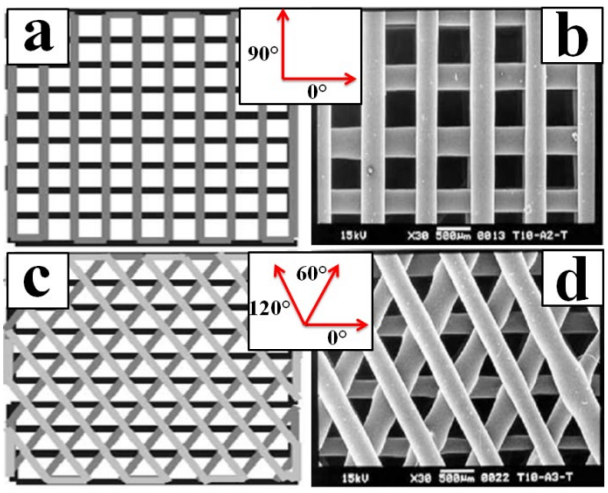

419

420 **Figure 9:** Fused deposition modeling scaffolds: (a) Computer-designed lay-down pattern of
421 0/90° forming square honeycomb pores gradient scaffolds, (b) PCL based bio-printed 0/90°
422 forming square honeycomb pores gradient scaffolds, (c) Computer-designed lay-down pattern
423 of 0/60/120° forming triangular honeycomb pores, (d) PCL based bio-printed 0/60/120°
424 forming triangular honeycomb pores. Adapted with permission from Ref. [74] © 2001 Elsevier
425 Science Ltd.

426

427 In a similar study, Song et al., have studied the effect of FDM processing parameter (build
428 orientation) on the tensile strength and porosity gradient of the poly (ether-ether-ketone)

scaffold. The platform was modified by pasting a polycarbonate plate by evenly spreading the glue attached to a printed circuit board to design four kinds of gradient scaffolds with varying pore sizes (0.4-2.0 mm). Electron micrographic examination of the scaffolds indicated the better interconnection between various ranges of pore size allowed easy attachment, migration, and differentiation of cells. The gradient scaffolds were also observed to have high tensile strength while the mechanical properties were comparable to that of human bone tissue [79].

As the patents for FDM were about to end in 2009, RepRap Ltd. community came up with a new name for the similar idea of FDM, and hence it was named as Fused Filament Fabrication (FFF). The absence of a heat chamber in FFF remains the only difference between both the techniques. FFF technique processes the scaffold designing with temperature fluctuations during material extrusion and deposition onto the heated bed. This technique has an advantage of producing complex pore structures with less energy and minimal cost as compared other techniques of AM like SL and SLS [80]. Recently, multilayered materials for gradient generation in scaffolds by the use of FFF technique are of particular interest in the field of tissue regeneration. In a study Portan et al., designed a PLA-based multi-layered porous gradient scaffold with varying pore sizes (60 μm-100 μm) by FFF, and investigated its mechanical stability, and biocompatibility. These experimental results signified that, the change in porosity of the gradient scaffolds along with the sample thickness can be of great interest for multi-functionality target [81]. Similarly, in another study, three compositions (varying ratios of HA and PCL) and four different simple and shifted gradient designed (Si-Grad1, Si-Grad2, Sh-Grad1, Sh-Grad) scaffolds shown in Figure 10, were prepared by FFF technique. It was observed that in shifted models, increasing the gradient slope weakened the mechanical performance but enhanced its biological activity when compared with the simple gradient scaffolds. The gradient scaffolds are necessary for biological assessments due to its morphological similarity with the cortical bone surrounded by trabecular bone [82].

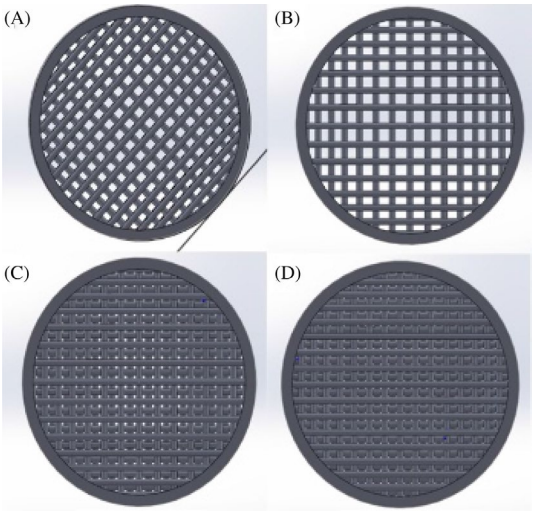

Figure 10: Gradient porous scaffold images constructed in the Solid Works software package. Design of scaffold (A) Si-Grad1, (B) Si-Grad2, (C) Sh-Grad1, (D) Sh-Grad2. Adapted with permission from Ref. [82] © 2022 Society of Plastics Engineers.

Although the material extrusion techniques are able to design large parts in less time, yet the scaffolds lack the smooth finishing and resolution that requires a lot of post processing. Moreover, this technique is not suitable for small details and intricate architecture and also is prone to breakage in the parts of joining area that results in reduced mechanical properties of the gradient scaffolds [83].

2.1.4. Sheet Lamination:

The technique of AM that manufactures each layer composed of paper, cellulose, plastic film, or metals and then super positioning them by the use of an adhesive or bonded through metallurgical process to generate a 3D scaffold is called sheet lamination [84,85]. The process of sheet lamination that is called as Laminated Object Manufacturing (LOM) is developed by Helisys Inc. and popularized by an Israel-based company named Solido. In the current years, this technology is mastered by EnvisionTEC Company and the Impossible Objects startup. In this technique, the 2D thin sheets of material are cut with laser according to the computer-aided

474 design and then stacked together by applying heat/pressure through a rolling heated cylinder
475 [86]. In addition, the unused parts are cut off and hence, generating an accurate piece of
476 scaffold. However, recently stacking of the metallic layers with thickness of ~100 μm by the
477 use of ultrasonic welding is in great demand. This technique is called Ultrasonic Additive
478 Manufacturing (UAM) that offers various advantages like low temperature processing, solid
479 state bonding, low geometric distortion, retaining of surface texture and making of large scale
480 parts to design functionally graded scaffolds with pre-defined gradients [87,88]. In a study by
481 S. Kumar, aimed to design a thermal conductivity-based gradient scaffold in the direction of
482 material (Al, Cu and stainless steel) stacking by changing the process parameters. They have
483 successfully created gradient scaffold with dimensions of 1300*200" by stacking 62 foils.
484 However, the generation of scaffolds with accuracy in the Z-direction is challenging due to the
485 swelling after effects. In addition, mechanical strength and production of overhangs are poor
486 due to absence of support while building the architecture [89].
487
488 **2.1.5. Direct Energy Deposition:**
489 Direct Energy Deposition (DED) is a method of AM that designs scaffolds by directly melting
490 the base materials by using high energy source (electron beam, laser or arc) inside a closed and
491 controlled frame environment. Although this is similar to that of the material extrusion process,
492 the nozzle in DED technique is movable in five multiple directions. This process is widely
493 known as Laser Engineered Net Shaping (LENS), Laser metal deposition (LMD), and Electron
494 Beam Additive Manufacturing (EBAM) depending on the energy source used [84,90]. In the
495 year 1998, US Sandia National Laboratories and Stanford University developed Laser-
496 engineered Net Shaping (LENS) technology that has now been commercialized by Optomec
497 Company as Directed Metal Deposition (DMD). This technique has the ability to design larger
498 parts because of its high rate of deposition of the material and hence is widely chosen over

material extrusion technique [91]. In a study, LMD was used to design stainless steel block with thermal gradients that showed larger track width in top zone as compared to the bottom zones. However, after powder layer deposition, incomplete melting local voids were formed due to air entrapment from moisture evaporation. In addition, the lack of proper fusion in the layers resulted in irregular porosity of the gradient block. This concluded that this technique has low fabrication efficiency resulting in rough surface in the scaffolds [92].

2.1.6. Material binder jetting:

Material binder jetting method is a faster and versatile rapid prototyping technique that designs gradient based scaffolds using a liquid binding agent to glue two different layers. This technique shows advantages of assimilating various components of (metals and ceramics) and colors during the process of designing gradient scaffolds over the direct 3D printing [93]. In a study, Li et al., have utilized the electro-hydrodynamic jet-binding technique to introduce biological gradients into the nerve conduits that is essential for regeneration of nerve tissues. They have fabricated collagen fibrous scaffolds with gradients of stromal cell-derived factor-1α. It was observed that, altering the process parameters influences the types of gradients formed such as shallow continuous, steep continuous, and step in the scaffolds. This novel technique not only allows good control over gradient structure but also enables long-term presentation of stable gradients in the scaffolds [94]. In order to print more complex gradient scaffolds, advancements in 3D printing accelerated giving rise to 3D bio-printing of different tissues and/or organs.

2.1.7. Bioplotter Printing:

Bioplotter printing uses a computer aided design to deposit layer upon layer of different biomaterials to print gradient scaffold by utilizing bioink. This system uses pneumatic

pressurized method to squeeze out the materials through the nozzle to print functional gradient scaffolds [95]. Therefore, 3D bioprinting in the recent years has enabled the printing of living constructs by combining choice of materials, cells, growth factors and chemical cues for tissue regeneration. However, bioprinting of multiple materials in a single small nozzle becomes quite challenging due to the mixing of different liquids. In addition, sheer force from different sized nozzles pose a disadvantage on the viability of the cells during the process of gradient scaffold printing [96]. Many alternative strategies have been explored to allow the precise printing of gradient scaffolds with controlled bioink viscosity, printing speed, extrusion flow rate, cell concentration, and reaction kinetics of the different molecules present in the bioink [75]. In a study, authors have modulated the stiffness, cell concentration and an immobilized peptide gradients printed on a carboxylated agarose scaffold with extrusion-based 3D bioprinting technology [97]. This paves the way for better development in various technique parameters for gradient tissue engineering. In another study to address the problem of recapitulating native gradients, a unique technique of Digital Light Processing (DLP)-based bioprinting system was developed by Wang et al., which is capable of fabricating multifunctional gradients into the hydrogel scaffold. The real time generation of controlled gradients were done by adjusting the flow ratios of bioink. The combination of DLP 3D bio printing with a microfluidic chaotic mixer-linked vat that has yielded both horizontal and vertical gradients in 2-D and 3D planes as demonstrated in Figure 11. The system could generate high resolution complicated hydrogel structures with gradients of varying properties in pore size, porosity, stiffness, cell densities, and growth factor concentration [2]. These AM techniques can be simulated, and the artifacts can be corrected well before printing therefore giving an upper edge over other techniques [98]. Hence, AM is beneficial for designing gradient scaffolds and integrating them within the biological systems for tissue regeneration.

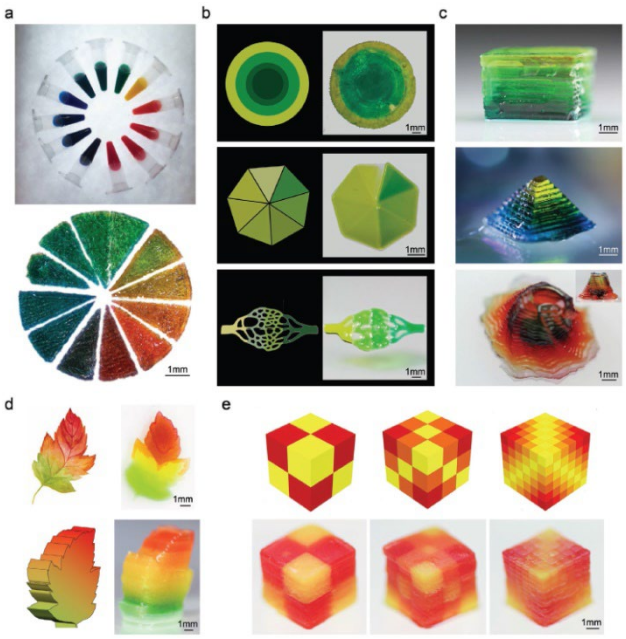

Figure 11: Illustrations of 2D and 3D structures produced by the composable-gradient DLP printing technique. a) The continual gradient of colors in the slices of a hydrogel pie printed by mixing merely three colored PEGDA inks. The inks in the Eppendorf tubes represent the colors collected after mixing before printing. b) The 2D structures including a circle with 4 color gradients, a heptagon with 7 color gradients, and a vascular network with 4 color gradients, generated by mixing two differently colored PEGDA inks at different ratios followed by printing. The corresponding designed patterns are shown at the left, while the actual printed results are presented at the right. c) The 3D constructs generated using PEGDA inks showing shapes of a cube, a pyramid, and a twisting hollow vase, featuring color gradients in the vertical direction. d) The 2D maple leaf with horizontal gradients and the 3D maple leaf with vertical gradients printed with the same composable gradient colors mixed from green to red in real time during the printing sessions. e) The cubes consisted of 2-by-2-by-2, 3-by-3-by-3, and 6-by-6-by-6 units presenting color gradients from discrete to continual. Adapted with permission from Ref. [2] © 2021 Wiley-VCH GmbH.

2.2. Component redistribution-based designing of scaffolds:

Component redistribution is another approach to design gradient scaffolds that uses physical parameters to re-distribute a homogenous fluidic mixture under the influence of a certain force. This technique increases the mechano-stability of the scaffolds and promotes the dispersion of nutrients, cells, metabolites, growth factors etc. in a differential manner and proliferation of cells [99,100]. This offers an advantage over other techniques as it utilizes differences in physical properties of the materials like density, thermal properties, temperature, size, etc. to form various gradients without modifying the bioactivity of the components and use of any external forces. Buoyancy, convective stretching, electric & magnetic field-based approaches are four important techniques available for component redistribution (Figure 12).

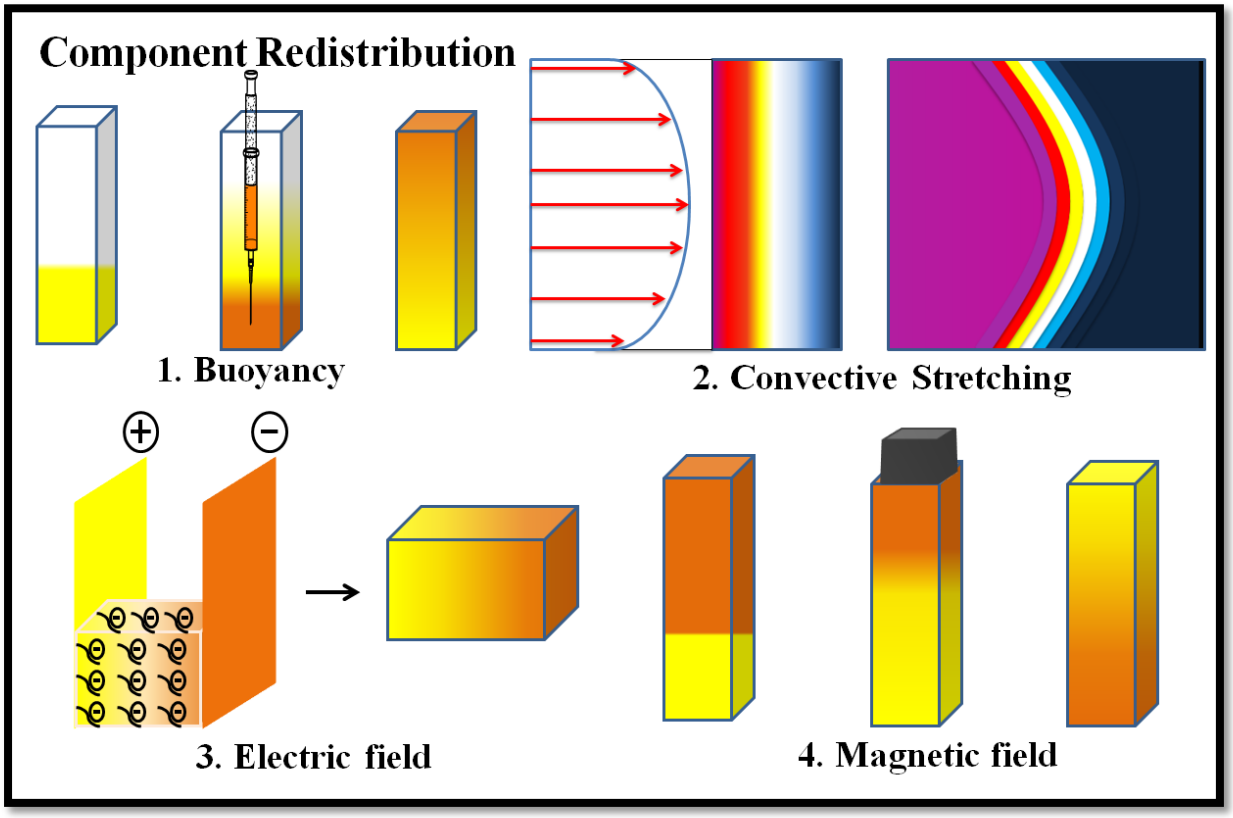

Figure 12: Different techniques of component redistribution for designing of gradient scaffolds.

2.2.1. Buoyancy

Buoyancy can be understood as the force exerted against gravity by a fluidic component on an immersed object [101]. This technique is beneficial for dispersal of growth factors for accelerating the cellular proliferation in a gradient scaffold. In a study, the authors have demonstrated the application of buoyance force to fabricate gradient scaffolds, Li et al., used gelatin metacryloyl, gellan gum, agarose, and acrylate polymers to incorporate physical gradients in the biomimetic 3D structure. The authors further tried to incorporated several macromolecular structures such as nanoparticles, liposomes etc. to induce biochemical gradients. During the design, three-phased liquid components were injected to the scaffold thus creating buoyancy within the architecture of the scaffold (Figure 13 A). Following the design, the Bone Morphogenetic Protein-2 release from the scaffold was observed over 28 days to reconstruct the bone cells. The study concluded that incorporation of buoyancy induced by liquids injected in multiple phases could be helpful in generating gradients that resembles the natural ones which can control the release of essential macromolecules for cartilage tissue regeneration (Figure 13 B) [102].

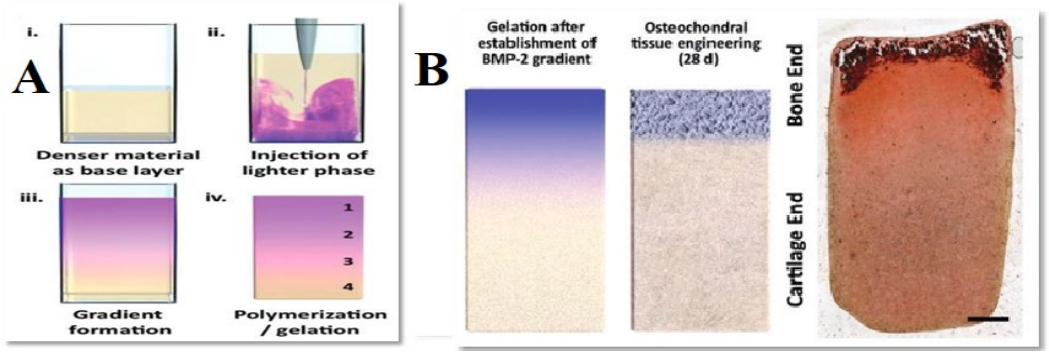

Figure 13: (A) Induction of gradients by sequestering of base components at different layers with sucrose density, (B) induction of osteo cell regeneration at the interface of cartilage and bone after 28 days by controlling the release of Bone Morphogenetic Protein-2. Adapted with permission from Ref. [102] © 2019 The Authors. Published by WILEY-VCH Verlag GmbH & Co. KGaA, Weinheim.

2.2.2. Convective Stretching:

Convective stretching technique is generally used to designing gradient scaffolds by faster moving of the center particle than the particles present near the wall due to difference in channel velocity [103]. In a study, Reis group of University Minho prepared HA gradient within the methacrylated gelatin and gellan-gum (GelMA-LAGG) scaffold by using convective stretching technique. In this system, porosity gradient was also incorporated which had no negative effect on the previously oriented HA gradients. This scaffold accelerated the prevasculature formation in the region of bone tissues but retarded in the cartilage region. This result demonstrated a great potential in regeneration of complex hierarchically organized osteochondral tissues [104].

In recent years, the channel used in convective stretching technique is replaced with microfluidic channel that allows the spreading of molecules inside the channel which is called as dispersion. This combination of convection and diffusion inside the channel can be used to generate gradients with desired architectural morphology that can mimic biological tissues which will be useful for tissue regeneration. In a recent study, Yanan and team developed a high-speed fluidic sheer offering convention-driven (hydrodynamic stretching) technique along with photo crosslinking to generate gradient of polymer, biomolecules, beads, cells and cross-gradients of two species in a micro channel which has been demonstrated in the Figure 14. This simple technique used to fabricate biomimetic anisotropic gradient scaffolds for tissue regeneration [101].

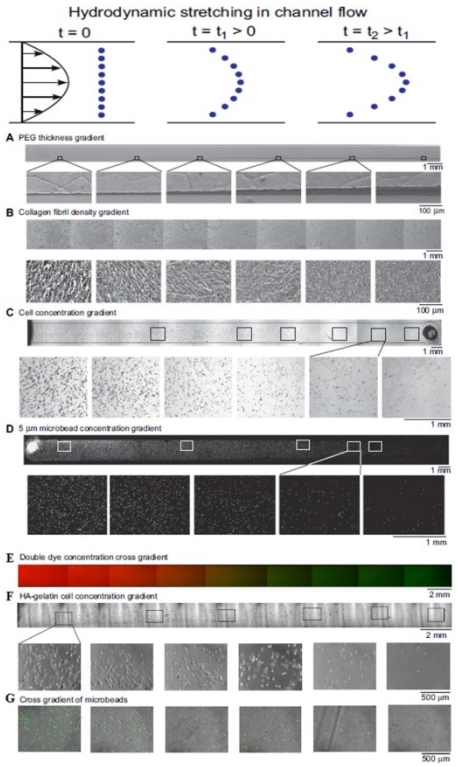

621

622 **Figure 14:** Convection-driven gradients of A. Poly(ethylene glycol-diacrylate) hydrogel
623 gradient; B. collagen gradient; C. endothelial cell gradient; D. fluorescent particle gradient
624 (diameter 5 mm); cross-gradients containing two species E. Merged fluorescence image of a
625 cross-gradient of FITC-dextran (green) and rhodamine dextran (red) F. Phase images (upper:
626 lower magnification; lower: higher magnification) of smooth muscle cells cultured on a
627 substrate made from a composite material with a HA-gelatin cross-gradient G. Merged phase
628 and fluorescence image of a cross-gradient of 10 mm fluorescent and non-fluorescent
629 microbeads. Adapted with permission from Ref. [105] © 2009 Elsevier Ltd.

630

631 **2.2.3. Electric & Magnetic field**

632 Bio-physical stimuli apart from chemical modifications are very important factors that needs
633 be taken into consideration while additively manufacturing the gradient scaffolds for tissue
634 regeneration. The electro-magnetic field-based component redistribution technique is
635 advantageous for designing of gradient scaffolds as the cellular migration, proliferation, and
636 adhesion can be controlled by externally inducing an electro-magnetic field towards desired

orientation [106,107]. In a study, Xu et al., have used electric field-driven crosslinking in β-sheet rich silk protein nanofibers to incorporate multiple gradients within the hydrogels. The gradients can be controlled accordingly by changing the influencing factors such as viscosity of the solution. The electric field imparted orientational gradient to the scaffold that could control the osteogenesis and chondrogenesis activity. It was observed that the fabricated mechanical gradient silk-based hydrogel scaffold was able to stimulate in vivo ectopic osteochondral tissue regeneration [108]. In another study, authors used a magnetic bio-technology system to design a gradient of two different magnetic nanoparticle labeled cell types; vascular and osteoprogenitor on the opposite sides of the PCL-Fe-doped HA magnetic scaffold fibers through material extrusion method. Computer-aided Multiphysics – Magnetostatics – 2D axial symmetry application was used for quantifying the influence of magnetic field on the gradient structuring of magnetized cells on the scaffold. The mathematical modeling unveiled that the gradient formation by the cells was guided by the permanent magnet whereas the non-homogenous distribution the cells were strongly modulated by the generated background magnetic field of the magnetic scaffold. Figure 15 a, b, and c shows the directions of magnetic gradients throughout the scaffold, along a single selected fiber and along the cross section of a complete row of fibers respectively. They concluded that this technology of manipulating magnetic cells to create gradient magnetic scaffold is highly useful for tissue regeneration without any pitfalls, although modifications and other alterations may be needed to optimize the model for further in vivo studies [109].

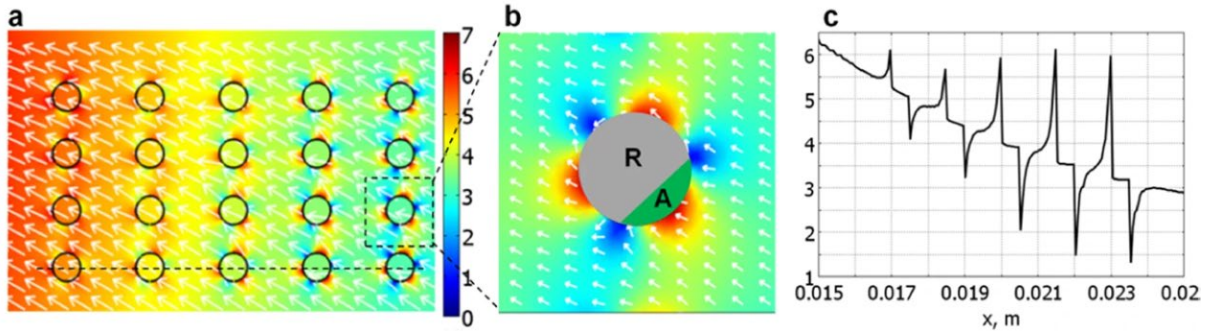

Figure 15: Magnetic gradient in T/m units: (a) distribution in the scaffold region: color scale indicates the magnitude while arrows show the direction of gradient and hence the direction of magnetic forces; (b) zooming around one fiber section, where green area delineates the attraction region (A), and grey area indicates the repulsion region (R); (c) gradient distribution along the dashed line in (a). Adapted with permission from Ref. [109] © The Author(s) 2020.

In a similar study, iron oxide nanoparticles have been used to design magnetized gradient multi-layered scaffold with porous nature, moderate mechanical stability and elasticity. This gradient scaffold was able to facilitate growth of neurons and successfully regenerated axon sprouting in the injured rat with nerve defect. The results demonstarted that the magnetic gradient could induce cell fate for nerve tissue regeneration due to magnetic stimulation in the implanted scaffold [110].

2.3.Controlled phase separation-based designing of scaffolds

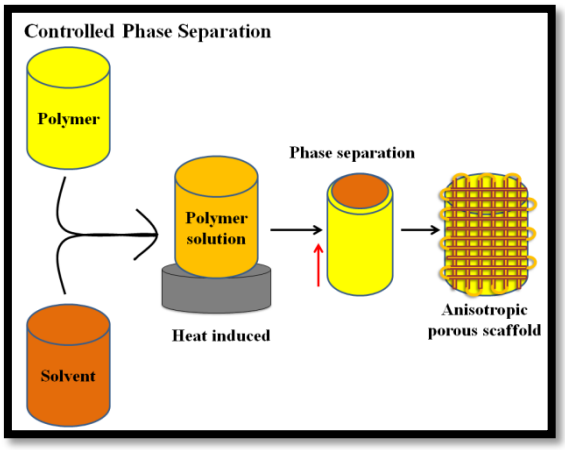

Figure 16: Different techniques of controlled phase separation for designing of gradient scaffolds.

Controlled phase changes in designing of gradient scaffolds involves the induction of an abiotic parameter such as temperature, pressure, light for changes in structural and/or physical

properties including density, porosity etc. [111–114]. The pictorial representation of this technique has been given in the Figure 16.

In tissue engineering, to regenerate tissue scaffolding biomaterial is essential with specific properties including interconnected porosity with sufficient mechanical strength and appropriate structural morphology. In bone tissue regeneration, it is compulsory for the technique to present a gradual variation of porosity along the scaffold thickness such as to mimic the native gradient structure. Ghersi et al., in a study used thermally induced phase separation (TIPS) to design a porous gradient of pore dimension along the thickness of the scaffold. In this method an experimental apparatus has been designed to impose different temperature vs. time pathway on both the sides of scaffolds (Figure 17 A). The nucleation-and-growth mechanism that occurs in the pore dimension is mainly influenced by the thermal history [115]. Hence, it is possible to achieve desired pore size by changing the residence time in the metastable region. The most interesting aspect of this technique is to control both temperature and cooling rate at the same time. The poly-L-lactic acid (PLLA) was mixed with HA at two different ratios (50/50 and 70/30) and exposed to various thermal environments to have pore size that increases along with increasing scaffold thickness. The micrograph images show that the scaffolds had well interconnected porous structure and the HA particles were also well blended into the polymer matrix. However, presence of HA was more evident in the scaffold with 50/50 PLLA/HA ratio than 70/30 ratio which can be concluded from the micrograph shown in Figure 17 B and C. Mammal bone tissues are known to contain 58% dry weight of ceramic HA and hence, shows good osteoconductive properties. Therefore, authors concluded that thermally induced porous HA-gradient scaffolds have promising aspects for bone tissue engineering [116].

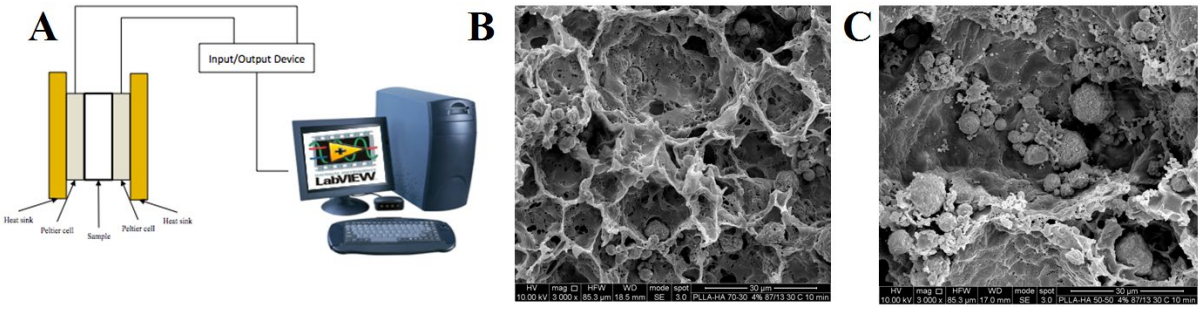

Figure 17: (A) Experimental setup of TIPS technique; High magnification SEM images of porous gradient scaffolds prepared using different ratio of HA:PLLA using TIPS (B) 70:30 (C) 50:50. Adapted with permission from Ref. [116] © 2016 AIDIC Servizi S.r.l.

A similar study by Mannella et al., prepared a porous-based gradient scaffold by using TIPS while generating foams with a single-step operation. This induced the scaffolds by monotonously varying pore size ranging from 45-260 µm, and de-mixing the temperatures ranging from 25°C-35°C along the scaffold thickness which suggests promising roles in bone regeneration [117]. Similarly Nie et al., combined TIPS technique with the sugar sphere template leaching process for designing PLLA scaffolds having a physical gradient of pore size ranging from 300 µm-600 µm [118].

Cardiovascular disease has become one of the leading causes of mortality in worldwide. Natural blood vessels consist of type I , II collagens and elastin which are of nanometer sizes. The designed nano-structured scaffolds to mimic the natural blood vessels needs to be biocompatible, biodegradable, adequate mechanical properties with high porosity suitable for arterial implantation [119]. In recent years, blood vessel tissue engineering plays an important role to design scaffolds that mimic nanosized fiber architecture. There are several strategies that have been adopted to design gradient scaffolds for blood-vessel tissue engineering but have various drawbacks and limitations to be used in clinic. In a study, the group of Peter Ma used TIPS technique to design biodegradable polymer scaffolds with oriented gradient interconnected microtubular pore structures in the axial or radial direction to facilitate cell

seeding and mass transfer for cell growth and function. Figure 18 A and B shows the SEM images of cross sections of vessel scaffolds wall with radial temperature gradient from inside to outside I/O structure and outside to inside O/I structure respectively. The migration and distribution of the cells within the oriented gradient scaffold were pronounced and healthy under haematoxylin and eosin (H-E) staining when compared with non-oriented porous scaffold (Figure 18 C). The structural features of such scaffolds can be conveniently adjusted by changing the polymer concentration, solvent ratio, TIPS temperature, and by thermal conductivities of different materials to mimic the nanofibrous features of an ECM to facilitate blood-vessel regeneration [120].

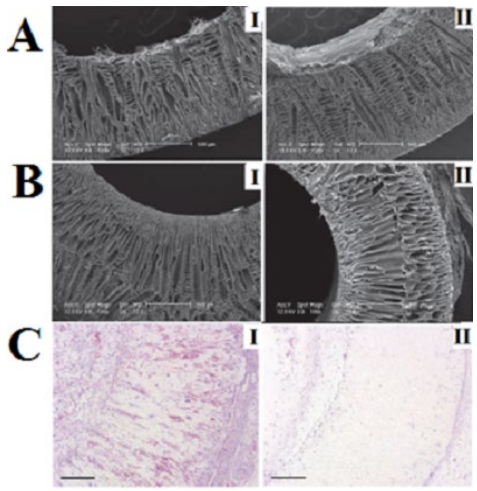

Figure 18: (A) SEM images of cross sections of a vessel scaffold prepared under a radial temperature gradient (I/O structure) at − 20 ° C for PLLA/ benzene solutions with different concentrations (w/v): I) 2.5%; I) 5.0%; (B) SEM images of cross sections of vessel scaffolds prepared under a radial temperature gradient (O/I structure) at − 20 ° C from PLLA/ benzene solutions with different concentrations (w/v): I) 2.5%; II) 5.0%; (C) After 2 weeks of implantation, H-E staining of the cross sections of implants showed that abundant host cells migrated into the scaffolds with orientated pores and the fibroblast-like cells appeared to be healthy in the microchannels; I) substantially fewer cells migrated into the scaffolds with non-oriented pores; II) Both types of scaffolds maintained their original shapes. Scale bar: 200 μ m.

743 Adapted with permission from Ref. [120] © 2010 WILEY-VCH Verlag GmbH & Co. KGaA,
744 Weinheim.
745
746 **2.4. Post modification-based designing of scaffolds:**
747 The techniques described above include the gradient fabrication during the designing process;
748 however compositional gradients introduced into the prior designed scaffold can be done in the
749 post-modification processes like diffusion, dip-coat, matrigel coats, immersion etc. [121,122].
750 This process helps in creating uneven gradual distribution of cells, proteins, biomolecules,
751 chemicals and hormones within the scaffold by varying the density, loading rate etc. of the
752 materials that are being loaded. In a study, Karpiak et al., have used the density variation within
753 the liquids for creating complex distinct layers in the hydrogel scaffold. They have chosen a
754 high density modifier (bisacrylamide and acrylamide or biocompatible c(PEGDA)) with
755 varying initial concentrations and settling time between the layers resulting in smooth gradient
756 hydrogels as shown in Figure 19. This one-step polymerization technique can be helpful in
757 designing complex matrices for tissue regeneration [20].

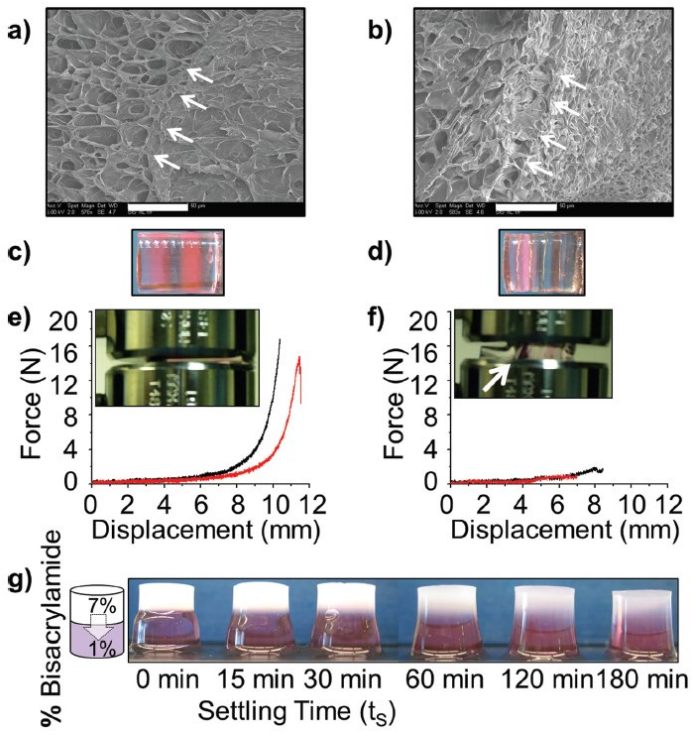

758

Figure 19: Density gradient multilayer polymerization (DGMP) results in continuous structures and mechanical stability at interfaces of adjacent compartments in mechanically heterogeneous hydrogels. a–b) Multicompartment PEGDA hydrogels fabricated via sucrose DGMP (a) are microstructurally more continuous at the interface between 10% (w/v, upper left) and 20% (w/v, lower right) prepolymer than sequentially photopolymerized PEGDA (b). White arrows highlight interfaces. Bar indicates 50 cm. c–f Five-layers PAM (10% w/v, 1% w/w crosslinker) hydrogels approximately 12 mm in diameter prepared by DGMP or sequential photopolymerization. DGMP produces hydrogels (c) that are macrostructurally more continuous than sequentially photopolymerized polyacrylamide (d). DGMP produces stronger hydrogels (e) than sequentially photopolymerized polyacrylamide (f) as indicated by perpendicular compression to failure and failure mode evaluation Photos are inset in force vs. displacement curves (n=2). Note that DGMP hydrogels bulk ruptured at around 90% strain while sequentially polymerized hydrogels delaminated at around 65% strain as indicated by white arrow. (g) Increasing tS prior to bulk polymerization modulates structural gradients in 10% (w/v) PAM bilayer hydrogels. As schematically represented (left), bisacrylamide crosslinker diffuses through the density interface to graduate the transition between 7% and 1% crosslinker (w/w monomer). Swelling in water demonstrates the transition from discrete to increasingly continuous mechanical gradients. Adapted with permission from Ref. [20] © 2012 WILEY-VCH Verlag GmbH & Co. KGaA, Weinheim.

However now-a-days, advanced techniques such as rapid prototyping computer-aided means and photopolymerization are used for post processing and surface modification of the pre-designed scaffolds. In a study, authors have combined 3D prototyping and surface polymerization to create multidirectional biochemical gradients onto the PCL scaffold. The PCL scaffolds were first fabricated with compositional variations of protein solution thus

producing a gradient along the axis. The scaffolds were further exposed to different compositions of electro-spun fibers in a bidirectional axis. The protein gradient scaffolds obtained were further cross-linked by exposing it to light which produced double gradients within the scaffolds along the x-axis & z-axis (Figure 20) [123].

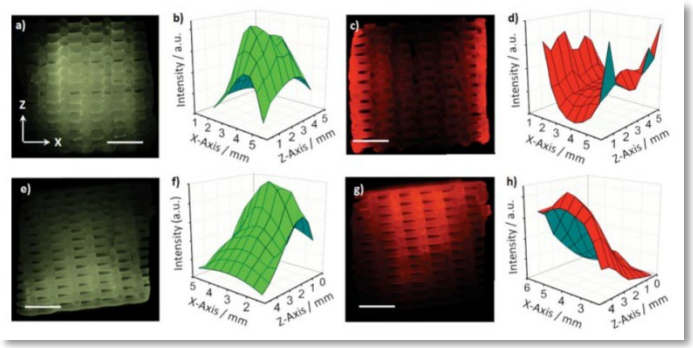

Figure 20: Double gradient induced in the designed scaffolds i.e. by diffusion, and light induced polymerization (a, e, c, g) depict the orthogonal views of the designed scaffolds when exposed to fluorescent stains; (b, d, f, h) intensity graphs corresponding to different views of the scaffolds along the x & z axis. Adapted with permission from Ref. [123] © 2015 WILEY-VCH Verlag GmbH & Co. KGaA, Weinheim.

In another study, authors have prepared vascular cell-laden gradient PEG hydrogels to study its potential for pre-vascularization and induction of spatial variations in complex tissues through the method of photo-polymerization. The authors have created five different decoupled and combined gradients of immobilized arginine-glycine-aspartic acid (RGD peptide) concentration, stiffness, and protease-sensitivity within the hydrogel to study the vascular sprouting activity in 3D culture. Their findings have concluded that vascularisation of complex tissues requires gradients of various properties like mechanical, degradation rate and adhesion ligand composition [124].

Basic Fibroblast Growth Factor (bFGF) is a potent mitogenic and chemotactic agent that plays an essential role in designing engineered tissues which mimic the structural and biological

functions of natural blood vessels along with enhancing in vivo directional cell migration. Furthermore, bFGF has the ability of binding covalently to scaffolds for fabricating growth factor gradients with retention of its bioactivity. In addition, bFGF covalently conjugated with RGD can enhance the proliferation and migration of vascular cells. Moreover, controlled bioactive signal in bFGF gradient scaffolds influenced their alignment and migration. In a study, authors have designed post modified PEG hydrogel, which is covalently conjugated with bFGF in combination with RGD by photopolymerization which retained its bioactivity on vascular smooth muscle cells (vSMC) proliferation and migration. This bioactive scaffold was further silver stained to analyse the bFGF gradient whose density was found to be linear in the direction of increasing bFGF concentration (Figure 21 A). The bFGF gradient also facilitates the alignment of more vSMCs in the direction of its increasing concentration which is not pronounced in case of scaffolds with constant or no bFGF (Figure 21 B). Therefore, designing of stable gradient of GF in the scaffold with known concentration profile will allow understanding the influence of gradients on cellular responses [125].

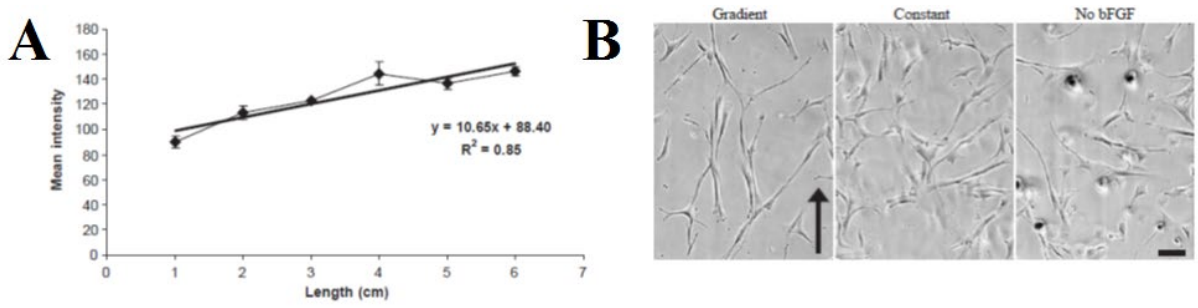

Figure 21: (A) The bFGF gradient was silver stained, analyzed under light microscopy, and found to be linear; (B) More cells were aligned on hydrogel surfaces with a bFGF gradient (indicated by arrow) than on the other hydrogel surfaces, which lacked a gradient of tethered bFGF (bar=10 mm). Adapted with permission from Ref. [125] © 2004 Elsevier Ltd.

Therefore, advancement in the fabricating techniques along with the use of tissue engineering has helped to expand the potential application of gradient scaffolds in research and medical

827 fields. The subsequent section explains the natural gradient of various tissues present in human
828 body and the application of gradient scaffolds for their successful recovery after being diseased
829 or damaged.
830
831 **3. Applications of gradient scaffolds in tissue engineering:**
832 The human body is full of gradient structures that guides various processes and events from
833 early embryonic stage to adult life. The designing of a scaffold must satisfy the basic structural
834 and functional requirements of the complex tissue/organ that may be addressed by gradient
835 scaffolds. Hence, recently, different fabrication techniques have been developed to design
836 gradient scaffolds that help accelerate various tissue regeneration. Gradient scaffold exhibit
837 several advantages over traditional scaffolds by exhibiting excellent penetration capacity for
838 nutrients & cells, increased cellular adhesion, cell viability & differentiation, improved
839 mechanical stability, and biocompatibility. Incorporating physical, chemical, and/or cellular
840 gradients into the scaffolds have shown enhanced efficacy in bone, cartilage, neural,
841 cardiovascular and skin tissue regeneration [126,127]. The wide applications of gradient
842 scaffolds in regeneration of various tissues has been described in detail in the subsequent
843 sections. Furthermore, Table 1 presents the wide applications of gradient scaffolds in tissue
844 regeneration.
845
846 **Table 1: Different gradient scaffolds used in various tissue regeneration**

Type of gradient	Base material	Designing Technique	Application	Advantages	Ref.
Structural and compositional	Randomly oriented PCL nanofibers (Bone) and -TCP nanoparticles PCL nanofibers	Hybrid twin-screw extrusion/electrospinning (TSEE)	Bone-Cartilage	Graded scaffold mimicked structural and compositional	[128]

				properties of natural interface	
Compositional	Random *poly(lactic-co-glycolic acid)* (PLGA) Nanofibers (Bone). Aligned PLGA Nanofibers (Tendon)	Electrospinning	Bone-Tendon	Mechanical properties similar to native tissue were achieved	[129,130]
HA gradient	Gelatin microribbon hydrogel	-	Bone-Tendon	Resemblance with the bone–cartilage–tendon transition with significant increase in tensile moduli of the resulting tissues	[131]
Porous	HA	Freeze-casting	Bone	Accelerated the self-seeding of cells	[132]
Porous	Biphasic calcium phosphate nanopowder and glass-ceramic	3D printing	Bone	Seeded cell number was found to be constantly increasing with decreased metabolic activity indicating cell differentiation	[133]
Topology and porous	316L stainless steel (based on a mathematical model)	3D printing (Direct metal laser sintering)	Bone	Young's modulus of the designed scaffolds was similar to that of trabecular bone, significant osteoblast growth was observed in in-vitro assay	[134]

Density	Collagen type II hydrogel	Bioprinting	Cartilage	Density gradient in cellular distribution in ECM components	[135]
Porous	Polylactone/4-arm poly(ethylene glycol) hydrogel (PCL@tetra-PEG) composite	3D-bioprinting	Cartilage	Excellent biochemical and biological (anti-inflammatory and anti-oxidant) properties with heterogeneous bionic structures	[136]
Substrate Stiffness, Thickness, Density	Collagen gels, 1% 3-aminopropyl tri methoxy silane, 0.5% glutaraldehyde	-	Osteogenic Cell Behavior	Osteogenic mechano-transduction	[137]
Compositional, porosity, and mechanical	PCL and gelatin	Casting, electrospinning and lyophilisation	Skin	Concurrent healing of the different layers of skin i.e. epidermis, dermis, and hypodermis. Proliferation, and differentiation of both keratinocytes &dermal fibroblasts was enhanced	[138]
Stiffness elastic modulus	n poly(dimethylsiloxane)/ poly(vinylidenefluoride-cotrifluoroethylene) polymers [(PDMS)/ P(VDF-TrFE)]	Solvent-assisted micromolding method and photolithographic technique with dry etching process	Skin	Compressibility, and contact area differences significantly improved	[139]

Pore size	Silk-based	Low temperature electrospinning	Skin	Differences in pore sizes enhanced the regeneration of skin	[140]
Pore and fibrous	Collagen-based	Flow, source-sink and point source method	Vascular endothelium	Higher cell density at the core & migration of growth factor (VEGF-165)	[141]
Vertical nanofibrous	Chitosan/PLA scaffolds	Electrospinning	Vascular tissue	Prevention of restenosis by rapid endothelial cell proliferation	[142]
Oxygen gradients	Collagen sponges	Diffusion	Myocardial tissue	Increased oxygen concentration within the construct and reduced the thickness of the mass transport boundary layer	[143]
Anisotropic and isotropic fibrous gradients	Block copolymer	Electrospinning	Region specific tissues	Guided cell migration, adhesion and spreading	[144]

3.1. Gradient scaffolds for bone tissue regeneration

Bone is a rigid connective tissue that not only provides structural support to the human body but also facilitates movement by providing attachment sites for muscles, tendons, ligaments, and protects vital soft organs and tissues [145–147]. This connective tissue has four different kinds of cells i.e., osteoblast, osteoclast, osteocytes, and bone linings (osteogenic). The bone comprises of two types of tissues; namely cancellous/spongy/trabecular and compact/cortical [145]. Spongy or cancellous bone contains osteocytes present in lacunae which are not arranged in concentric circles, but in compact bone these osteocytes are arranged in concentric circles

as shown in Figure 22 [148]. Bone, ligament and fibrocartilage are three different regions in the natural constituent of ligament-bone graded transition interface. The bone consists of a well-organized gradient macro to nano-scale structures with 9 wt% water, 22 wt% organic (type I, II, IV collagen, and 200 types of noncollagenous matrix protein such as glycoproteins, proteoglycans, sialoproteins, etc.), and 69 wt% inorganic crystalline components (hydroxyapatite and calcium phosphate).

The bone-cartilage interface shows regional gradation in proteoglycan, mineral and collagen concentration through four cartilaginous region namely surface zone cartilage (SZC), middle zone cartilage (MZC), to deep zone cartilage (DZC), then calcified cartilage (CC), and finally to bone [149–152]. In bone tissues, a structural gradient is observed in an axial direction in flat bones. In contrast, in the radial direction of long bones, the bone density varies from the cancellous bone to the cortical bone. In addition, the bone also has a biochemical gradient composed of different minerals with high percentage of calcium, phosphorous, and trace quantities of sodium, potassium which creates an ionic gradient in the cancellous, and trabecular bones. The structural architecture and porosity influence the overall bone properties. However, the compact bone are more resistant to longitudinal stress compared to radial and compression than to tension [26].

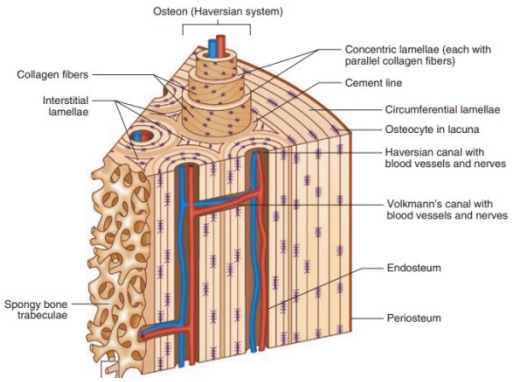

Figure 22: Structural (compact and spongy) and cellular gradients (collagen fibers, and osteocytes) in bone tissue. Adapted with permission from Ref. [148] © 2017 Springer International Publishing Switzerland.

The gradients in bone structure helps in facilitation of nutrients, bone cells, mineralization, and contributes to high mechanical strength thereby providing rigidity to the structure of the body, strength for performing physical activities and accelerate bone regeneration [153–155]. Organic components present in the bone tissue impart flexibility, whereas inorganic components provide toughness and strength. Moreover, the presence of HA and collagen fibers in the bone tissue instigates interaction with the local physiological, and biochemical environment [156–158].

Bone tissue regeneration is the repair of bone defects generated for various reasons. Bone transplantation is the second most common clinical application after blood transfusion due to the increase in the aging population in the world. Although bone tissue has its natural self-healing ability, but many-a-times larger or more complex defects face difficulties as the occurrence of bone traumatic cases range from 33.4-64% worldwide [18]. In the clinic, the current bone therapies for bone replacement include autografts and allografts, which are not ideal solutions till date. Hence, there is an alternative for restoring and improving the function of bone by using gradient scaffolds, which can provide an appropriate regenerative signal to cells and a biomimetic environment for bone tissue repair or regeneration [159,160]. In a study to design multi-layered gradient scaffold, Surmeneva et al., applied EBM on titanium-based alloy (Ti_6Al_4V) for segmental bone reconstruction. The process of EBM utilizes electron beams allowing temperature reaching up to 1000° C, which generates gradient within the material. By using this process, five different lattice designs were created, with four of them presenting a solid tubular architecture similar to that of human bone (Figure 23 A & B) [161].

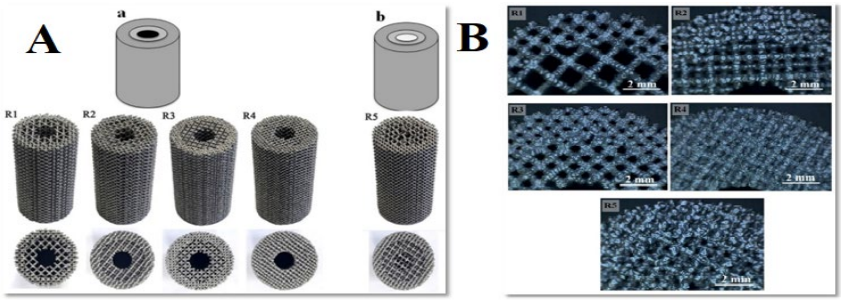

Figure 23: (A) Titanium-based multi-layered porous gradient scaffolds obtained by electron beam melting by (a) 2-step and (b) 3-step layering, (B) Microscopic images of multi-layered gradient scaffolds with varying porosities. Adapted with permission from Ref. [161] © 2017 Elsevier Ltd.

In addition, it was found that the tubular scaffolds had high energy absorption, which resulted in a higher compressive strength (31-22 MPa). The multi-layered lattice scaffolds presented excellent compatibility for the ingrowth and vascularization of bone tissue. Interestingly, the multi-layered scaffolds could be seeded with different biomaterials by exploring their porosity, which could further improve the mechano-durability of the grafted bone. [161]study This This suggested that Ti_6Al_4V based scaffold architectures could trigger bone regeneration by enhancing the mechanical strength, and augmented ductility [161].

In another attempt to develop scaffolds with porous gradients, Sobral et al., took the approach of a rapid prototyping technique for bone tissue engineering. The authors designed two gradient scaffolds (Grad 1, Grad 2) and two homogenous scaffolds (Homog 1 & Homog 2), each with different porosities and pore aspect ratios (Figure 24). The scaffolds were produced by three-dimensional plotting while using a blended mixture of starch and PCL.

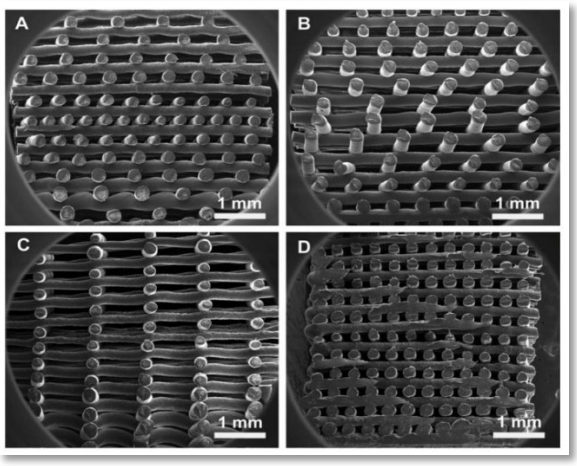

Figure 24: SEM images of porous gradient scaffold (A) Grad 1, (B) Grad 2, (C) Homog 1, and (D) Homog 2 scaffolds. Adapted with permission from Ref. [162] © 2010 Acta Materialia Inc. Published by Elsevier Ltd.

When the seeding of cells was studied *in-vitro,* 70% and 56% efficiency was observed in Grad 1 and Grad 2 scaffolds, whereas the seeding efficiencies for the Homog 1 & Homog 2 scaffolds was observed to be 30% and 40%. This demonstrates that the gradient in porosity of the scaffolds results in enhanced cell seeding efficiency. This shows that gradient scaffolds prepared under controlled conditions can be of benefit over homogeneous scaffolds for engineering of bone tissue [162]. In a similar study, Xie et al., designed 3D mineral gradient scaffolds composed of HA with spatial calcium (Ca^{2+}) distribution for differentiation of the rat bone marrow stem cells. The scaffold was designed using a combination of the traditional textile manufacturing, and electrospinning strategies (Figure 25). The authors observed that the scaffolds efficiently released the Ca^{2+} ions in a gradient manner for up to 10 weeks. From the *in-vitro* studies, the cells of mouse embryo osteoblast precursor cells were noticed to proliferate and the osteogens differentiation of bone marrow of rat (rBMSCs) were also boosted by the mineralized segments whereas the tenocytes differentiation of rBMSCs was enhanced by the non-mineralized segment [163].

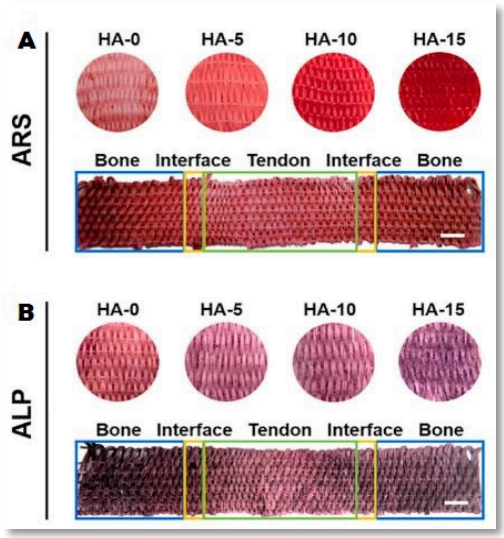

Figure 25: Osteogenic induction by the continuous mineral gradient scaffolds with different concentration of HA: (A) Alizarin Red S stained of scaffolds segments, and whole segments containing rBMSCs, (B) Alkaline phosphatase expression of scaffolds incorporated with rBMSCs. Adapted with permission from Ref. [163] © 2021 Elsevier Ltd.

The results suggests that HA gradient scaffold can be a good asset for tendon-bone tissue regeneration as it have the capacity to guide the spatial differentiation of rBMSCs; thus playing a major role in providing structural, biochemical, and biomechanical characteristics to the neo-tissues same as the native tissue [163]. In a similar study, mineral gradations of HA nanoparticle was fabricated within gelatin microbead by infiltration with PLGA using a simple inverse opal scaffolding process. The prepared scaffolds with HA gradient were observed to control the spatial arrangement of adipose derived mesenchymal stem cells (ASCs) for osteogenesis with high cell viability potential. In addition, the scaffolds had uniformly distributed pores that could facilitate transport of nutrients and metabolic wastes. Figure 26, SEM and Micro-CT images show the mineral gradient in scaffold structure which shows a potential future in fabricating the interfaces between mineralised and unmineralized tissues [10].

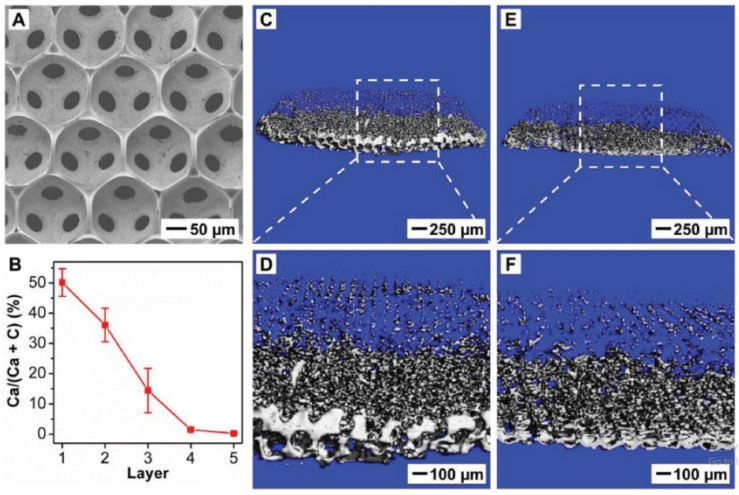

954

955 **Figure 26:** Characterization of the distribution of HA nanoparticles in the PLGA inverse opal
956 scaffold. A) Top-view SEM image. B) EDX quantification of calcium content along the vertical
957 direction (n=3). The layer number refers to the layer of pores after template removal. (C−F)
958 Micro-CT images of an HAp-graded PLGA scaffold (C,D) and its sagittal sectioning plane
959 (E,F). Adapted with permission from Ref. [10] © 2018 WILEY-VCH Verlag GmbH & Co.
960 KGaA, Weinheim.

961

962 However, the recovery of irregular shaped bone defects and soft tissues has become a major
963 problem. To overcome such limitations, Wang et.al, have tried to develop scaffolds with super
964 elastic SiO_2 nanofibers with chitosan as bonding sites (SiO_2 NF-CS) through lyophilisation
965 process. Furthermore, they have developed stiffness gradient in SiO_2 nanofibers (Figure 27)
966 that helped spatial differentiation of human mesenchymal stem cells (hMSCs) into
967 chondrocytes and osteoblasts. The scaffold demonstrated stiffness gradient, high elasticity,
968 good fatigue resistance, and quick recovery in aqueous medium. Histomorphological analysis
969 in rat having calvarial defect confirmed the efficiency of the gradient scaffold by enhancing
970 vascularization and bone formation. This strategy will be helpful in recovery of irregular
971 defects and subcondral sites of bone [164].

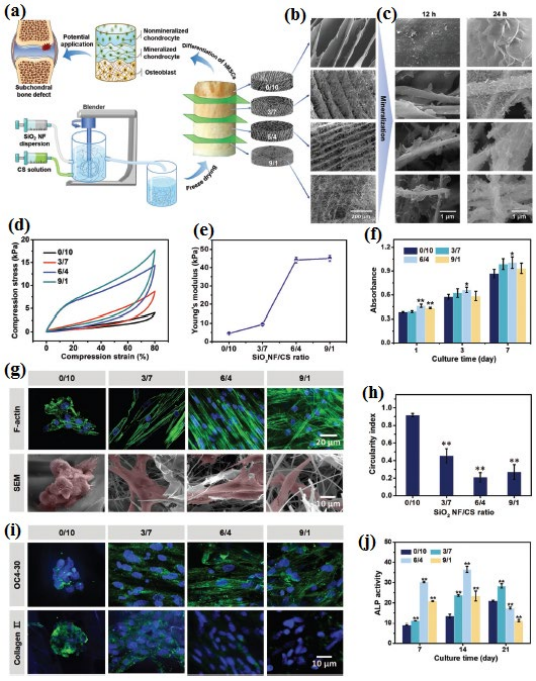

Figure 27: SiO_2 NF-CS scaffold with gradations in SiO_2 nanofibers to mimic subchondral bone sites. a) Schematic for fabrication of gradient SiO_2 NF-CS scaffold. SEM images of b) gradient scaffolds and c) mineralized gradient scaffolds at different locations. d) Compression curves and e) Young's modulus of each section in the gradient scaffold. f) Cellular viability of hMSCs cultured in each section of gradient SiO_2 NF-CS scaffold. g) F-actin staining, SEM images (hMSCs were in pseudocolored red for contrast), and h) cellular circularity index of hMSCs cultured in each section in the gradient scaffold, indicating enhanced cell stretching and proliferation with increase in SiO_2 nanofiber content. i) OC4-30 and collagen II immunostaining and j) alkaline phosphatase activity of hMSCs cultured in each section in gradient SiO_2 NF-CS scaffolds after 21-day culture. Data are presented as mean ± SD.* and ** indicates $P < 0.05$ and $P < 0.01$ for SiO2 NF-CS scaffold section (3/7, 6/4, and 9/1) compared with CS scaffold section (0/10), respectively. Adapted with permission from Ref. [164] © 2019 WILEY-VCH Verlag GmbH & Co. KGaA, Weinheim.

Melt Electrowritten (MEW) technique is a solvent free process used to design gradient scaffolds with specific ordered and tuneable architecture. The technique is therefore non-toxic

and creates aligned orientation, uniform pore size, distribution & interconnectivity. This results in accelerated angiogenesis and cell penetration leading to quicker repair of bone defects. In a study Stephen Hamlet group, used a new technique of MEW to design PCL scaffold with three different pore structure (two offset scaffold with different fiber layout and complex scaffold with three gradient pore size). The obtained results revealed that the gradient scaffold enhanced the alkaline phosphatase activity in the osteoblasts. However, the scaffold mineralization was higher in obtained scaffold. The immuno-staining showed significant expression of osteocalcin gradient scaffold structure [165]. The same Hamlet group in another study, designed MEW tri-layered PCL gradient scaffold with different architectures that showed different capacities of in vivo osteo-conductivity. The results demonstrated that the expression of osteogenic marker was present in all scaffolds whereas, the mineralization marker osteocalcin was observed in the gradient scaffold. Furthermore, the expression of endothelial marker showed that induced angiogenesis was also involved in the repair process [166]. The MEW based scaffold showed accelerated osteogenesis of osteoblasts and has potential of opening a new avenue for superior bone tissue regeneration system.

3.2. Gradient scaffolds for cartilage tissue regeneration

Cartilage is dense structured flexible connective tissue resembling a firm gel made up of collagen and elastic fibres. It is an important structural component of the body found in between joints of bones, ear, nose, bronchia etc. and has higher stiffness than muscles but less than that of bones [167,168]. The cartilage is of three types i.e. hyaline, elastic, fibrous, and all three have cellular and macromolecular gradient composed of chondrocytes, perichondrium, chondroitin sulfate [164]. Hyaline cartilage is the most common tissue found in the body amongst all the three types. It is closely packed with collagen fibers that make it tough but slightly flexible with smooth surface. For example, articular cartilage is a type of hyaline

cartilage which has a decreasing gradient of cartilage thickness in the transition (~40-60%), deep (~30%) and calcified cartilage zone (very low amount). Similarly, collagen II and water content gradient also decrease down the layers from the articular surface [169]. However, the concentration gradient of glycosaminoglycans, chondrocyte size and thickness increases from the top layer to the deep zone that finally attaches to the calcified zone. All the gradients present in the articular cartilage has been illustrated in the Figure 28. However fibrocartilage is the toughest tissue among all, that consists of widely dispersed dense masses of white collagen fibers. The bundles of dense collagen fibers are embedded along with condrocytes without perichondrium making it a perfect site for providing support and rigidity to the joints between intervertebral discs, pubic symphysis, junction where tendons insert into bone, etc. However, elastic cartilage is covered with a perichondrium and presence of abundant elastic fibers make it flexible. The chondrocytes are present between the network of elastic fibers providing it with high resilience. The strength of the cartilage lies in the amount of collagen, proteoglycan, and interstitial fluid present at the junction of cartilage connected structures which present a structural gradient. Moreover, the presence of chondrocytes in the cartilage impart a nutritional gradient [170].

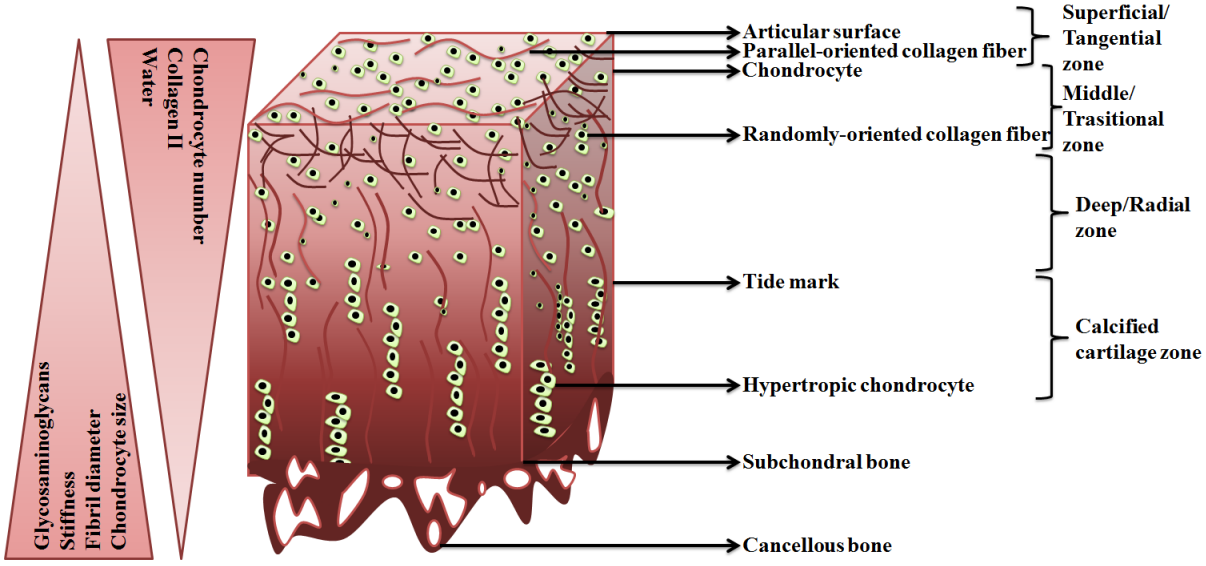

Figure 28: Structural and compositional gradient present in articular cartilage.

The injury associated with cartilage is very common, but it has poor self-regeneration ability due to its low cellularity and avascular properties. In recent years, a significant number of population have suffered from cartilage defects caused by ageing, trauma, repeated overloading, and various diseases leading to inflammation, stiffness, chronic pain, and disability. The complex physiological structure of cartilage creates significant hurdles for self-healing. Currently, two techniques have been used in the clinic such as autologous or allogeneic tissue to treat cartilage defects. However, these techniques are inadequate due to limited donors and poor therapeutic efficacy [171]. To design tissue-specific biomimetic synthetic gradient scaffolds, the fundamental knowledge of the structural composition and functional properties of cartilage must be known. Recently, due to the development of advanced 3D printing technology, patient-specific tissue regeneration for functional repair of cartilage can be a potential alternative approach. Due to the presence of multiple biological gradients and the depreciation of the biological role of the cartilage tissue with aging such as dehydrated matrix, subchondral sclerosis, etc., designing gradient scaffolds can be promising for cartilage tissue regeneration [167,172,173]. In this section, the designing of 3D bioprinted gradient anisotropic structured scaffolds for cartilage regeneration will be discussed in detail.

Sun et al., designed a dual-factor releasing gradient scaffolds incorporated with mesenchymal stem cell-laden hydrogels containing PLGA associated bone morphogenetic protein 4, transforming growth factor (TGFβ3), and PCL fibers for regeneration of cartilage tissue. The gradient scaffolds were 3D printed by keeping the laden hydrogel in-between the PCL fibers with a spacing of 150 μm for biochemical stimulus, and 750 μm for biomechanical stimulus. The electron microscopic results of these 3D printed gradient scaffolds had excellent alignment & interconnection between PCL and laden hydrogels when compared to those of non-gradient scaffolds (Figure 29 A).

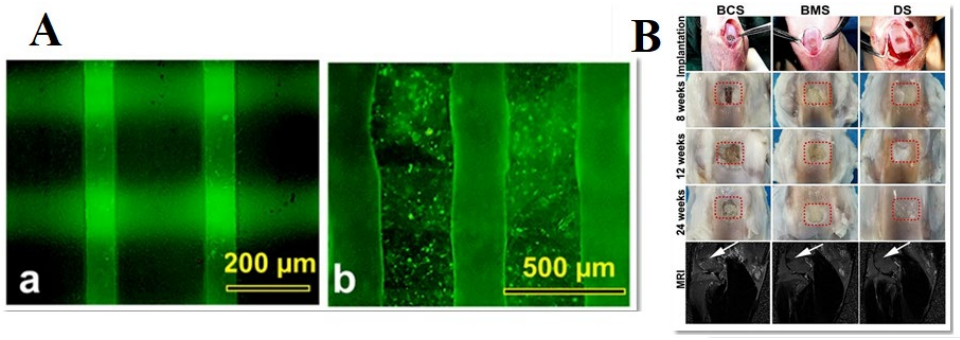

Figure 29: (A) Microscopic images of interconnection & alignment between the PCL fibers and laden hydrogels at different resolutions, (B) implantation, regeneration, and magnetic resonance imaging of the designed gradient scaffolds with biochemical stimulation (BCS), biomechanical stimulation (BMS), and double stimulus (DS) over 24 weeks of time. Adapted with permission from Ref. [174] © 2022 American Association for the Advancement of Science.

The authors also reported that gradient scaffolds exhibited a sequential, and time dependent release of the dual factors demonstrating a controlled release feature of the scaffold. The viability when studied over a time period of 21 days, showed a survival rate of >95% at the time of study maintained up to 75% till the end of the study, while the proliferation rate was observed to increase as a function of time. The authors further implanted the gradient scaffolds in an artificially created cartilage injury, and studied the regenerative efficacy (Figure 29 B). It was concluded that the gradient scaffolds with double stimulus showed enhanced regenerative efficacy than scaffolds with BCS, and BMS throughout 24 weeks. Moreover, all the gradient scaffolds exhibited better chondro-protective effect as compared to those of non-gradient scaffolds [174]. In a similar study, authors have designed a four layered gradient scaffolds using PCL fiber-laden hydrogel with different porosities, that exhibited enhanced biological efficacy (Figure 30 A & B). The designed gradient scaffolds demonstrated heterogeneous differentiation of chondrogenic cells, and enhanced the angiogenesis, and vascularization

within the tissue (Figure 30 C). The histochemical staining of the regenerated tissues implanted with gradient scaffolds demonstrated higher rate of tissue vascularization than those implanted with non-gradient scaffolds. The mechanism was attributed to the gradation observed in pore sizes within the gradient scaffolds, and induction of axis activation by hypoxia induced factor-1 alpha (HIF1α), and focal adhesion tyrosine kinase (FAK) genes.

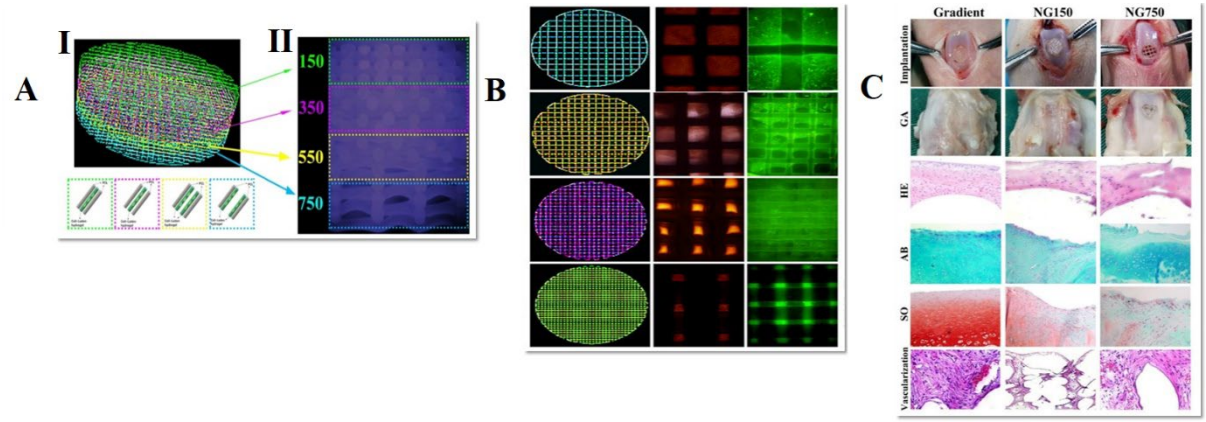

Figure 30: (A) Designed gradient scaffold: (I) 4-layered gradient scaffold (II) Layers with different porosities (150 µm, 350 µm, 550 µm & 750 µm), (B) PCL-laden hydrogel based gradient scaffolds with different porosities (a) 150 µm (in blue); (b) 350 µm (in yellow) (c) 550 µm (in purple) (d) 750 µm (in green), (C) Implantation, histochemical staining (H-E; alcian blue; Safranin O and vascularization of tissues by the designed gradient scaffolds. Adapted with permission from Ref. [175] © 2021 Elsevier Inc.

The immunofluorescent staining of regenerated cartilage tissue suggested that expression of HIF1 and FAK is relatively higher in gradient based scaffolds than those in non-gradient scaffolds. The authors also reported that the ECM in regenerated cartilage tissue resembled the native ones. This results demonstrates that the HIF1/FAK activation results in the enhancement of biocompatibility in gradient scaffolds [175]. In another recent study, a 3D-printed three-layer gradient GelMA-PEGDA scaffold has been developed with an RNTK coating (GelMA-PEGDA-RNTK) using an SL-based printer to mimic the hierarchical structure of cartilage

(Figure 31). The differentiation of adipose-derived mesenchymal stem cells seeded onto the gradient scaffold was enhanced due to the presence of RNTK, confirmed through histological analysis and a real-time quantitative polymerase chain reaction (RT-PCR) assay. The outcome of the study suggests the potential utility of nucleic acid incorporated gradient scaffolds have promising therapeutic efficacy for cartilage tissue engineering [176].

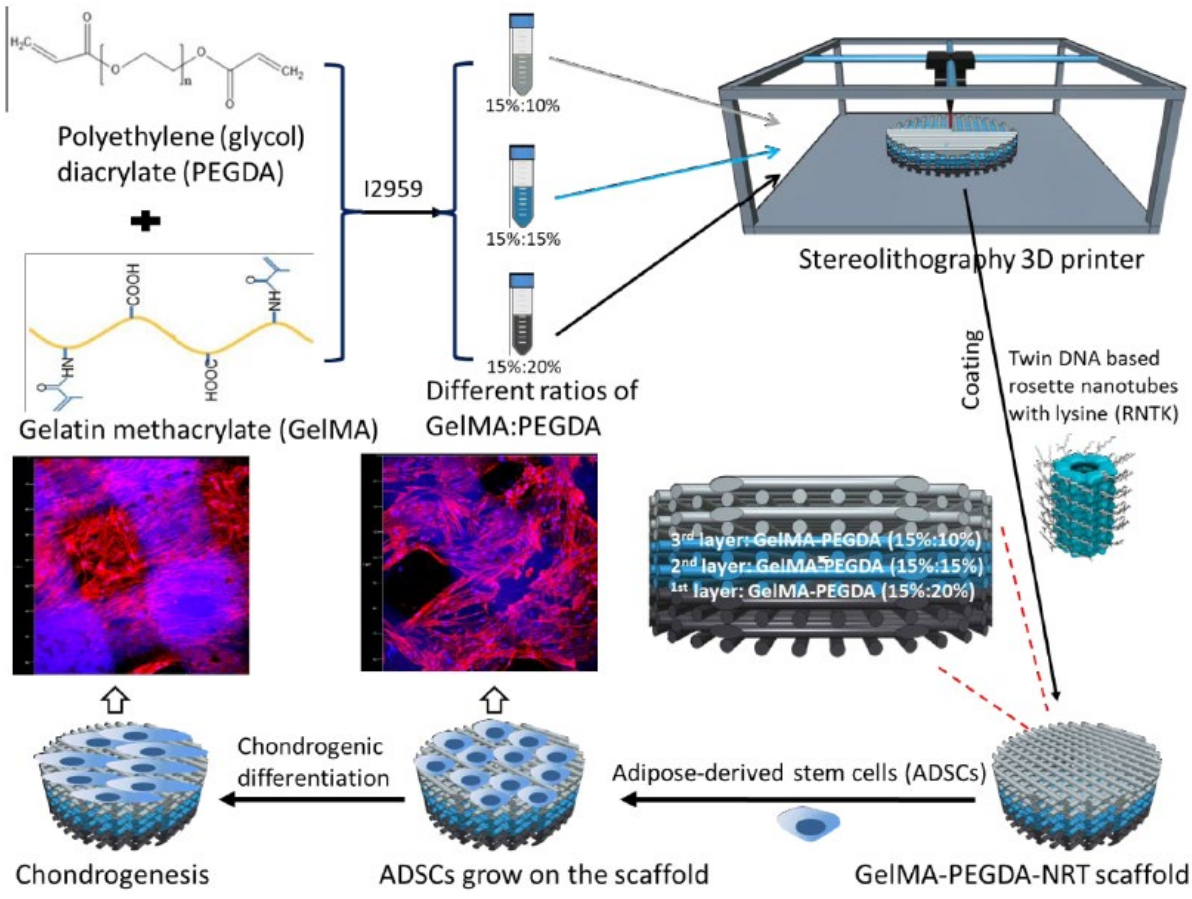

Figure 31: Schematic diagram of a 3D printed gradient scaffold for cartilage regeneration. Adapted with permission from Ref. [176] © American Chemical Society.

However, osteochondral defects face a major challenge to get entirely satisfactory results from the existing therapies. To address this, a complete hydrogel and nano-HA (nHA)/hydrogel mixture based system with different ratio were used to print a similar gradient structure as that of the top, intermediate and bottom cartilage layer (Figure 32). The researchers evaluated different parameters (physicochemical, mechanical, and biological) of the 3D printed scaffolds.

BMSCs were loaded onto the porous gradient scaffold which was further implanted into the mouse models with osteochondral defects. The results and regeneration efficiency of the 3D printed porous gradient scaffold were remarkable both in vitro and in vivo [177].

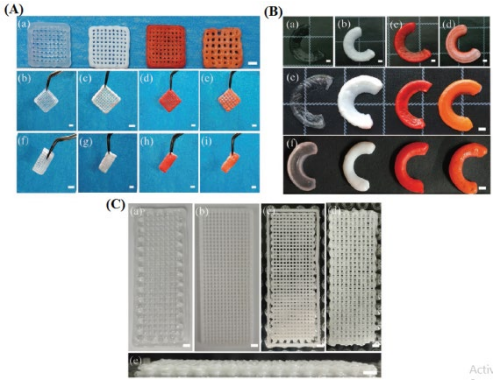

Figure 32: Photographs of various 3D printed scaffolds. A) From left to right in a) were "0% nHA", "40% nHA", "70% nHA" (dyed in red with rhodamine), and "G-nHA", respectively; b–e,f–i) the states of removal from the supporting and bending of the corresponding samples in (A). B) Macroscopic appearance of 3D printed artificial meniscus geometric models based on a) "0% nHA", b) "40% nHA", c) "70% nHA" (dyed in red with rhodamine), and d) "G-nHA" gel, respectively; d,f) before and after soaking CaCl2 solution (100 × 10−3 m). C) Digital images of 3D printed hydrogel scaffolds before immersing in CaCl2 solution for the tensile testing: top-view images of a) "0% nHA", b) "40% nHA", c) "70% nHA," and d) "G nHA" and e) side-view image of "G-nHA" scaffolds. (Scale bars = 5 mm). Adapted with permission from Ref. [177] © 2020 Wiley-VCH GmbH.

3.3. Gradient scaffolds for neural tissue regeneration

A neuron is a specialized cell present in several well developed organisms, and plays a major role in control, and coordination of the body [178–180]. It is divided into three parts including soma, dendrite, and an axon that has three major functionalities. Its sensory role responds to the external stimulus whereas the motor neurons are responsible for coordination in the organisms. The third role is to connect between two different neurons, and such neurons are

known as interconnecting neurons [180]. For proper functioning, multiple gradients are present in the neuron such as an electrochemical gradient helps in conduction of voltage across the neurons whereas, biochemical gradients control the passage of neurotransmitters, and a structural gradient in the myelin sheath. However, depreciation in neural function can happen due to severe trauma, aging, improper development etc. can lead to neurodegenerative disorder, neural tube defects, loss of coordination in individuals, and multiple sclerosis etc. [181,182]. The global rate of neural dysfunctions is quite high, ranging from thousands to millions, and in various age groups as well [183–186]. Moreover, the conventional approaches such as neural reconstruction, physiotherapy, medications etc. do not prove to be much effective, and absence of any other advanced systematic approach for treatment of affected individuals makes the situation worse. Under such circumstances, engineering of neural tissues using gradient based scaffolds emerge as potential strategy. The gradient scaffolds for neural tissues are therefore suitable to be integrated considering the structural, electrical, & biochemical gradients in the neurons [179].

Huang et al., designed scaffolds with orientational and biochemical gradient by using 3D printing combined with directional freezing technique. The scaffolds were fabricated by incorporating silk fibroin, collagen, and Nerve Growth Factor (NGF) thus creating a biochemical gradient. The scaffolds demonstrated the development of an orientation gradient of NGFs which enhanced the regeneration of neural tissues while promoting myelination as well (Figure 33 A & B). The sciatic functional index and the von Frey test was estimated, the results suggested promoting motor-sensory functions. Thus the study concluded that designing of gradient scaffolds by combining multiple cues could lead to regeneration of neural tissues at an accelerated rate, along with enhancing its functionality [187].

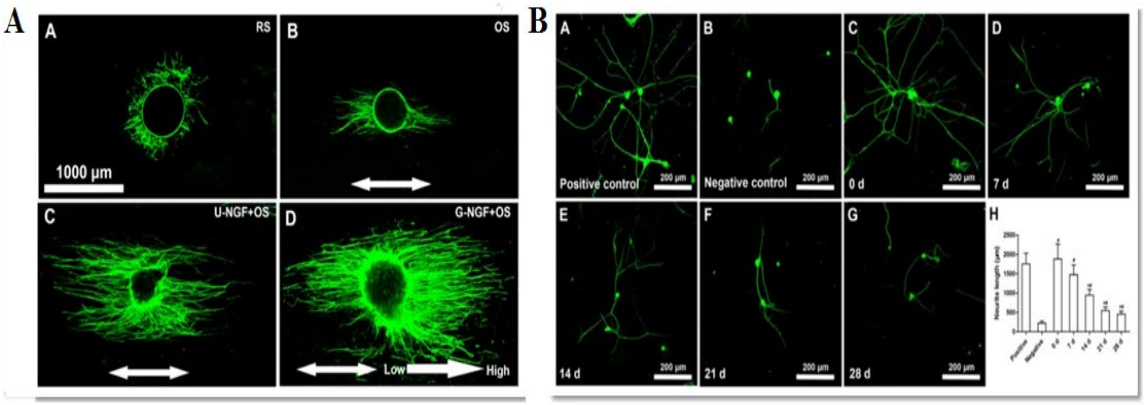

Figure 33: (A) Orientational gradients created by neural tissues along the longitudinal axis of the designed gradient scaffolds (A) random scaffold (B) orientational scaffold (C) uniform NGF based scaffold (D) gradient NGF based scaffold, (B) Release of nerve growth factors from the designed orientational gradient scaffolds (A) Positive control with 10 ng/ml of NGF (B) Negative control with 0 ng/ml of NGF (C) incubated for 0 day (D) incubated for 7 days (E) incubated for 14 days (F) incubated for 21 days (G) incubated for 28 days (H) Release profile of NGF from the gradient scaffold. Adapted with permission from Ref. [187] © 2020 American Chemical Society.

The repair of injured spinal cord needs aligned structural support, and biological gradients from the periphery to the center and endogenous neural stem cells (NSCs) from the central canal region to the abrasion site to re-establish neural interconnectivity. In a study Jianwu Dai et al., developed a simple and versatile method to design continuous protein gradient of stromal-cell-derived factor-1α (SDF1α) encapsulated in the radially aligned electrospun collagen/PCL fiber mats. In electrospinning method (Figure 34 A), controllable and reproducible biological gradient fiber mats can be achieved with the adjustment of collector size and collection time. A continuous gradient of SDF1α was formed along the aligned fibers by incorporation of collagen-binding domain (CBD) fused SDF1α (CBD-SDF1α), with reduction of fiber concentration gradually from the center to the periphery. The aligned CBD-SDF1α gradients

show steady, persistent, and gradual release during 7 days on the collagen/PCL fibers (Figure 34 B). Furthermore, the aligned CBD-SDF1α gradients effect on the NSCs was evaluated and the results demonstrated that the cells were elongated along with the aligned electrospun fibers and their periphery to the center migration of the scaffold, which was enhanced along with the CBD-SDF1α gradients (Figure 34 C). The outcome of this study demonstrated that structural architecture of gradient scaffolds with aligned topography offers NSC migration and better guidance of nerve regeneration. The CBD-SDF1α distribution and release on the newly designed gradient scaffolds were investigated by using three equally divided segments (Segment I, II, III) of electrospun mats from the central to peripheral region. The CBD-SDF1α binding was higher than that of native-SDF1α in all segment apart from the center shown in Figure 34 BII, which is similar with the Figure 34 BI. However, CBD-SDF1α binding decreases at the sequential segments along the x -axis, which demonstrated that SDF1α gradient was successfully generated along the radially aligned fibrous scaffold. The cumulative SDF1α sustained and stable release was achieved from all the segments of CBD-SDF1α containing radially aligned scaffolds in 7 days, which decreased in sequential manner from segments excluding the center (34 BIII) [188].

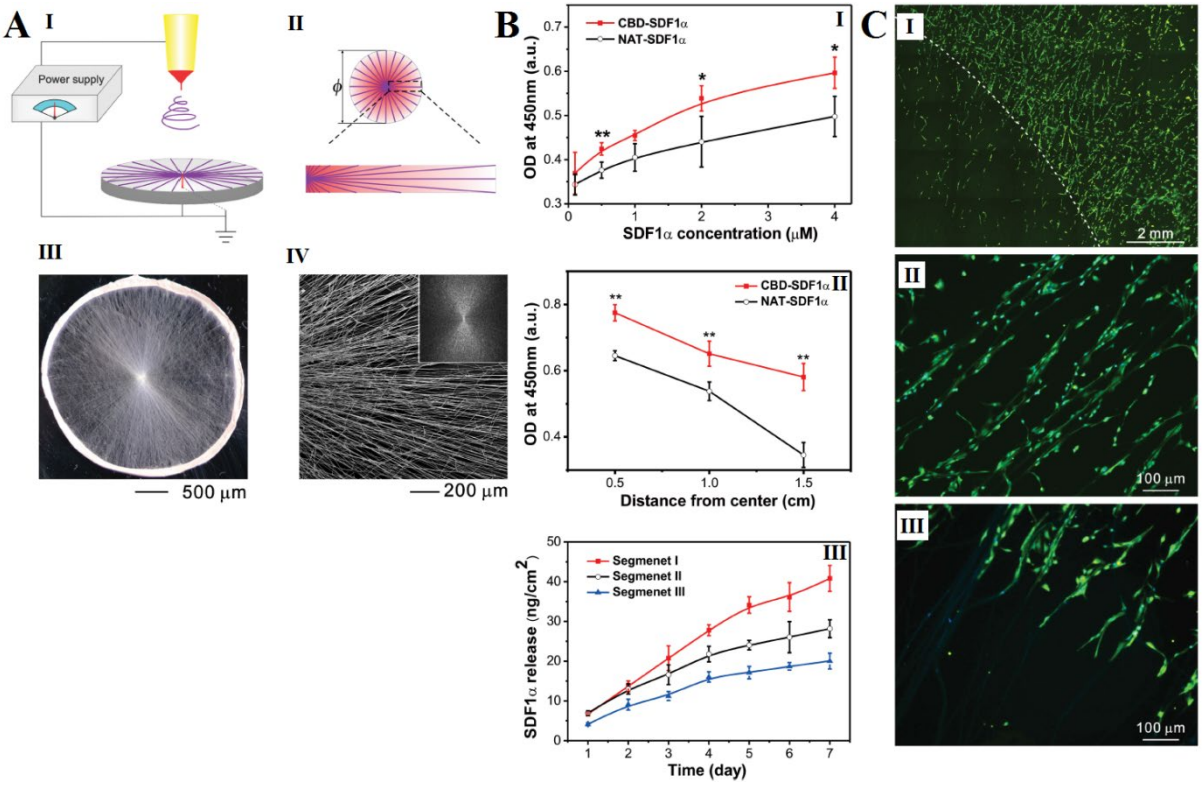

Figure 34: (A) Fabrication of continuous protein gradients embedded in the radially aligned electrospun mats (I) Schematic showing the fabrication of radially aligned fibers (II) Schematic illustration of protein gradients from the center to the periphery (III) Photograph of the collagen/PCL scaffold composed of radially aligned fibers (IV) SEM image showing the morphology and radial alignment. The inset shows the Fourier fast transfer pattern; (B) Binding and release properties of CBD-SDF1α (I) Binding curves of native-SDF1α and CBD-SDF1α to aligned electrospun collagen/ PCL mats (II) The binding of native-SDF1α and CBD-SDF1α to the sequential segments of the radially aligned scaffolds from the center to the periphery (III) Cumulative release of SDF1α from the sequential segments on radially aligned CBD-SDF1α scaffolds from the center to the periphery within 7 days; (C) (I) Fluorescence image showing the migration of NSCs on the radially aligned fibers immobilized with CBD-SDF1α after 1 day of culture (II) Higher magnification view of the cells in the source zone (III) Higher magnification view of the cells in the leading zone. The dashed line indicates the border of

NSC seeding. Adapted with permission from Ref. [188] © 2016 Wiley-VCH Verlag GmbH & Co. KGaA, Weinheim.

In a similar study, authors have expanded the use of electrospun fibrous mats by altering the electrical and topographical signals to design piezoelectric scaffolds for neuronal tissue regeneration. The developed scaffolds had radially aligned fibrous patterns with topological gradient structures that enabled stress fibre formation in neural cells for Yes Associated Protein (YAP) activation of nuclear localization. The developed fibrous gradient scaffolds with completely different topological and crystal features could be used to access the neuronal differentiation and predict neural cell response. Further studies with various chemical cues and in vivo studies can expand the application of 3D electrospun piezoelectric gradient scaffolds for neuronal tissue engineering [189].

3.4. Gradient scaffolds for cardiovascular regeneration

The cardiovascular system which is comprised of heart (the blood pumping organ), three blood carrying organs namely arteries, veins and capillaries and the most importantly the blood itself. The cardiac tissue comprises of chambers, valves, and the cardiac tissue wall is composed of the endocardium, myocardium, and the epicardium which makes up the pericardium [190]. There are different structural, functional, transmural and electrochemical gradients that play major roles in the normal functioning of the cardiovascular tissues [191,192]. Those gradients are central-to-peripheral arterial stiffness gradient, pressure gradients across the wall, and gradients of cell types, nutrients, growth factors and most importantly oxygen gradients [141]. This helps in controlling the functions of heart at different hierarchical levels [193]. Several reports on cardio vascular disease (angina, and stroke) suggest that annual morbidity and mortality rate is quite high thus is a major reason for global death rate [194–197]. According

to World Health Organization (WHO), the global death rate reached up to ~18 million accounting for 32 % of the total death [198]. The regeneration capacity of heart tissues is limited in case of any injury or disease and hence gradient scaffold can be a better therapeutic option for heart tissue regeneration [199]. The gradient in the heart can therefore be explored to design scaffolds which can promote accelerated cellular proliferation, migration, and faster regeneration of the cardiovascular tissues. The goal of cardiovascular tissue engineering mainly focuses on the generation of cardiac gradients with retention of same architecture, structure, and physiological functions of native tissues [200]. Now-a-days, cardiovascular tissues can be regenerated from human induced pluripotent stem cells (hiPSCs) that are functionally and morphologically similar to human embryonic stem cells. Dattola et al., constructed 3D PVA porous gradient scaffolds to support the proliferation and differentiation of hiPSCs into cardiomycetes. Figure 35 a shows the physical morphology of the porous scaffold with an irregular pore structure having an average diameter of 82±60 µm. The histogram shows the size distribution in which ~ 90% of the pores diameters fall below 200 µm (Figure 35 b). Surprisingly, cross-sections of the gradient scaffolds showed densely populated cardiomyocytes in the edges when compared to the inner parts. In addition, due to chemotaxis, a gradient of nutrients was generated owing to higher growth of hiPSCs cell in the edges of the scaffold [201].

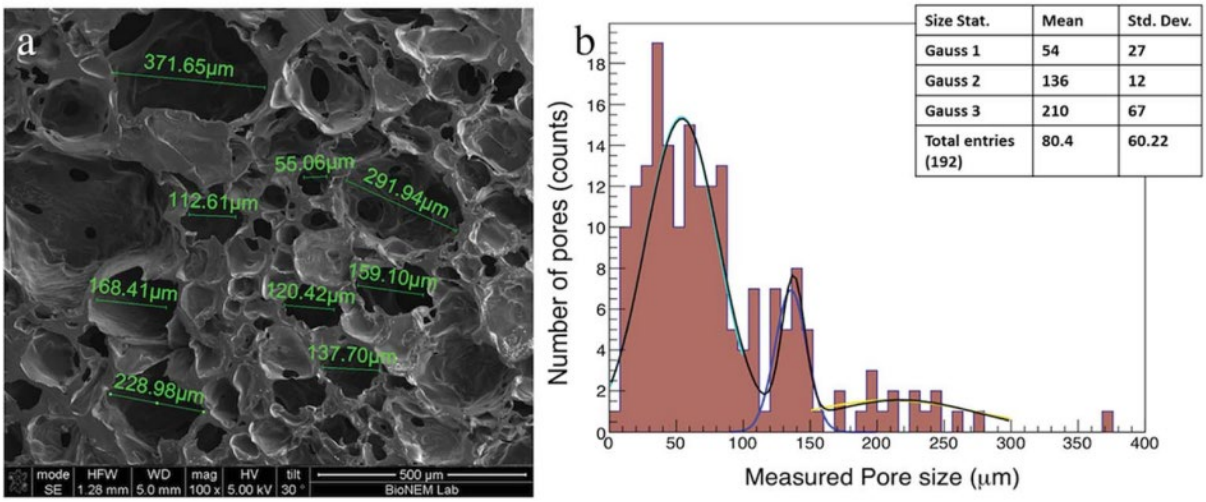

Figure 35: (a) The morphological characteristics of cross-sections of PVA scaffolds examined with a SEM (magnifications 100X, scale bar 500 mm), (b) Histograms of pore diameter distribution of the PVA scaffolds. The PVA scaffolds show an average pore size of 82±60 μm. Adapted with permission from Ref. [201] © The Royal Society of Chemistry 2019.

Odedra et al., designed collagen-based porous gradient scaffolds, and immobilized growth factors (VEGF-165). The scaffolds were constructed by activitating 1-ethyl-3-(3-Dimethylaminopropyl) carbodiimide /sulfo N-hydroxysuccinimide and seeded into the scaffold by perfusion, source-sink, or directly delivering to the center of the scaffold. The authors observed that a VEGF-165 gradient was radially formed, and guided the endothelial cells for migration to the center. It was further observed that the scaffolds contained higher density of cells at the center and gradually decreased to the outer side (Figure 36) however; substantial proliferation was not observed. The migration rate of the endothelial cells was further observed to be substantial even at low concentrations thus demonstrating the high efficacy of the designed gradient scaffolds [141].

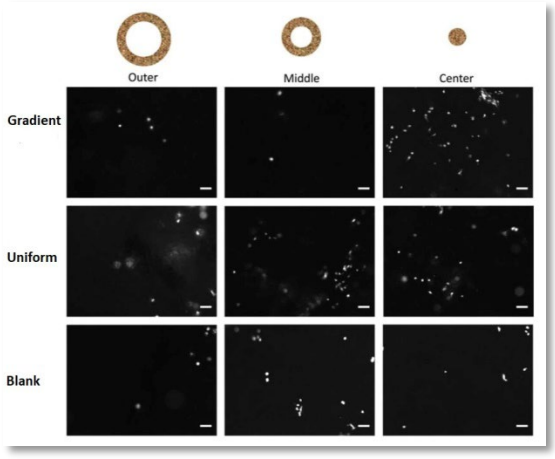

Figure 36: Scaffolds with VEGF gradients lead to a more centralized cell distribution. The scaffolds prepared by the point source method were seeded with 5000 cells and cultured for 3 days. At the end of the culture period the scaffolds were stained with a live cell marker, CFDA.

Serial images were acquired on the two axes of the circular scaffold. Adapted with permission from Ref. [141] 2011 Acta Materialia Inc. Published by Elsevier Ltd.

3.5. Gradient scaffolds for skin tissue regeneration

The human skin is one of the important tissues comprising several dermal layers (Figure 37). It also serves as a primary defense barrier to invading opportunistic microorganisms [8,202,203]. The presence of compositional and structural gradient like epithelial tissues (squamous, columnar, and cuboidal) modulates the tissue stiffness, porosity, topology, nutrition, and respiration within the tissue. Moreover, the biochemical gradients promote the moist environment, and presence of cells for skin tissue & immune system present a cellular gradient [8,9,103,202,204,205]. In addition, damage to the skin by infectious agents or injury to the skin at multiple layers may lead to chronic wounds. The regeneration of such multilayered tissue using gradient based scaffolds may help to prevent further aggravation of the injury, and lead to tissue rejuvenation by maintaining a moist environment, and providing a high surface to volume ratio, thus leading to enhanced reconstruction of epithelial cells [206–208]. However, the varying differences in the physical (layer's stiffness, architecture, and composition), biochemical (signaling biomolecules), and Ca^{2+} ion concentration gradients of the skin tissue should be carefully considered while choosing a suitable biomaterial and/or designing techniques for gradient scaffolds fabrication.

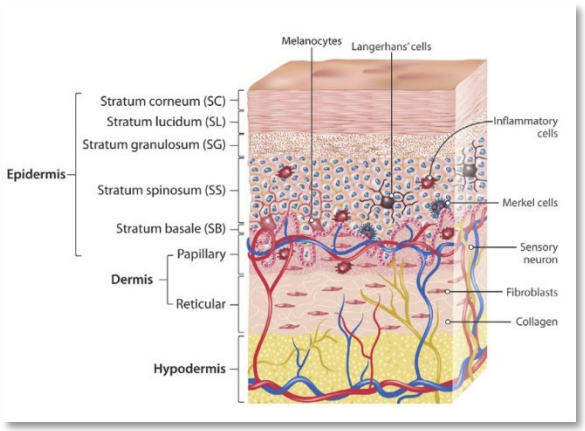

Figure 37: Structural organization with sub layers of epidermis having a physical gradient of collagen from top to bottom layers (different concentrations and orientations of collagen fibers); and gradients of thin, loose, and thick, dense irregular connective tissue layers in skin tissue. Adapted with permission from Ref. [8] © 2019 The Author(s). Published by Elsevier Ltd.

Wang et al., constructed a three-layered artificial dermis by designing porous gradient scaffolds which was packed with fibroblasts as the seeding material (Figure 38). The designed scaffolds had a varying collagen concentration from 0.13 to 0.26 % with a pore size ranging from 87.7 µm-166.9 µm. The scaffold seeded with fibroblasts promoted granulation of the tissue, and accelerated re-epithelialization of the wound. The authors concluded that designed "Sandwich" scaffold mimicked the natural human dermis with greater pores on the outer side whereas the middle part showed smaller pores thus making it a suitable biomimetic for skin tissue regeneration [209].

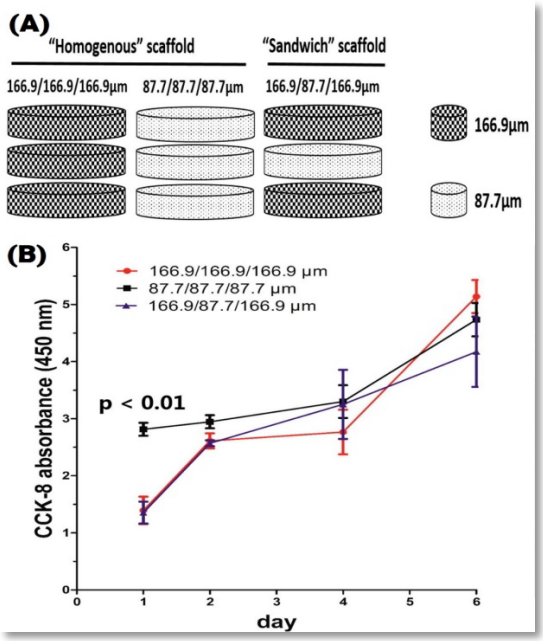

Figure 38: Three-layered porous scaffold designed with high porosity (A) Homogenous architecture and sandwich architecture of the scaffolds (B) Cell proliferation over time. Adapted with permission from Ref. [209] 2015 Acta Materialia Inc. Published by Elsevier Ltd.

In another study, Zhang et al., fabricated eight models of alginate based scaffolds with a stage cooling method, resulting in gradient of pore architecture by modulating the temperature, and incubation time. The pore size of scaffolds varied gradually from 100.0 to 137.0 μm at the top whereas 20.0 to 130.0 μm at the base (Figure 39 Model A-H). Two of the scaffold models A and D were found to have pore sizes ranging between 25-120 μm which closely resembles the pore size of the human skin whereas the other six models had invariant pore size, and might not be helpful for controlled release of seeding materials. They observed that varying the initial temperatures and duration affected the pore size whereas the pore shape could be modulated by changing temperature steps. The author further suggested that the modulation of temperature between -60° C to -75° C, could lead to gain control over the pore sizes, shapes, and gradients in the scaffold. The modulation of both temperature, and incubation time also played a major role in controlling the wall thickness of the scaffolds suggesting the beneficial role of such gradient scaffolds for skin regeneration [210].

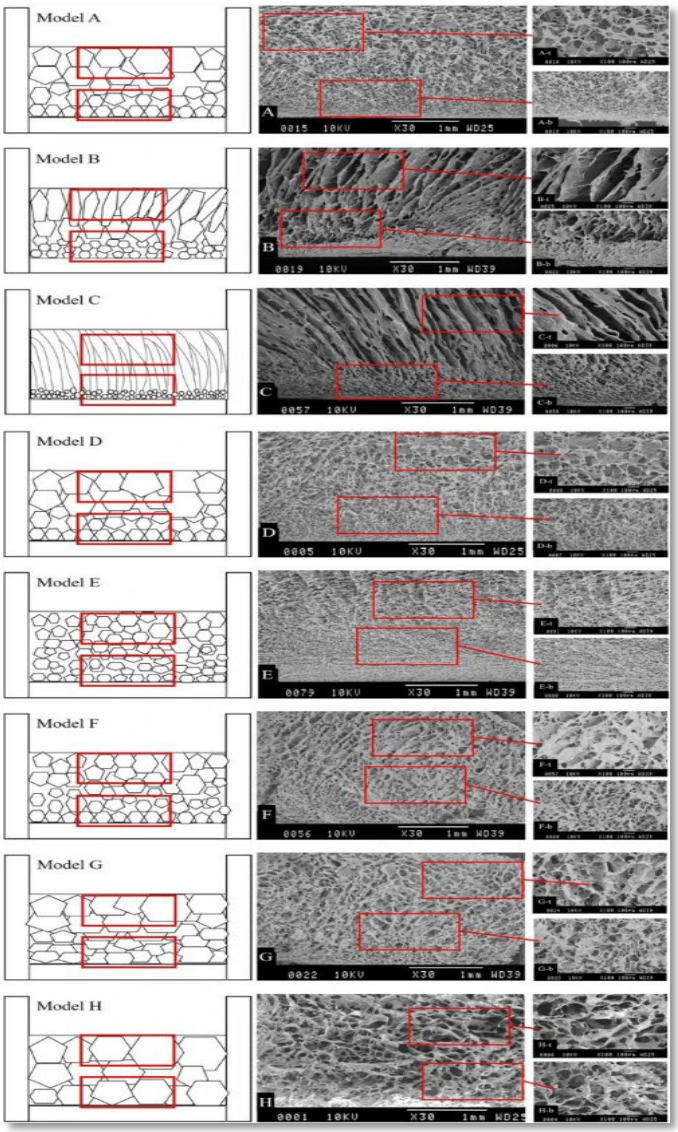

Figure 39: Influence of stage cooling method on pore architecture of biomimetic models of alginate scaffolds (A-H). Adapted with permission from Ref. [210] © 2017, The Author(s).

Skin regeneration in case of wounds demand treatments having the capacity of withstanding high bursting force and quick recruitment of MSCs. These properties are provided by various patches that are available in the market. Recently, a programmable nanofibrous patches having radial gradient, inspired from royal water lily-like radially branched architecture has been developed by Jingtao Du team [28]. The patch was integrated with center-to-periphery gradient migration of SDF1α (Figure 40). The patches were coated with gelatin methacryloyl were used

for studies to recover the skin when applied on the incision done in the mouse. These patches were successful in providing a suitable microenvironment for decreased inflammation and subsequently increased MSC recruitment. Above mentioned properties along with robust bursting bearing capability and fast deployment property of the patches lead to the accelerated wound healing in the mouse model within 12 days when compared to gauze and Tegaderm^{TM} film.

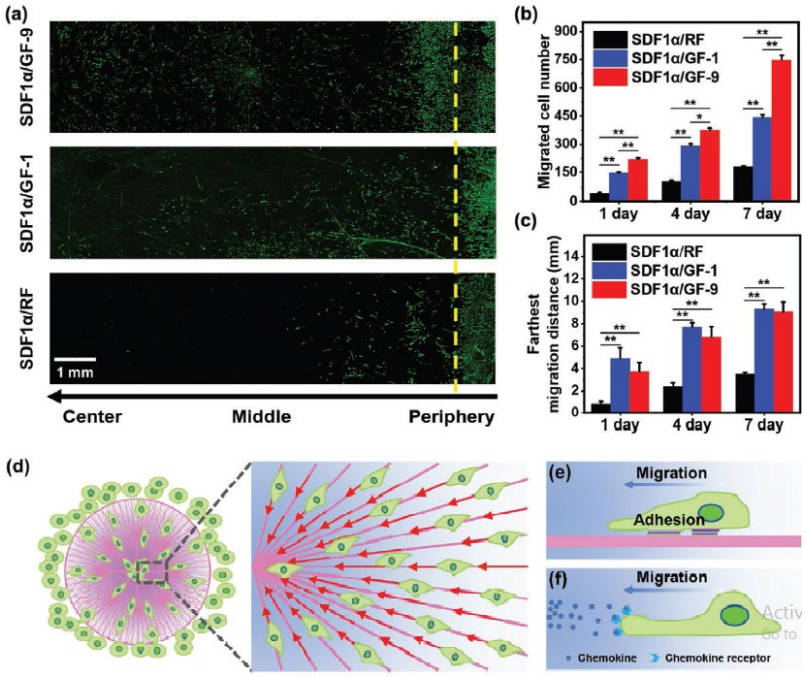

Figure 40: GF patches with "center-to-periphery" SDF1α gradient directed MSC migration to the center region. a) MSC distribution on SDF1α immobilized RF, GF-1, and GF-9 patches after 7 d of culture. The dashed line indicates the border between MSC seeding domain and migration domain. Quantification of b) migrated cell number and c) maximum migration distance. d) Schematic illustrating that e) the aligned nanofiber topography and f) gradient chemokine cues induced MSC migration from the periphery to the central region synergistically. Data are presented as mean ± SD.* $P < 0.05$, ** $P < 0.01$. Adapted with permission from Ref. [28] © 2021 Wiley-VCH GmbH.

4. Conclusion and future prospective:

Gradient scaffolds have been considered as a potential and promising biomaterial for therapeutic applications as compared to conventional scaffolds. Recapitulating the natural gradients present in human cells and tissues are integrated into the scaffolds by the use of advanced fabrication techniques of additive manufacturing, component redistribution, controlled phase changes, and post modification. These techniques show promising outcome by allowing the design of gradient/multi gradient scaffolds with controlled geometrical features, for enhancing the biocompatibility, mechanical strength, bio toxicity, biodegradability, and successfully integrated into the biological system in vivo (bone, cartilage, neural, cardiovascular, and skin tissues). In addition, multi gradient scaffolds using natural/synthetic polymers have emerged as a great alternative for designing of biomimetic tissues to be used in clinics for tissue regeneration applications.

In this review it was observed that there are several reports that show the efficiency of the advanced designing techniques for fabrication of gradient scaffolds for tissue regeneration, yet detailed understanding of natural gradients in the biological system is unclear. However, the existing techniques to design gradient scaffolds are less effective, hence appropriate use of high-throughput techniques for designing, and optimizing gradient scaffolds is highly desirable. Furthermore, the utilization of combinatorial designing methods will enable to fabricate new gradient scaffolds by non-invasive approach with better penetration into the cellular micro environment. Future significant progress in the field of designing gradient/ multi gradient scaffolds for tissue regeneration will focus on improvisation of available fabrication techniques to incorporate the specific designed gradient scaffolds for more complex biological systems.

5. Acknowledgments

Ms. Ananya Patnaik acknowledges the Indian Council for Medical Research for awarding the fellowship of ICMR-SRF (Letter No. 45/01/2022-Nano/BMS). Mr. A.Swaroop Sanket is thankful to Indian Council for Medical Research for awarding the fellowship ICMR-SRF (File No. 5/3/8/88/ITR-F/2020). Ms. Swarnaprabha Pany expresses thanks to CSIR-SRF [09/547(0005)/2018-EMR-I]. Dr. Sangram Keshari Samal highly acknowledges the Ramanujan fellowship (SB/S2/RJN-038/2016) of the Department of Science and Technology, and Ramalingaswami Re-entry fellowship (Ref: D.O. No. BT/HRD/35/02/ 2006) of Department of Biotechnology, Government of India. The authors also thank the Indian Council of Medical Research-Regional Medical Research Centre, Bhubaneswar for providing a scientific platform.

6. Conflict of Interest

The authors have declared no conflict of interest.

7. References:

[1] J.M. Lowen, J.K. Leach, Functionally Graded Biomaterials for Use as Model Systems and Replacement Tissues, Adv. Funct. Mater. 30 (2020) 1909089. https://doi.org/10.1002/adfm.201909089.

[2] M. Wang, W. Li, L.S. Mille, T. Ching, Z. Luo, G. Tang, C.E. Garciamendez, A. Lesha, M. Hashimoto, Y.S. Zhang, Digital Light Processing Based Bioprinting with Composable Gradients, Adv. Mater. 34 (2022) 2107038. https://doi.org/10.1002/adma.202107038.

[3] C.P. Grey, S.T. Newton, G.L. Bowlin, T.W. Haas, D.G. Simpson, Gradient fiber electrospinning of layered scaffolds using controlled transitions in fiber diameter, Biomaterials. 34 (2013) 4993–5006. https://doi.org/10.1016/j.biomaterials.2013.03.033.

[4] S. Chen, A. McCarthy, J. V. John, Y. Su, J. Xie, Converting 2D Nanofiber Membranes to 3D Hierarchical Assemblies with Structural and Compositional Gradients Regulates Cell Behavior, Adv. Mater. 32 (2020) 2003754. https://doi.org/10.1002/adma.202003754.

[5] Y. Li, Y. Xiao, C. Liu, The Horizon of Materiobiology: A Perspective on Material-Guided Cell Behaviors and Tissue Engineering, Chem. Rev. 117 (2017) 4376–4421.

https://doi.org/10.1021/acs.chemrev.6b00654.

[6] Z. Liu, M.A. Meyers, Z. Zhang, R.O. Ritchie, Functional gradients and heterogeneities in biological materials: Design principles, functions, and bioinspired applications, Prog. Mater. Sci. 88 (2017) 467–498. https://doi.org/10.1016/j.pmatsci.2017.04.013.

[7] C.F. Guimarães, L. Gasperini, A.P. Marques, R.L. Reis, The stiffness of living tissues and its implications for tissue engineering, Nat. Rev. Mater. 5 (2020) 351–370. https://doi.org/10.1038/s41578-019-0169-1.

[8] M. Rahmati, J.J. Blaker, S.P. Lyngstadaas, J.F. Mano, H.J. Haugen, Designing multigradient biomaterials for skin regeneration, Mater. Today Adv. 5 (2020) 100051. https://doi.org/10.1016/j.mtadv.2019.100051.

[9] M.P. Nikolova, M.S. Chavali, Recent advances in biomaterials for 3D scaffolds: A review, Bioact. Mater. 4 (2019) 271–292. https://doi.org/10.1016/j.bioactmat.2019.10.005.

[10] C. Zhu, J. Qiu, S. Pongkitwitoon, S. Thomopoulos, Y. Xia, Inverse Opal Scaffolds with Gradations in Mineral Content for Spatial Control of Osteogenesis, Adv. Mater. 30 (2018) 1706706. https://doi.org/10.1002/adma.201706706.

[11] M.T.I. Mredha, I. Jeon, Biomimetic anisotropic hydrogels: Advanced fabrication strategies, extraordinary functionalities, and broad applications, Prog. Mater. Sci. 124 (2022) 100870. https://doi.org/10.1016/j.pmatsci.2021.100870.

[12] X. Li, J. Xie, J. Lipner, X. Yuan, S. Thomopoulos, Y. Xia, Nanofiber Scaffolds with Gradations in Mineral Content for Mimicking the Tendon-to-Bone Insertion Site, Nano Lett. 9 (2009) 2763–2768. https://doi.org/10.1021/nl901582f.

[13] L.C. Palmer, C.J. Newcomb, S.R. Kaltz, E.D. Spoerke, S.I. Stupp, Biomimetic Systems for Hydroxyapatite Mineralization Inspired By Bone and Enamel, Chem. Rev. 108 (2008) 4754–4783. https://doi.org/10.1021/cr8004422.

[14] S. Wu, X. Liu, K.W.K. Yeung, C. Liu, X. Yang, Biomimetic porous scaffolds for bone tissue engineering, Mater. Sci. Eng. R Reports. 80 (2014) 1–36. https://doi.org/10.1016/j.mser.2014.04.001.

[15] J.W. Vogel, R. La Joie, M.J. Grothe, A. Diaz-Papkovich, A. Doyle, E. Vachon-Presseau, C. Lepage, R. Vos de Wael, R.A. Thomas, Y. Iturria-Medina, B. Bernhardt, G.D. Rabinovici, A.C. Evans, A molecular gradient along the longitudinal axis of the human hippocampus informs large-scale behavioral systems, Nat. Commun. 11 (2020) 960. https://doi.org/10.1038/s41467-020-14518-3.

[16] J.B. Gurdon, P.-Y. Bourillot, Morphogen gradient interpretation, Nature. 413 (2001) 797–803. https://doi.org/10.1038/35101500.

[17] G.L. Koons, M. Diba, A.G. Mikos, Materials design for bone-tissue engineering, Nat. Rev. Mater. 5 (2020) 584–603. https://doi.org/10.1038/s41578-020-0204-2.

[18] M.H. Bolin, K. Svennersten, D. Nilsson, A. Sawatdee, E.W.H. Jager, A. Richter-Dahlfors, M. Berggren, Active Control of Epithelial Cell-Density Gradients Grown Along the Channel of an Organic Electrochemical Transistor, Adv. Mater. 21 (2009) 4379–4382. https://doi.org/10.1002/adma.200901191.

[19] A. Pattnaik, S. Pati, S.K. Samal, Chitosan-Polyphenol Conjugates for Human Health, Life. 12 (2022) 1768. https://doi.org/10.3390/life12111768.

[20] J. V. Karpiak, Y. Ner, A. Almutairi, Density Gradient Multilayer Polymerization for Creating Complex Tissue, Adv. Mater. 24 (2012) 1466–1470. https://doi.org/10.1002/adma.201103501.

[21] K. Chatterjee, L. Sun, L.C. Chow, M.F. Young, C.G. Simon, Combinatorial screening of osteoblast response to 3D calcium phosphate/poly(ε-caprolactone) scaffolds using gradients and arrays, Biomaterials. 32 (2011) 1361–1369. https://doi.org/10.1016/j.biomaterials.2010.10.043.

[22] P. Deb, A.B. Deoghare, A. Borah, E. Barua, S. Das Lala, Scaffold Development Using Biomaterials: A Review, Mater. Today Proc. 5 (2018) 12909–12919. https://doi.org/10.1016/j.matpr.2018.02.276.

[23] Z. Wang, W.J. Lee, B.T.H. Koh, M. Hong, W. Wang, P.N. Lim, J. Feng, L.S. Park, M. Kim, E.S. Thian, Functional regeneration of tendons using scaffolds with physical anisotropy engineered via microarchitectural manipulation, Sci. Adv. 4 (2018). https://doi.org/10.1126/sciadv.aat4537.

[24] L.W. Chow, A. Armgarth, J.-P. St-Pierre, S. Bertazzo, C. Gentilini, C. Aurisicchio, S.D. McCullen, J.A.M. Steele, M.M. Stevens, Biomimetic Materials: Peptide-Directed Spatial Organization of Biomolecules in Dynamic Gradient Scaffolds (Adv. Healthcare Mater. 9/2014), Adv. Healthc. Mater. 3 (2014) 1350–1350. https://doi.org/10.1002/adhm.201470044.

[25] C. Li, L. Ouyang, J.P.K. Armstrong, M.M. Stevens, Advances in the Fabrication of Biomaterials for Gradient Tissue Engineering, Trends Biotechnol. 39 (2021) 150–164. https://doi.org/10.1016/j.tibtech.2020.06.005.

[26] B. Zhang, J. Huang, R.J. Narayan, Gradient scaffolds for osteochondral tissue engineering and regeneration, J. Mater. Chem. B. 8 (2020) 8149–8170. https://doi.org/10.1039/D0TB00688B.

[27] T. Novak, B. Seelbinder, C.M. Twitchell, C.C. van Donkelaar, S.L. Voytik-Harbin, C.P. Neu, Mechanisms and Microenvironment Investigation of Cellularized High Density Gradient Collagen Matrices via Densification, Adv. Funct. Mater. 26 (2016) 2617–2628. https://doi.org/10.1002/adfm.201503971.

[28] J. Du, Y. Yao, M. Wang, R. Su, X. Li, J. Yu, B. Ding, Programmable Building of Radially Gradient Nanofibrous Patches Enables Deployment, Bursting Bearing Capability, and Stem Cell Recruitment, Adv. Funct. Mater. 32 (2022) 2109833. https://doi.org/10.1002/adfm.202109833.

[29] F.N. Alaribe, S.L. Manoto, S.C.K.M. Motaung, Scaffolds from biomaterials: advantages and limitations in bone and tissue engineering, Biologia (Bratisl). 71 (2016) 353–366. https://doi.org/10.1515/biolog-2016-0056.

[30] C.G. Simon, S. Lin-Gibson, Combinatorial and High-Throughput Screening of Biomaterials, Adv. Mater. 23 (2011) 369–387. https://doi.org/10.1002/adma.201001763.

[31] S.J. Hollister, Scaffold Design and Manufacturing: From Concept to Clinic, Adv. Mater. 21 (2009) 3330–3342. https://doi.org/10.1002/adma.200802977.

[32] M. Mohseni, O. Bas, N.J. Castro, B. Schmutz, D.W. Hutmacher, Additive biomanufacturing of scaffolds for breast reconstruction, Addit. Manuf. 30 (2019) 100845. https://doi.org/10.1016/j.addma.2019.100845.

[33] J.R. Clegg, A.M. Wagner, S.R. Shin, S. Hassan, A. Khademhosseini, N.A. Peppas, Modular fabrication of intelligent material-tissue interfaces for bioinspired and biomimetic devices, Prog. Mater. Sci. 106 (2019) 100589. https://doi.org/10.1016/j.pmatsci.2019.100589.

[34] A. du Plessis, S.M.J. Razavi, M. Benedetti, S. Murchio, M. Leary, M. Watson, D. Bhate, F. Berto, Properties and applications of additively manufactured metallic cellular materials: A review, Prog. Mater. Sci. 125 (2022) 100918. https://doi.org/10.1016/j.pmatsci.2021.100918.

[35] Y. Lakhdar, C. Tuck, J. Binner, A. Terry, R. Goodridge, Additive manufacturing of advanced ceramic materials, Prog. Mater. Sci. 116 (2021) 100736. https://doi.org/10.1016/j.pmatsci.2020.100736.

[36] L.E. Freed, G.C. Engelmayr, J.T. Borenstein, F.T. Moutos, F. Guilak, Advanced Material Strategies for Tissue Engineering Scaffolds, Adv. Mater. 21 (2009) 3410–3418. https://doi.org/10.1002/adma.200900303.

[37] E. MacDonald, R. Wicker, Multiprocess 3D printing for increasing component functionality, Science (80-.). 353 (2016). https://doi.org/10.1126/science.aaf2093.

[38] P. Szymczyk-Ziółkowska, M.B. Łabowska, J. Detyna, I. Michalak, P. Gruber, A review of fabrication polymer scaffolds for biomedical applications using additive manufacturing techniques, Biocybern. Biomed. Eng. 40 (2020) 624–638. https://doi.org/10.1016/j.bbe.2020.01.015.

[39] No Title, (n.d.). https://www.grandviewresearch.com/industry-analysis/healthcare-additive-manufacturing-market.

[40] F. Gao, Z. Xu, Q. Liang, B. Liu, H. Li, Y. Wu, Y. Zhang, Z. Lin, M. Wu, C. Ruan, W. Liu, Direct 3D Printing of High Strength Biohybrid Gradient Hydrogel Scaffolds for Efficient Repair of Osteochondral Defect, Adv. Funct. Mater. 28 (2018) 1706644. https://doi.org/10.1002/adfm.201706644.

[41] S. Singh, S. Mehla, S.K. Bhargava, S. Ramakrishna, History and Evolution of Additive Manufacturing, in: Addit. Manuf. Chem. Sci. Eng., Springer Nature Singapore, Singapore, 2022: pp. 19–51. https://doi.org/10.1007/978-981-19-2293-0_2.

[42] B.P. Chan, Biomedical Applications of Photochemistry, Tissue Eng. Part B Rev. 16 (2010) 509–522. https://doi.org/10.1089/ten.teb.2009.0797.

[43] S. Upadhyay, A Photochemical Reaction and Applications in Organic Synthesis, Insights Chem. Biochem. 1 (2021). https://doi.org/10.33552/ICBC.2021.01.000520.

[44] A.A. Pawar, G. Saada, I. Cooperstein, L. Larush, J.A. Jackman, S.R. Tabaei, N.-J. Cho, S. Magdassi, High-performance 3D printing of hydrogels by water-dispersible photoinitiator nanoparticles, Sci. Adv. 2 (2016).

https://doi.org/10.1126/sciadv.1501381.

[45] K.L. Sampson, B. Deore, A. Go, M.A. Nayak, A. Orth, M. Gallerneault, P.R.L. Malenfant, C. Paquet, Multimaterial Vat Polymerization Additive Manufacturing, ACS Appl. Polym. Mater. 3 (2021) 4304–4324. https://doi.org/10.1021/acsapm.1c00262.

[46] M. Pagac, J. Hajnys, Q.-P. Ma, L. Jancar, J. Jansa, P. Stefek, J. Mesicek, A Review of Vat Photopolymerization Technology: Materials, Applications, Challenges, and Future Trends of 3D Printing, Polymers (Basel). 13 (2021) 598. https://doi.org/10.3390/polym13040598.

[47] F. Liu, R. Quan, C. Vyas, E. Aslan, Hybrid biomanufacturing systems applied in tissue regeneration, Int. J. Bioprinting. 9 (2022). https://doi.org/10.18063/ijb.v9i1.646.

[48] D.A. Walker, J.L. Hedrick, C.A. Mirkin, Rapid, large-volume, thermally controlled 3D printing using a mobile liquid interface, Science (80-.). 366 (2019) 360–364. https://doi.org/10.1126/science.aax1562.

[49] N.A. Chartrain, C.B. Williams, A.R. Whittington, A review on fabricating tissue scaffolds using vat photopolymerization, Acta Biomater. 74 (2018) 90–111. https://doi.org/10.1016/j.actbio.2018.05.010.

[50] Z. Wang, C. Huang, J. Wang, B. Zou, C.A. Abbas, X. Wang, Design and Characterization of Hydroxyapatite Scaffolds Fabricated by Stereolithography for Bone Tissue Engineering Application, Procedia CIRP. 89 (2020) 170–175. https://doi.org/10.1016/j.procir.2020.05.138.

[51] F.P.W. Melchels, K. Bertoldi, R. Gabbrielli, A.H. Velders, J. Feijen, D.W. Grijpma, Mathematically defined tissue engineering scaffold architectures prepared by stereolithography, Biomaterials. 31 (2010) 6909–6916. https://doi.org/10.1016/j.biomaterials.2010.05.068.

[52] C. Zhou, H. Ye, F. Zhang, A Novel Low-Cost Stereolithography Process Based on Vector Scanning and Mask Projection for High-Accuracy, High-Speed, High-Throughput, and Large-Area Fabrication, J. Comput. Inf. Sci. Eng. 15 (2015). https://doi.org/10.1115/1.4028848.

[53] J. Gotman, J.R. Ives, P. Gloor, Automatic recognition of inter-ictal epileptic activity in prolonged EEG recordings., Electroencephalogr. Clin. Neurophysiol. 46 (1979) 510–20. https://doi.org/10.1016/0013-4694(79)90004-x.

[54] X. Wu, Q. Lian, D. Li, Z. Jin, Biphasic osteochondral scaffold fabrication using multi-material mask projection stereolithography, Rapid Prototyp. J. 25 (2019) 277–288. https://doi.org/10.1108/RPJ-07-2017-0144.

[55] M. Bahraminasab, Challenges on optimization of 3D-printed bone scaffolds, Biomed. Eng. Online. 19 (2020) 69. https://doi.org/10.1186/s12938-020-00810-2.

[56] A.M. Greiner, M. Jäckel, A.C. Scheiwe, D.R. Stamow, T.J. Autenrieth, J. Lahann, C.M. Franz, M. Bastmeyer, Multifunctional polymer scaffolds with adjustable pore size and chemoattractant gradients for studying cell matrix invasion, Biomaterials. 35 (2014) 611–619. https://doi.org/10.1016/j.biomaterials.2013.09.095.

[57] A.C. Weems, M.M. Pérez-Madrigal, M.C. Arno, A.P. Dove, 3D Printing for the

Clinic: Examining Contemporary Polymeric Biomaterials and Their Clinical Utility, Biomacromolecules. 21 (2020) 1037–1059. https://doi.org/10.1021/acs.biomac.9b01539.

[58] G. Lipkowitz, T. Samuelsen, K. Hsiao, B. Lee, M.T. Dulay, I. Coates, H. Lin, W. Pan, G. Toth, L. Tate, E.S.G. Shaqfeh, J.M. DeSimone, Injection continuous liquid interface production of 3D objects, Sci. Adv. 8 (2022). https://doi.org/10.1126/sciadv.abq3917.

[59] S.A. Khairallah, A.A. Martin, J.R.I. Lee, G. Guss, N.P. Calta, J.A. Hammons, M.H. Nielsen, K. Chaput, E. Schwalbach, M.N. Shah, M.G. Chapman, T.M. Willey, A.M. Rubenchik, A.T. Anderson, Y.M. Wang, M.J. Matthews, W.E. King, Controlling interdependent meso-nanosecond dynamics and defect generation in metal 3D printing, Science (80-.). 368 (2020) 660–665. https://doi.org/10.1126/science.aay7830.

[60] D.G. Tamay, T. Dursun Usal, A.S. Alagoz, D. Yucel, N. Hasirci, V. Hasirci, 3D and 4D Printing of Polymers for Tissue Engineering Applications, Front. Bioeng. Biotechnol. 7 (2019). https://doi.org/10.3389/fbioe.2019.00164.

[61] J.C. Najmon, S. Raeisi, A. Tovar, Review of additive manufacturing technologies and applications in the aerospace industry, in: Addit. Manuf. Aerosp. Ind., Elsevier, 2019: pp. 7–31. https://doi.org/10.1016/B978-0-12-814062-8.00002-9.

[62] A. Muzaffar, M.B. Ahamed, K. Deshmukh, T. Kovářík, T. Křenek, S.K.K. Pasha, 3D and 4D printing of pH-responsive and functional polymers and their composites, in: 3D 4D Print. Polym. Nanocomposite Mater., Elsevier, 2020: pp. 85–117. https://doi.org/10.1016/B978-0-12-816805-9.00004-1.

[63] G.V. Salmoria, C.H. Ahrens, P. Klauss, R.A. Paggi, R.G. Oliveira, A. Lago, Rapid manufacturing of polyethylene parts with controlled pore size gradients using selective laser sintering, Mater. Res. 10 (2007) 211–214. https://doi.org/10.1590/S1516-14392007000200019.

[64] Y. Du, H. Liu, Q. Yang, S. Wang, J. Wang, J. Ma, I. Noh, A.G. Mikos, S. Zhang, Selective laser sintering scaffold with hierarchical architecture and gradient composition for osteochondral repair in rabbits, Biomaterials. 137 (2017) 37–48. https://doi.org/10.1016/j.biomaterials.2017.05.021.

[65] L. Guo, S. Ataollah Naghavi, Z. Wang, S. Nath Varma, Z. Han, Z. Yao, L. Wang, L. Wang, C. Liu, On the design evolution of hip implants: A review, Mater. Des. 216 (2022) 110552. https://doi.org/10.1016/j.matdes.2022.110552.

[66] Y. Lv, G. Liu, B. Wang, Y. Tang, Z. Lin, J. Liu, G. Wei, L. Wang, Pore Strategy Design of a Novel NiTi-Nb Biomedical Porous Scaffold Based on a Triply Periodic Minimal Surface, Front. Bioeng. Biotechnol. 10 (2022). https://doi.org/10.3389/fbioe.2022.910475.

[67] F. Mangano, L. Chambrone, R. van Noort, C. Miller, P. Hatton, C. Mangano, Direct Metal Laser Sintering Titanium Dental Implants: A Review of the Current Literature, Int. J. Biomater. 2014 (2014) 1–11. https://doi.org/10.1155/2014/461534.

[68] T. Traini, C. Mangano, R.L. Sammons, F. Mangano, A. Macchi, A. Piattelli, Direct laser metal sintering as a new approach to fabrication of an isoelastic functionally graded material for manufacture of porous titanium dental implants, Dent. Mater. 24

(2008) 1525–1533. https://doi.org/10.1016/j.dental.2008.03.029.

[69] S. Megahed, V. Aniko, J.H. Schleifenbaum, Electron Beam-Melting and Laser Powder Bed Fusion of Ti6Al4V: Transferability of Process Parameters, Metals (Basel). 12 (2022) 1332. https://doi.org/10.3390/met12081332.

[70] K.C. Nune, R.D.K. Misra, S.M. Gaytan, L.E. Murr, Interplay between cellular activity and three-dimensional scaffold-cell constructs with different foam structure processed by electron beam melting, J. Biomed. Mater. Res. Part A. 103 (2015) 1677–1692. https://doi.org/10.1002/jbm.a.35307.

[71] H. Shi, P. Zhou, J. Li, C. Liu, L. Wang, Functional Gradient Metallic Biomaterials: Techniques, Current Scenery, and Future Prospects in the Biomedical Field, Front. Bioeng. Biotechnol. 8 (2021). https://doi.org/10.3389/fbioe.2020.616845.

[72] R. Winarso, P.W. Anggoro, R. Ismail, J. Jamari, A.P. Bayuseno, Application of fused deposition modeling (FDM) on bone scaffold manufacturing process: A review, Heliyon. 8 (2022) e11701. https://doi.org/10.1016/j.heliyon.2022.e11701.

[73] P.K. Penumakala, J. Santo, A. Thomas, A critical review on the fused deposition modeling of thermoplastic polymer composites, Compos. Part B Eng. 201 (2020) 108336. https://doi.org/10.1016/j.compositesb.2020.108336.

[74] I. Zein, D.W. Hutmacher, K.C. Tan, S.H. Teoh, Fused deposition modeling of novel scaffold architectures for tissue engineering applications, Biomaterials. 23 (2002) 1169–1185. https://doi.org/10.1016/S0142-9612(01)00232-0.

[75] L.G. Bracaglia, B.T. Smith, E. Watson, N. Arumugasaamy, A.G. Mikos, J.P. Fisher, 3D printing for the design and fabrication of polymer-based gradient scaffolds, Acta Biomater. 56 (2017) 3–13. https://doi.org/10.1016/j.actbio.2017.03.030.

[76] M. ERYILDIZ, Effect of Build Orientation on Mechanical Behaviour and Build Time of FDM 3D-Printed PLA Parts: An Experimental Investigation, Eur. Mech. Sci. 5 (2021) 116–120. https://doi.org/10.26701/ems.881254.

[77] D.W. Hutmacher, T. Schantz, I. Zein, K.W. Ng, S.H. Teoh, K.C. Tan, Mechanical properties and cell cultural response of polycaprolactone scaffolds designed and fabricated via fused deposition modeling, J. Biomed. Mater. Res. 55 (2001) 203–216. https://doi.org/10.1002/1097-4636(200105)55:2<203::AID-JBM1007>3.0.CO;2-7.

[78] J.W. Lee, J.Y. Kim, D.-W. Cho, Solid Free-form Fabrication Technology and Its Application to Bone Tissue Engineering, Int. J. Stem Cells. 3 (2010) 85–95. https://doi.org/10.15283/ijsc.2010.3.2.85.

[79] X. Song, D. Shi, P. Song, X. Han, Q. Wei, C. Huang, Fused deposition modeling of poly(ether ether ketone) scaffolds, High Temp. Mater. Process. 40 (2021) 1–11. https://doi.org/10.1515/htmp-2021-0009.

[80] D. Jiang, F. Ning, Fused Filament Fabrication of Biodegradable PLA/316L Composite Scaffolds: Effects of Metal Particle Content, Procedia Manuf. 48 (2020) 755–762. https://doi.org/10.1016/j.promfg.2020.05.110.

[81] D. V. Portan, C. Ntoulias, G. Mantzouranis, A.P. Fortis, D.D. Deligianni, D. Polyzos, V. Kostopoulos, Gradient 3D Printed PLA Scaffolds on Biomedical Titanium:

Mechanical Evaluation and Biocompatibility, Polymers (Basel). 13 (2021) 682. https://doi.org/10.3390/polym13050682.

[82] M. Karimi, M. Asadi-Eydivand, N. Abolfathi, Y. Chehrehsaz, M. Solati-Hashjin, The effect of pore size and layout on mechanical and biological properties of <scp>3D</scp> -printed bone scaffolds with gradient porosity, Polym. Compos. (2022). https://doi.org/10.1002/pc.27174.

[83] T. Jiang, J.G. Munguia-Lopez, S. Flores-Torres, J. Kort-Mascort, J.M. Kinsella, Extrusion bioprinting of soft materials: An emerging technique for biological model fabrication, Appl. Phys. Rev. 6 (2019) 011310. https://doi.org/10.1063/1.5059393.

[84] C. Gao, C. Wang, H. Jin, Z. Wang, Z. Li, C. Shi, Y. Leng, F. Yang, H. Liu, J. Wang, Additive manufacturing technique-designed metallic porous implants for clinical application in orthopedics, RSC Adv. 8 (2018) 25210–25227. https://doi.org/10.1039/C8RA04815K.

[85] M. Hofmann, 3D Printing Gets a Boost and Opportunities with Polymer Materials, ACS Macro Lett. 3 (2014) 382–386. https://doi.org/10.1021/mz4006556.

[86] Y. Zhang, W. Jarosinski, Y.-G. Jung, J. Zhang, Additive manufacturing processes and equipment, in: Addit. Manuf., Elsevier, 2018: pp. 39–51. https://doi.org/10.1016/B978-0-12-812155-9.00002-5.

[87] R.J. Friel, R.A. Harris, Ultrasonic Additive Manufacturing – A Hybrid Production Process for Novel Functional Products, Procedia CIRP. 6 (2013) 35–40. https://doi.org/10.1016/j.procir.2013.03.004.

[88] Y. Li, Z. Feng, L. Hao, L. Huang, C. Xin, Y. Wang, E. Bilotti, K. Essa, H. Zhang, Z. Li, F. Yan, T. Peijs, A Review on Functionally Graded Materials and Structures via Additive Manufacturing: From Multi-Scale Design to Versatile Functional Properties, Adv. Mater. Technol. 5 (2020) 1900981. https://doi.org/10.1002/admt.201900981.

[89] S. Kumar, Development of Functionally Graded Materials by Ultrasonic Consolidation, CIRP J. Manuf. Sci. Technol. 3 (2010) 85–87. https://doi.org/10.1016/j.cirpj.2010.07.006.

[90] A. Saboori, D. Gallo, S. Biamino, P. Fino, M. Lombardi, An Overview of Additive Manufacturing of Titanium Components by Directed Energy Deposition: Microstructure and Mechanical Properties, Appl. Sci. 7 (2017) 883. https://doi.org/10.3390/app7090883.

[91] G. Piscopo, L. Iuliano, Current research and industrial application of laser powder directed energy deposition, Int. J. Adv. Manuf. Technol. 119 (2022) 6893–6917. https://doi.org/10.1007/s00170-021-08596-w.

[92] Z.E. Tan, J.H.L. Pang, J. Kaminski, H. Pepin, Characterisation of porosity, density, and microstructure of directed energy deposited stainless steel AISI 316L, Addit. Manuf. 25 (2019) 286–296. https://doi.org/10.1016/j.addma.2018.11.014.

[93] A. Mostafaei, A.M. Elliott, J.E. Barnes, F. Li, W. Tan, C.L. Cramer, P. Nandwana, M. Chmielus, Binder jet 3D printing—Process parameters, materials, properties, modeling, and challenges, Prog. Mater. Sci. 119 (2021) 100707.

https://doi.org/10.1016/j.pmatsci.2020.100707.

[94] X. Li, H. Liang, J. Sun, Y. Zhuang, B. Xu, J. Dai, Electrospun Collagen Fibers with Spatial Patterning of SDF1α for the Guidance of Neural Stem Cells, Adv. Healthc. Mater. 4 (2015) 1869–1876. https://doi.org/10.1002/adhm.201500271.

[95] J.H.Y. Chung, S. Naficy, Z. Yue, R. Kapsa, A. Quigley, S.E. Moulton, G.G. Wallace, Bio-ink properties and printability for extrusion printing living cells, Biomater. Sci. 1 (2013) 763. https://doi.org/10.1039/c3bm00012e.

[96] W. Liu, Y.S. Zhang, M.A. Heinrich, F. De Ferrari, H.L. Jang, S.M. Bakht, M.M. Alvarez, J. Yang, Y.-C. Li, G. Trujillo-de Santiago, A.K. Miri, K. Zhu, P. Khoshakhlagh, G. Prakash, H. Cheng, X. Guan, Z. Zhong, J. Ju, G.H. Zhu, X. Jin, S.R. Shin, M.R. Dokmeci, A. Khademhosseini, Bioprinting: Rapid Continuous Multimaterial Extrusion Bioprinting (Adv. Mater. 3/2017), Adv. Mater. 29 (2017). https://doi.org/10.1002/adma.201770016.

[97] M. Kuzucu, G. Vera, M. Beaumont, S. Fischer, P. Wei, V.P. Shastri, A. Forget, Extrusion-Based 3D Bioprinting of Gradients of Stiffness, Cell Density, and Immobilized Peptide Using Thermogelling Hydrogels, ACS Biomater. Sci. Eng. 7 (2021) 2192–2197. https://doi.org/10.1021/acsbiomaterials.1c00183.

[98] R. Sinha, M. Cámara-Torres, P. Scopece, E. Verga Falzacappa, A. Patelli, L. Moroni, C. Mota, A hybrid additive manufacturing platform to create bulk and surface composition gradients on scaffolds for tissue regeneration, Nat. Commun. 12 (2021) 500. https://doi.org/10.1038/s41467-020-20865-y.

[99] Y. Zhang, D. Wu, X. Zhao, M. Pakvasa, A.B. Tucker, H. Luo, K.H. Qin, D.A. Hu, E.J. Wang, A.J. Li, M. Zhang, Y. Mao, M. Sabharwal, F. He, C. Niu, H. Wang, L. Huang, D. Shi, Q. Liu, N. Ni, K. Fu, C. Chen, W. Wagstaff, R.R. Reid, A. Athiviraham, S. Ho, M.J. Lee, K. Hynes, J. Strelzow, T.-C. He, M. El Dafrawy, Stem Cell-Friendly Scaffold Biomaterials: Applications for Bone Tissue Engineering and Regenerative Medicine, Front. Bioeng. Biotechnol. 8 (2020). https://doi.org/10.3389/fbioe.2020.598607.

[100] F.P.W. Melchels, B. Tonnarelli, A.L. Olivares, I. Martin, D. Lacroix, J. Feijen, D.J. Wendt, D.W. Grijpma, The influence of the scaffold design on the distribution of adhering cells after perfusion cell seeding, Biomaterials. 32 (2011) 2878–2884. https://doi.org/10.1016/j.biomaterials.2011.01.023.

[101] Y. Du, M.J. Hancock, J. He, J.L. Villa-Uribe, B. Wang, D.M. Cropek, A. Khademhosseini, Convection-driven generation of long-range material gradients, Biomaterials. 31 (2010) 2686–2694. https://doi.org/Adapted with permission from Ref.

[102] C. Li, L. Ouyang, I.J. Pence, A.C. Moore, Y. Lin, C.W. Winter, J.P.K. Armstrong, M.M. Stevens, Buoyancy-Driven Gradients for Biomaterial Fabrication and Tissue Engineering, Adv. Mater. 31 (2019) 1900291. https://doi.org/10.1002/adma.201900291.

[103] S. Sant, M.J. Hancock, J.P. Donnelly, D. Iyer, A. Khademhosseini, Biomimetic gradient hydrogels for tissue engineering, Can. J. Chem. Eng. 88 (2010) 899–911. https://doi.org/10.1002/cjce.20411.

[104] R.F. Canadas, T. Ren, A.P. Marques, J.M. Oliveira, R.L. Reis, U. Demirci, Biochemical Gradients to Generate 3D Heterotypic-Like Tissues with Isotropic and Anisotropic Architectures, Adv. Funct. Mater. 28 (2018) 1804148. https://doi.org/10.1002/adfm.201804148.

[105] Y. Du, M.J. Hancock, J. He, J.L. Villa-Uribe, B. Wang, D.M. Cropek, A. Khademhosseini, Convection-driven generation of long-range material gradients, Biomaterials. 31 (2010) 2686–2694. https://doi.org/10.1016/j.biomaterials.2009.12.012.

[106] C.L. Ross, The use of electric, magnetic, and electromagnetic field for directed cell migration and adhesion in regenerative medicine, Biotechnol. Prog. 33 (2017) 5–16. https://doi.org/10.1002/btpr.2371.

[107] S. Kopyl, R. Surmenev, M. Surmeneva, Y. Fetisov, A. Kholkin, Magnetoelectric effect: principles and applications in biology and medicine– a review, Mater. Today Bio. 12 (2021) 100149. https://doi.org/10.1016/j.mtbio.2021.100149.

[108] G. Xu, Z. Ding, Q. Lu, X. Zhang, X. Zhou, L. Xiao, G. Lu, D.L. Kaplan, Electric field-driven building blocks for introducing multiple gradients to hydrogels, Protein Cell. 11 (2020) 267–285. https://doi.org/10.1007/s13238-020-00692-z.

[109] V. Goranov, T. Shelyakova, R. De Santis, Y. Haranava, A. Makhaniok, A. Gloria, A. Tampieri, A. Russo, E. Kon, M. Marcacci, L. Ambrosio, V.A. Dediu, 3D Patterning of cells in Magnetic Scaffolds for Tissue Engineering, Sci. Rep. 10 (2020) 2289. https://doi.org/10.1038/s41598-020-58738-5.

[110] Y. Qian, Z. Yan, X. Li, S. Chen, H. Jiang, C. Chen, W.-E. Yuan, C. Fan, Gradient Nanoaggregation in a Magnetically Actuated Scaffold for Multiscale Immunoregulation and Microenvironment Remodeling Accelerates Nerve and Muscle Repair, ACS Mater. Lett. (2023) 580–595. https://doi.org/10.1021/acsmaterialslett.2c00684.

[111] P. Sofokleous, M.H.W. Chin, R. Day, Phase-separation technologies for 3D scaffold engineering, in: Funct. 3D Tissue Eng. Scaffolds, Elsevier, 2018: pp. 101–126. https://doi.org/10.1016/B978-0-08-100979-6.00005-7.

[112] R. Zeinali, L.J. del Valle, J. Torras, J. Puiggalí, Recent Progress on Biodegradable Tissue Engineering Scaffolds Prepared by Thermally-Induced Phase Separation (TIPS), Int. J. Mol. Sci. 22 (2021) 3504. https://doi.org/10.3390/ijms22073504.

[113] E. Sachlos, J. Czernuszka, Making Tissue Engineering Scaffolds Work. Review: The application of solid freeform fabrication technology to the production of tissue engineering scaffolds, Eur. Cells Mater. 5 (2003) 29–40. https://doi.org/10.22203/eCM.v005a03.

[114] R. Akbarzadeh, A.-M. Yousefi, Effects of processing parameters in thermally induced phase separation technique on porous architecture of scaffolds for bone tissue engineering, J. Biomed. Mater. Res. Part B Appl. Biomater. 102 (2014) 1304–1315. https://doi.org/10.1002/jbm.b.33101.

[115] F.C. Pavia, V. La Carrubba, S. Piccarolo, V. Brucato, Polymeric scaffolds prepared via thermally induced phase separation: Tuning of structure and morphology, J. Biomed.

Mater. Res. Part A. 86A (2008) 459–466. https://doi.org/10.1002/jbm.a.31621.

[116] G. Ghersi, F.C. Pavia, G. Conoscenti, G.A. Mannella, S. Greco, S. Rigogliuso, V. La Carrubba, V. Brucato, PLLA scaffold via TIPS for bone tissue engineering, Chem. Eng. Trans. 49 (2016) 301–306. https://doi.org/10.3303/CET1649051.

[117] G.A. Mannella, G. Conoscenti, F. Carfì Pavia, V. La Carrubba, V. Brucato, Preparation of polymeric foams with a pore size gradient via Thermally Induced Phase Separation (TIPS), Mater. Lett. 160 (2015) 31–33. https://doi.org/10.1016/j.matlet.2015.07.055.

[118] T. Nie, L. Xue, M. Ge, H. Ma, J. Zhang, Fabrication of poly(L-lactic acid) tissue engineering scaffolds with precisely controlled gradient structure, Mater. Lett. 176 (2016) 25–28. https://doi.org/10.1016/j.matlet.2016.04.078.

[119] B.C. Isenberg, C. Williams, R.T. Tranquillo, Small-Diameter Artificial Arteries Engineered In Vitro, Circ. Res. 98 (2006) 25–35. https://doi.org/10.1161/01.RES.0000196867.12470.84.

[120] H. Ma, J. Hu, P.X. Ma, Polymer Scaffolds for Small-Diameter Vascular Tissue Engineering, Adv. Funct. Mater. 20 (2010) 2833–2841. https://doi.org/10.1002/adfm.201000922.

[121] J.E. Phillips, K.L. Burns, J.M. Le Doux, R.E. Guldberg, A.J. Garcia, Engineering graded tissue interfaces, Proc. Natl. Acad. Sci. 105 (2008) 12170–12175. https://doi.org/10.1073/pnas.0801988105.

[122] W. Liu, J. Lipner, J. Xie, C.N. Manning, S. Thomopoulos, Y. Xia, Nanofiber Scaffolds with Gradients in Mineral Content for Spatial Control of Osteogenesis, ACS Appl. Mater. Interfaces. 6 (2014) 2842–2849. https://doi.org/10.1021/am405418g.

[123] M.K. Gunnewiek, A. Di Luca, H.Z. Bollemaat, C.A. van Blitterswijk, G.J. Vancso, L. Moroni, E.M. Benetti, Creeping Proteins in Microporous Structures: Polymer Brush-Assisted Fabrication of 3D Gradients for Tissue Engineering, Adv. Healthc. Mater. 4 (2015) 1169–1174. https://doi.org/10.1002/adhm.201400797.

[124] Y.J. He, M.F. Santana, A. Staneviciute, M.B. Pimentel, F. Yang, J. Goes, K. Kawaji, M.K. Vaicik, R. Abdulhadi, N. Hibino, G. Papavasiliou, Cell-Laden Gradient Hydrogel Scaffolds for Neovascularization of Engineered Tissues, Adv. Healthc. Mater. 10 (2021) 2001706. https://doi.org/10.1002/adhm.202001706.

[125] S.A. DeLong, J.J. Moon, J.L. West, Covalently immobilized gradients of bFGF on hydrogel scaffolds for directed cell migration, Biomaterials. 26 (2005) 3227–3234. https://doi.org/10.1016/j.biomaterials.2004.09.021.

[126] A. Forget, D. Rojas, M. Waibel, D. Pencko, S. Gunenthiran, N. Ninan, T. Loudovaris, C. Drogemuller, P.T. Coates, N.H. Voelcker, A. Blencowe, Facile preparation of tissue engineering scaffolds with pore size gradients using the muesli effect and their application to cell spheroid encapsulation, J. Biomed. Mater. Res. Part B Appl. Biomater. 108 (2020) 2495–2504. https://doi.org/10.1002/jbm.b.34581.

[127] A. Marrella, M. Aiello, R. Quarto, S. Scaglione, Chemical and morphological gradient scaffolds to mimic hierarchically complex tissues: From theoretical modeling to their

fabrication, Biotechnol. Bioeng. 113 (2016) 2286–2297. https://doi.org/10.1002/bit.25994.

[128] C. Erisken, D.M. Kalyon, H. Wang, Functionally graded electrospun polycaprolactone and β-tricalcium phosphate nanocomposites for tissue engineering applications, Biomaterials. 29 (2008) 4065–4073. https://doi.org/10.1016/j.biomaterials.2008.06.022.

[129] K.L. Moffat, A.S.-P. Kwei, J.P. Spalazzi, S.B. Doty, W.N. Levine, H.H. Lu, Novel Nanofiber-Based Scaffold for Rotator Cuff Repair and Augmentation, Tissue Eng. Part A. 15 (2009) 115–126. https://doi.org/10.1089/ten.tea.2008.0014.

[130] J. Xie, X. Li, J. Lipner, C.N. Manning, A.G. Schwartz, S. Thomopoulos, Y. Xia, "Aligned-to-random" nanofiber scaffolds for mimicking the structure of the tendon-to-bone insertion site, Nanoscale. 2 (2010) 923. https://doi.org/10.1039/c0nr00192a.

[131] A.E. Stanton, X. Tong, S.L. Jing, A. Behn, H. Storaci, F. Yang, Aligned Gelatin Microribbon Scaffolds with Hydroxyapatite Gradient for Engineering the Bone–Tendon Interface, Tissue Eng. Part A. 28 (2022) 712–723. https://doi.org/10.1089/ten.tea.2021.0099.

[132] H. Bai, D. Wang, B. Delattre, W. Gao, J. De Coninck, S. Li, A.P. Tomsia, Biomimetic gradient scaffold from ice-templating for self-seeding of cells with capillary effect, Acta Biomater. 20 (2015) 113–119. https://doi.org/10.1016/j.actbio.2015.04.007.

[133] F. Cestari, Y. Yang, J. Wilbig, J. Günster, A. Motta, V.M. Sglavo, Powder 3D Printing of Bone Scaffolds with Uniform and Gradient Pore Sizes Using Cuttlebone-Derived Calcium Phosphate and Glass-Ceramic, Materials (Basel). 15 (2022) 5139. https://doi.org/10.3390/ma15155139.

[134] S. Kanwar, O. Al-Ketan, S. Vijayavenkataraman, A novel method to design biomimetic, 3D printable stochastic scaffolds with controlled porosity for bone tissue engineering, Mater. Des. 220 (2022) 110857. https://doi.org/10.1016/j.matdes.2022.110857.

[135] X. Ren, F. Wang, C. Chen, X. Gong, L. Yin, L. Yang, Engineering zonal cartilage through bioprinting collagen type II hydrogel constructs with biomimetic chondrocyte density gradient, BMC Musculoskelet. Disord. 17 (2016) 301. https://doi.org/10.1186/s12891-016-1130-8.

[136] B. Xu, J. Ye, B.-S. Fan, X. Wang, J.-Y. Zhang, S. Song, Y. Song, W.-B. Jiang, X. Wang, J.-K. Yu, Protein-spatiotemporal partition releasing gradient porous scaffolds and anti-inflammatory and antioxidant regulation remodel tissue engineered anisotropic meniscus, Bioact. Mater. 20 (2023) 194–207. https://doi.org/10.1016/j.bioactmat.2022.05.019.

[137] C.A. Mullen, T.J. Vaughan, K.L. Billiar, L.M. McNamara, The Effect of Substrate Stiffness, Thickness, and Cross-Linking Density on Osteogenic Cell Behavior, Biophys. J. 108 (2015) 1604–1612. https://doi.org/10.1016/j.bpj.2015.02.022.

[138] S. Haldar, A. Sharma, S. Gupta, S. Chauhan, P. Roy, D. Lahiri, Bioengineered smart trilayer skin tissue substitute for efficient deep wound healing, Mater. Sci. Eng. C. 105 (2019) 110140. https://doi.org/10.1016/j.msec.2019.110140.

[139] M. Ha, S. Lim, S. Cho, Y. Lee, S. Na, C. Baig, H. Ko, Skin-Inspired Hierarchical Polymer Architectures with Gradient Stiffness for Spacer-Free, Ultrathin, and Highly Sensitive Triboelectric Sensors, ACS Nano. 12 (2018) 3964–3974. https://doi.org/10.1021/acsnano.8b01557.

[140] L. Huang, J. Huang, H. Shao, X. Hu, C. Cao, S. Fan, L. Song, Y. Zhang, Silk scaffolds with gradient pore structure and improved cell infiltration performance, Mater. Sci. Eng. C. 94 (2019) 179–189. https://doi.org/10.1016/j.msec.2018.09.034.

[141] D. Odedra, L.L.Y. Chiu, M. Shoichet, M. Radisic, Endothelial cells guided by immobilized gradients of vascular endothelial growth factor on porous collagen scaffolds, Acta Biomater. 7 (2011) 3027–3035. https://doi.org/10.1016/j.actbio.2011.05.002.

[142] F. Du, H. Wang, W. Zhao, D. Li, D. Kong, J. Yang, Y. Zhang, Gradient nanofibrous chitosan/poly ε-caprolactone scaffolds as extracellular microenvironments for vascular tissue engineering, Biomaterials. 33 (2012) 762–770. https://doi.org/10.1016/j.biomaterials.2011.10.037.

[143] M. Radisic, J. Malda, E. Epping, W. Geng, R. Langer, G. Vunjak-Novakovic, Oxygen gradients correlate with cell density and cell viability in engineered cardiac tissue, Biotechnol. Bioeng. 93 (2006) 332–343. https://doi.org/10.1002/bit.20722.

[144] L. Chen, Q. Yu, Y. Jia, M. Xu, Y. Wang, J. Wang, T. Wen, L. Wang, Micro-and-nanometer topological gradient of block copolymer fibrous scaffolds towards region-specific cell regulation, J. Colloid Interface Sci. 606 (2022) 248–260. https://doi.org/10.1016/j.jcis.2021.08.021.

[145] R. Florencio-Silva, G.R. da S. Sasso, E. Sasso-Cerri, M.J. Simões, P.S. Cerri, Biology of Bone Tissue: Structure, Function, and Factors That Influence Bone Cells, Biomed Res. Int. 2015 (2015) 1–17. https://doi.org/10.1155/2015/421746.

[146] A.M. Mohamed, An overview of bone cells and their regulating factors of differentiation., Malays. J. Med. Sci. 15 (2008) 4–12. http://www.ncbi.nlm.nih.gov/pubmed/22589609.

[147] A.M. Weatherholt, R.K. Fuchs, S.J. Warden, Specialized Connective Tissue: Bone, the Structural Framework of the Upper Extremity, J. Hand Ther. 25 (2012) 123–132. https://doi.org/10.1016/j.jht.2011.08.003.

[148] A. Rehfeld, M. Nylander, K. Karnov, Bone Tissue, in: Compend. Histol., Springer International Publishing, Cham, 2017: pp. 157–185. https://doi.org/10.1007/978-3-319-41873-5_9.

[149] A. Di Luca, B. Ostrowska, I. Lorenzo-Moldero, A. Lepedda, W. Swieszkowski, C. Van Blitterswijk, L. Moroni, Gradients in pore size enhance the osteogenic differentiation of human mesenchymal stromal cells in three-dimensional scaffolds, Sci. Rep. 6 (2016) 22898. https://doi.org/10.1038/srep22898.

[150] R.I. Sharma, J.G. Snedeker, Biochemical and biomechanical gradients for directed bone marrow stromal cell differentiation toward tendon and bone, Biomaterials. 31 (2010) 7695–7704. https://doi.org/10.1016/j.biomaterials.2010.06.046.

[151] L.E. Iannucci, A.J. Boys, M.C. McCorry, L.A. Estroff, L.J. Bonassar, Cellular and Chemical Gradients to Engineer the Meniscus-to-Bone Insertion, Adv. Healthc. Mater. 8 (2019) 1800806. https://doi.org/10.1002/adhm.201800806.

[152] W. Luo, H. Liu, C. Wang, Y. Qin, Q. Liu, J. Wang, Bioprinting of Human Musculoskeletal Interface, Adv. Eng. Mater. 21 (2019) 1900019. https://doi.org/10.1002/adem.201900019.

[153] N.H. Hart, S. Nimphius, T. Rantalainen, A. Ireland, A. Siafarikas, R.U. Newton, Mechanical basis of bone strength: influence of bone material, bone structure and muscle action., J. Musculoskelet. Neuronal Interact. 17 (2017) 114–139. https://doi.org/28860414.

[154] B. Clarke, Normal Bone Anatomy and Physiology, Clin. J. Am. Soc. Nephrol. 3 (2008) S131–S139. https://doi.org/10.2215/CJN.04151206.

[155] S.K. Samal, M. Dash, P. Dubruel, Enzymatically Mineralized Cationic Cellulose-Graphene Oxide Scaffolds for Bone Tissue Engineering Applications, (2013) 2013.

[156] S. Panseri, C. Cunha, T. D'Alessandro, M. Sandri, A. Russo, G. Giavaresi, M. Marcacci, C.T. Hung, A. Tampieri, Magnetic hydroxyapatite bone substitutes to enhance tissue regeneration: evaluation in vitro using osteoblast-like cells and in vivo in a bone defect., PLoS One. 7 (2012) e38710. https://doi.org/10.1371/journal.pone.0038710.

[157] B.C. Isenberg, J.Y. Wong, Building structure into engineered tissues, Mater. Today. 9 (2006) 54–60. https://doi.org/10.1016/S1369-7021(06)71743-6.

[158] M.A. Lopez-Heredia, A. Łapa, A.C. Mendes, L. Balcaen, S.K. Samal, F. Chai, P. Van der Voort, C. V. Stevens, B. V. Parakhonskiy, I.S. Chronakis, F. Vanhaecke, N. Blanchemain, E. Pamuła, A.G. Skirtach, T.E.L. Douglas, Bioinspired, biomimetic, double-enzymatic mineralization of hydrogels for bone regeneration with calcium carbonate, Mater. Lett. 190 (2017) 13–16. https://doi.org/10.1016/j.matlet.2016.12.122.

[159] L.M. Cross, A. Thakur, N.A. Jalili, M. Detamore, A.K. Gaharwar, Nanoengineered biomaterials for repair and regeneration of orthopedic tissue interfaces, Acta Biomater. 42 (2016) 2–17. https://doi.org/10.1016/j.actbio.2016.06.023.

[160] D. Shi, J. Shen, Z. Zhang, C. Shi, M. Chen, Y. Gu, Y. Liu, Preparation and properties of dopamine-modified alginate/chitosan–hydroxyapatite scaffolds with gradient structure for bone tissue engineering, J. Biomed. Mater. Res. Part A. (2019) jbm.a.36678. https://doi.org/10.1002/jbm.a.36678.

[161] M.A. Surmeneva, R.A. Surmenev, E.A. Chudinova, A. Koptioug, M.S. Tkachev, S.N. Gorodzha, L.E. Rännar, Fabrication of multiple-layered gradient cellular metal scaffold via electron beam melting for segmental bone reconstruction, Mater. Des. 133 (2017) 195–204. https://doi.org/10.1016/j.matdes.2017.07.059.

[162] J.M. Sobral, S.G. Caridade, R.A. Sousa, J.F. Mano, R.L. Reis, Three-dimensional plotted scaffolds with controlled pore size gradients: Effect of scaffold geometry on mechanical performance and cell seeding efficiency, Acta Biomater. 7 (2011) 1009–1018. https://doi.org/10.1016/j.actbio.2010.11.003.

[163] X. Xie, J. Cai, Y. Yao, Y. Chen, A. ur R. Khan, J. Wu, X. Mo, A woven scaffold with continuous mineral gradients for tendon-to-bone tissue engineering, Compos. Part B Eng. 212 (2021) 108679. https://doi.org/10.1016/j.compositesb.2021.108679.

[164] L. Wang, Y. Qiu, H. Lv, Y. Si, L. Liu, Q. Zhang, J. Cao, J. Yu, X. Li, B. Ding, 3D Superelastic Scaffolds Constructed from Flexible Inorganic Nanofibers with Self-Fitting Capability and Tailorable Gradient for Bone Regeneration, Adv. Funct. Mater. 29 (2019) 1901407. https://doi.org/10.1002/adfm.201901407.

[165] N. Abbasi, R.S.B. Lee, S. Ivanovski, R.M. Love, S. Hamlet, In vivo bone regeneration assessment of offset and gradient melt electrowritten (MEW) PCL scaffolds, Biomater. Res. 24 (2020) 17. https://doi.org/10.1186/s40824-020-00196-1.

[166] N. Abbasi, S. Ivanovski, K. Gulati, R.M. Love, S. Hamlet, Role of offset and gradient architectures of 3-D melt electrowritten scaffold on differentiation and mineralization of osteoblasts, Biomater. Res. 24 (2020) 2. https://doi.org/10.1186/s40824-019-0180-z.

[167] A.M. Bhosale, J.B. Richardson, Articular cartilage: structure, injuries and review of management, Br. Med. Bull. 87 (2008) 77–95. https://doi.org/10.1093/bmb/ldn025.

[168] R.S. Decker, E. Koyama, M. Pacifici, Articular Cartilage: Structural and Developmental Intricacies and Questions, Curr. Osteoporos. Rep. 13 (2015) 407–414. https://doi.org/10.1007/s11914-015-0290-z.

[169] N. Fahy, M. Alini, M.J. Stoddart, Mechanical stimulation of mesenchymal stem cells: Implications for cartilage tissue engineering, J. Orthop. Res. (2017). https://doi.org/10.1002/jor.23670.

[170] Y. Liu, K.M. Shah, J. Luo, Strategies for Articular Cartilage Repair and Regeneration, Front. Bioeng. Biotechnol. 9 (2021). https://doi.org/10.3389/fbioe.2021.770655.

[171] H. Hu, W. Liu, C. Sun, Q. Wang, W. Yang, Z. Zhang, Z. Xia, Z. Shao, B. Wang, Endogenous Repair and Regeneration of Injured Articular Cartilage: A Challenging but Promising Therapeutic Strategy, Aging Dis. 12 (2021) 886. https://doi.org/10.14336/AD.2020.0902.

[172] A.J. Sophia Fox, A. Bedi, S.A. Rodeo, The Basic Science of Articular Cartilage: Structure, Composition, and Function, Sport. Heal. A Multidiscip. Approach. 1 (2009) 461–468. https://doi.org/10.1177/1941738109350438.

[173] S.L. Francis, C. Di Bella, G.G. Wallace, P.F.M. Choong, Cartilage Tissue Engineering Using Stem Cells and Bioprinting Technology—Barriers to Clinical Translation, Front. Surg. 5 (2018). https://doi.org/10.3389/fsurg.2018.00070.

[174] Y. Sun, Y. You, W. Jiang, B. Wang, Q. Wu, K. Dai, 3D bioprinting dual-factor releasing and gradient-structured constructs ready to implant for anisotropic cartilage regeneration, Sci. Adv. 6 (2020). https://doi.org/10.1126/sciadv.aay1422.

[175] Y. Sun, Q. Wu, Y. Zhang, K. Dai, Y. Wei, 3D-bioprinted gradient-structured scaffold generates anisotropic cartilage with vascularization by pore-size-dependent activation of HIF1α/FAK signaling axis, Nanomedicine Nanotechnology, Biol. Med. 37 (2021) 102426. https://doi.org/10.1016/j.nano.2021.102426.

[176] X. Zhou, S. Tenaglio, T. Esworthy, S.Y. Hann, H. Cui, T.J. Webster, H. Fenniri, L.G.

Zhang, Three-Dimensional Printing Biologically Inspired DNA-Based Gradient Scaffolds for Cartilage Tissue Regeneration, ACS Appl. Mater. Interfaces. 12 (2020) 33219–33228. https://doi.org/10.1021/acsami.0c07918.

[177] H. Zhang, H. Huang, G. Hao, Y. Zhang, H. Ding, Z. Fan, L. Sun, 3D Printing Hydrogel Scaffolds with Nanohydroxyapatite Gradient to Effectively Repair Osteochondral Defects in Rats, Adv. Funct. Mater. 31 (2021) 2006697. https://doi.org/10.1002/adfm.202006697.

[178] K. Sidiropoulou, E.K. Pissadaki, P. Poirazi, Inside the brain of a neuron, EMBO Rep. 7 (2006) 886–892. https://doi.org/10.1038/sj.embor.7400789.

[179] L.R. Doblado, C. Martínez-Ramos, M.M. Pradas, Biomaterials for Neural Tissue Engineering, Front. Nanotechnol. 3 (2021). https://doi.org/10.3389/fnano.2021.643507.

[180] A. Subramanian, U.M. Krishnan, S. Sethuraman, Development of biomaterial scaffold for nerve tissue engineering: Biomaterial mediated neural regeneration, J. Biomed. Sci. 16 (2009) 108. https://doi.org/10.1186/1423-0127-16-108.

[181] S. Grade, M. Götz, Neuronal replacement therapy: previous achievements and challenges ahead, Npj Regen. Med. 2 (2017) 29. https://doi.org/10.1038/s41536-017-0033-0.

[182] A.Y. Chiu, M.S. Rao, Cell-Based Therapy for Neural Disorders — Anticipating Challenges, Neurotherapeutics. 8 (2011) 744–752. https://doi.org/10.1007/s13311-011-0066-9.

[183] V.L. Feigin, E. Nichols, T. Alam, M.S. Bannick, E. Beghi, N. Blake, W.J. Culpepper, E.R. Dorsey, A. Elbaz, R.G. Ellenbogen, J.L. Fisher, C. Fitzmaurice, G. Giussani, L. Glennie, S.L. James, C.O. Johnson, N.J. Kassebaum, G. Logroscino, B. Marin, W.C. Mountjoy-Venning, M. Nguyen, R. Ofori-Asenso, A.P. Patel, M. Piccininni, G.A. Roth, T.J. Steiner, L.J. Stovner, C.E.I. Szoeke, A. Theadom, S.E. Vollset, M.T. Wallin, C. Wright, J.R. Zunt, N. Abbasi, F. Abd-Allah, A. Abdelalim, I. Abdollahpour, V. Aboyans, H.N. Abraha, D. Acharya, A.A. Adamu, O.M. Adebayo, A.M. Adeoye, J.C. Adsuar, M. Afarideh, S. Agrawal, A. Ahmadi, M.B. Ahmed, A.N. Aichour, I. Aichour, M.T.E. Aichour, R.O. Akinyemi, N. Akseer, A. Al-Eyadhy, R. Al-Shahi Salman, F. Alahdab, K.A. Alene, S.M. Aljunid, K. Altirkawi, N. Alvis-Guzman, N.H. Anber, C.A.T. Antonio, J. Arabloo, O. Aremu, J. Ärnlöv, H. Asayesh, R.J. Asghar, H.T. Atalay, A. Awasthi, B.P. Ayala Quintanilla, T.B. Ayuk, A. Badawi, M. Banach, J.A.M. Banoub, M.A. Barboza, S.L. Barker-Collo, T.W. Bärnighausen, B.T. Baune, N. Bedi, M. Behzadifar, M. Behzadifar, Y. Béjot, B.B. Bekele, A.B. Belachew, D.A. Bennett, I.M. Bensenor, A. Berhane, M. Beuran, K. Bhattacharyya, Z.A. Bhutta, B. Biadgo, A. Bijani, N. Bililign, M.S. Bin Sayeed, C.K. Blazes, C. Brayne, Z.A. Butt, I.R. Campos-Nonato, C. Cantu-Brito, M. Car, R. Cárdenas, J.J. Carrero, F. Carvalho, C.A. Castañeda-Orjuela, F. Castro, F. Catalá-López, E. Cerin, Y. Chaiah, J.-C. Chang, I. Chatziralli, P.P.-C. Chiang, H. Christensen, D.J. Christopher, C. Cooper, P.A. Cortesi, V.M. Costa, M.H. Criqui, C.S. Crowe, A.A.M. Damasceno, A. Daryani, V. De la Cruz-Góngora, F.P. De la Hoz, D. De Leo, G.T. Demoz, K. Deribe, S.D. Dharmaratne, D. Diaz, M.T. Dinberu, S. Djalalinia, D.T. Doku, M. Dubey, E. Dubljanin, E.E. Duken, D. Edvardsson, Z. El-Khatib, M. Endres, A.Y. Endries, S. Eskandarieh, A. Esteghamati, S. Esteghamati, F. Farhadi, A. Faro, F. Farzadfar, M.H.

Farzaei, B. Fatima, S.-M. Fereshtehnejad, E. Fernandes, G.T. Feyissa, I. Filip, F. Fischer, T. Fukumoto, M. Ganji, F.G. Gankpe, M.A. Garcia-Gordillo, A.K. Gebre, T.G. Gebremichael, B.K. Gelaw, J.M. Geleijnse, D. Geremew, K.E. Gezae, M. Ghasemi-Kasman, M.Y. Gidey, P.S. Gill, T.K. Gill, E.T. Girma, E. V Gnedovskaya, A.C. Goulart, A. Grada, G. Grosso, Y. Guo, R. Gupta, R. Gupta, J.A. Haagsma, T.B. Hagos, A. Haj-Mirzaian, A. Haj-Mirzaian, R.R. Hamadeh, S. Hamidi, G.J. Hankey, Y. Hao, J.M. Haro, H. Hassankhani, H.Y. Hassen, R. Havmoeller, S.I. Hay, M.I. Hegazy, B. Heidari, A. Henok, F. Heydarpour, C.L. Hoang, M.K. Hole, E. Homaie Rad, S.M. Hosseini, G. Hu, E.U. Igumbor, O.S. Ilesanmi, S.S.N. Irvani, S.M.S. Islam, M. Jakovljevic, M. Javanbakht, R.P. Jha, Y.B. Jobanputra, J.B. Jonas, J.J. Jozwiak, M. Jürisson, A. Kahsay, R. Kalani, Y. Kalkonde, T.A. Kamil, T. Kanchan, M. Karami, A. Karch, N. Karimi, A. Kasaeian, T.D. Kassa, Z.Y. Kassa, A. Kaul, A.T. Kefale, P.N. Keiyoro, Y.S. Khader, M.A. Khafaie, I.A. Khalil, E.A. Khan, Y.-H. Khang, H. Khazaie, A.A. Kiadaliri, D.N. Kiirithio, A.S. Kim, D. Kim, Y.-E. Kim, Y.J. Kim, A. Kisa, Y. Kokubo, A. Koyanagi, R. V Krishnamurthi, B. Kuate Defo, B. Kucuk Bicer, M. Kumar, B. Lacey, A. Lafranconi, V.C. Lansingh, A. Latifi, C.T. Leshargie, S. Li, Y. Liao, S. Linn, W.D. Lo, J.C.F. Lopez, S. Lorkowski, P.A. Lotufo, R.M. Lucas, R. Lunevicius, M.T. Mackay, N.B. Mahotra, M. Majdan, R. Majdzadeh, A. Majeed, R. Malekzadeh, D.C. Malta, N. Manafi, M.A. Mansournia, L.G. Mantovani, W. März, T.P. Mashamba-Thompson, B.B. Massenburg, K.K. V Mate, C. McAlinden, J.J. McGrath, V. Mehta, T. Meier, H.G. Meles, A. Melese, P.T.N. Memiah, Z.A. Memish, W. Mendoza, D.T. Mengistu, G. Mengistu, A. Meretoja, T.J. Meretoja, T. Mestrovic, B. Miazgowski, T. Miazgowski, T.R. Miller, G. Mini, E.M. Mirrakhimov, B. Moazen, B. Mohajer, N. Mohammad Gholi Mezerji, M. Mohammadi, M. Mohammadi-Khanaposhtani, R. Mohammadibakhsh, M. Mohammadnia-Afrouzi, S. Mohammed, F. Mohebi, A.H. Mokdad, L. Monasta, S. Mondello, Y. Moodley, M. Moosazadeh, G. Moradi, M. Moradi-Lakeh, M. Moradinazar, P. Moraga, I. Moreno Velásquez, S.D. Morrison, S.M. Mousavi, O.S. Muhammed, W. Muruet, K.I. Musa, G. Mustafa, M. Naderi, G. Nagel, A. Naheed, G. Naik, F. Najafi, V. Nangia, I. Negoi, R.I. Negoi, C.R.J. Newton, J.W. Ngunjiri, C.T. Nguyen, L.H. Nguyen, D.N.A. Ningrum, Y.L. Nirayo, M.R. Nixon, B. Norrving, J.J. Noubiap, M. Nourollahpour Shiadeh, P.S. Nyasulu, O.S. Ogah, I.-H. Oh, A.T. Olagunju, T.O. Olagunju, P.R. Olivares, O.E. Onwujekwe, E. Oren, M.O. Owolabi, M. PA, A.H. Pakpour, W.-H. Pan, S. Panda-Jonas, J.D. Pandian, S.K. Patel, D.M. Pereira, M. Petzold, J.D. Pillay, M.A. Piradov, G. V Polanczyk, S. Polinder, M.J. Postma, R. Poulton, H. Poustchi, S. Prakash, V. Prakash, M. Qorbani, A. Radfar, A. Rafay, A. Rafiei, F. Rahim, V. Rahimi-Movaghar, M. Rahman, M.H.U. Rahman, M.A. Rahman, F. Rajati, U. Ram, A. Ranta, D.L. Rawaf, S. Rawaf, N. Reinig, C. Reis, A.M.N. Renzaho, S. Resnikoff, S. Rezaeian, M.S. Rezai, C.M. Rios González, N.L.S. Roberts, L. Roever, L. Ronfani, E.M. Roro, G. Roshandel, A. Rostami, P. Sabbagh, R.L. Sacco, P.S. Sachdev, B. Saddik, H. Safari, R. Safari-Faramani, S. Safi, S. Safiri, R. Sagar, R. Sahathevan, A. Sahebkar, M.A. Sahraian, P. Salamati, S. Salehi Zahabi, Y. Salimi, A.M. Samy, J. Sanabria, I.S. Santos, M.M. Santric Milicevic, N. Sarrafzadegan, B. Sartorius, S. Sarvi, B. Sathian, M. Satpathy, A.R. Sawant, M. Sawhney, I.J.C. Schneider, B. Schöttker, D.C. Schwebel, S. Seedat, S.G. Sepanlou, H. Shabaninejad, A. Shafieesabet, M.A. Shaikh, R.A. Shakir, M. Shams-Beyranvand, M. Shamsizadeh, M. Sharif, M. Sharif-Alhoseini, J. She, A. Sheikh, K.N. Sheth, M. Shigematsu, R. Shiri, R. Shirkoohi, I. Shiue, S. Siabani, T.J. Siddiqi, I.D. Sigfusdottir, R. Sigurvinsdottir, D.H. Silberberg, J.P. Silva, D.G.A. Silveira, J.A. Singh, D.N. Sinha, E. Skiadaresi, M. Smith, B.H. Sobaih, S. Sobhani, M. Soofi, I.N. Soyiri, L.A. Sposato, D.J. Stein, M.B. Stein, M.A. Stokes,

M.B. Sufiyan, B.L. Sykes, P. Sylaja, R. Tabarés-Seisdedos, B.J. Te Ao, A. Tehrani-Banihashemi, M.-H. Temsah, O. Temsah, J.S. Thakur, A.G. Thrift, R. Topor-Madry, M. Tortajada-Girbés, M.R. Tovani-Palone, B.X. Tran, K.B. Tran, T.C. Truelsen, A.G. Tsadik, L. Tudor Car, K.N. Ukwaja, I. Ullah, M.S. Usman, O.A. Uthman, P.R. Valdez, T.J. Vasankari, R. Vasanthan, Y. Veisani, N. Venketasubramanian, F.S. Violante, V. Vlassov, K. Vosoughi, G.T. Vu, I.S. Vujcic, F.S. Wagnew, Y. Waheed, Y.-P. Wang, E. Weiderpass, J. Weiss, H.A. Whiteford, T. Wijeratne, A.S. Winkler, C.S. Wiysonge, C.D.A. Wolfe, G. Xu, A. Yadollahpour, T. Yamada, Y. Yano, M. Yaseri, H. Yatsuya, E.M. Yimer, P. Yip, E. Yisma, N. Yonemoto, M. Yousefifard, C. Yu, Z. Zaidi, S. Bin Zaman, M. Zamani, H. Zandian, Z. Zare, Y. Zhang, S. Zodpey, M. Naghavi, C.J.L. Murray, T. Vos, Global, regional, and national burden of neurological disorders, 1990–2016: a systematic analysis for the Global Burden of Disease Study 2016, Lancet Neurol. 18 (2019) 459–480. https://doi.org/10.1016/S1474-4422(18)30499-X.

[184] B.G. Mohney, R.C. Young, N. Diehl, Incidence and Associated Endocrine and Neurologic Abnormalities of Optic Nerve Hypoplasia, JAMA Ophthalmol. 131 (2013) 898. https://doi.org/10.1001/jamaophthalmol.2013.65.

[185] G. Singh, M. Sharma, G.A. Kumar, N.G. Rao, K. Prasad, P. Mathur, J.D. Pandian, J.D. Steinmetz, A. Biswas, P.K. Pal, S. Prakash, P.N. Sylaja, E. Nichols, T. Dua, H. Kaur, S. Alladi, V. Agarwal, S. Aggarwal, A. Ambekar, B.S. Bagepally, T.K. Banerjee, R.G. Bender, S. Bhagwat, S. Bhargava, R. Bhatia, J.K. Chakma, N. Chowdhary, S. Dey, M.A. Dirac, V.L. Feigin, A. Ganguli, M.J. Golechha, M. Gourie-Devi, V. Goyal, G. Gupta, P.C. Gupta, R. Gupta, G. Gururaj, R. Hemalatha, P. Jeemon, C.O. Johnson, P. Joshi, R. Kant, A.C. Kataki, D. Khurana, R.P. Krishnankutty, H.H. Kyu, S.S. Lim, R. Lodha, R. Ma, R. Malhotra, R. Malhotra, M. Mathai, R. Mehrotra, U.K. Misra, P. Mutreja, M. Naghavi, N. Naik, M. Nguyen, A. Pandey, P. Parmar, A. Perianayagam, D. Prabhakaran, G.K. Rath, N. Reinig, G.A. Roth, R. Sagar, M.J. Sankar, K.S. Shaji, R.S. Sharma, S. Sharma, R. Singh, M.V.P. Srivastava, B.A. Stark, N. Tandon, J.S. Thakur, A.S. ThekkePurakkal, S. V Thomas, M. Tripathi, A. Vongpradith, H.Y. Wunrow, D. Xavier, D.K. Shukla, K.S. Reddy, S. Panda, R. Dandona, C.J.L. Murray, T. Vos, R.S. Dhaliwal, L. Dandona, The burden of neurological disorders across the states of India: the Global Burden of Disease Study 1990–2019, Lancet Glob. Heal. 9 (2021) e1129–e1144. https://doi.org/10.1016/S2214-109X(21)00164-9.

[186] S. Poliak, E. Peles, The local differentiation of myelinated axons at nodes of Ranvier, Nat. Rev. Neurosci. 4 (2003) 968–980. https://doi.org/10.1038/nrn1253.

[187] L. Huang, J. Gao, H. Wang, B. Xia, Y. Yang, F. Xu, X. Zheng, J. Huang, Z. Luo, Fabrication of 3D Scaffolds Displaying Biochemical Gradients along Longitudinally Oriented Microchannels for Neural Tissue Engineering, ACS Appl. Mater. Interfaces. 12 (2020) 48380–48394. https://doi.org/10.1021/acsami.0c15185.

[188] X. Li, M. Li, J. Sun, Y. Zhuang, J. Shi, D. Guan, Y. Chen, J. Dai, Radially Aligned Electrospun Fibers with Continuous Gradient of SDF1α for the Guidance of Neural Stem Cells, Small. 12 (2016) 5009–5018. https://doi.org/10.1002/smll.201601285.

[189] J.I. Kim, T.I. Hwang, J.C. Lee, C.H. Park, C.S. Kim, Regulating Electrical Cue and Mechanotransduction in Topological Gradient Structure Modulated Piezoelectric Scaffolds to Predict Neural Cell Response, Adv. Funct. Mater. 30 (2020) 1907330. https://doi.org/10.1002/adfm.201907330.

[190] J. Veldhuizen, R.Q. Migrino, M. Nikkhah, Three-dimensional microengineered models of human cardiac diseases, J. Biol. Eng. 13 (2019) 29. https://doi.org/10.1186/s13036-019-0155-6.

[191] M. Easterling, S. Rossi, A.J. Mazzella, M. Bressan, Assembly of the Cardiac Pacemaking Complex: Electrogenic Principles of Sinoatrial Node Morphogenesis, J. Cardiovasc. Dev. Dis. 8 (2021) 40. https://doi.org/10.3390/jcdd8040040.

[192] E.D. Carruth, A.D. McCulloch, J.H. Omens, Transmural gradients of myocardial structure and mechanics: Implications for fiber stress and strain in pressure overload, Prog. Biophys. Mol. Biol. 122 (2016) 215–226. https://doi.org/10.1016/j.pbiomolbio.2016.11.004.

[193] K.D. Dwyer, K.L.K. Coulombe, Cardiac mechanostructure: Using mechanics and anisotropy as inspiration for developing epicardial therapies in treating myocardial infarction, Bioact. Mater. 6 (2021) 2198–2220. https://doi.org/10.1016/j.bioactmat.2020.12.015.

[194] Y. Ruan, Y. Guo, Y. Zheng, Z. Huang, S. Sun, P. Kowal, Y. Shi, F. Wu, Cardiovascular disease (CVD) and associated risk factors among older adults in six low-and middle-income countries: results from SAGE Wave 1, BMC Public Health. 18 (2018) 778. https://doi.org/10.1186/s12889-018-5653-9.

[195] M. Amini, F. Zayeri, M. Salehi, Trend analysis of cardiovascular disease mortality, incidence, and mortality-to-incidence ratio: results from global burden of disease study 2017, BMC Public Health. 21 (2021) 401. https://doi.org/10.1186/s12889-021-10429-0.

[196] G.A. Roth, C. Johnson, A. Abajobir, F. Abd-Allah, S.F. Abera, G. Abyu, M. Ahmed, B. Aksut, T. Alam, K. Alam, F. Alla, N. Alvis-Guzman, S. Amrock, H. Ansari, J. Ärnlöv, H. Asayesh, T.M. Atey, L. Avila-Burgos, A. Awasthi, A. Banerjee, A. Barac, T. Bärnighausen, L. Barregard, N. Bedi, E. Belay Ketema, D. Bennett, G. Berhe, Z. Bhutta, S. Bitew, J. Carapetis, J.J. Carrero, D.C. Malta, C.A. Castañeda-Orjuela, J. Castillo-Rivas, F. Catalá-López, J.Y. Choi, H. Christensen, M. Cirillo, L. Cooper, M. Criqui, D. Cundiff, A. Damasceno, L. Dandona, R. Dandona, K. Davletov, S. Dharmaratne, P. Dorairaj, M. Dubey, R. Ehrenkranz, M. El Sayed Zaki, E.J.A. Faraon, A. Esteghamati, T. Farid, M. Farvid, V. Feigin, E.L. Ding, G. Fowkes, T. Gebrehiwot, R. Gillum, A. Gold, P. Gona, R. Gupta, T.D. Habtewold, N. Hafezi-Nejad, T. Hailu, G.B. Hailu, G. Hankey, H.Y. Hassen, K.H. Abate, R. Havmoeller, S.I. Hay, M. Horino, P.J. Hotez, K. Jacobsen, S. James, M. Javanbakht, P. Jeemon, D. John, J. Jonas, Y. Kalkonde, C. Karimkhani, A. Kasaeian, Y. Khader, A. Khan, Y.H. Khang, S. Khera, A.T. Khoja, J. Khubchandani, D. Kim, D. Kolte, S. Kosen, K.J. Krohn, G.A. Kumar, G.F. Kwan, D.K. Lal, A. Larsson, S. Linn, A. Lopez, P.A. Lotufo, H.M.A. El Razek, R. Malekzadeh, M. Mazidi, T. Meier, K.G. Meles, G. Mensah, A. Meretoja, H. Mezgebe, T. Miller, E. Mirrakhimov, S. Mohammed, A.E. Moran, K.I. Musa, J. Narula, B. Neal, F. Ngalesoni, G. Nguyen, C.M. Obermeyer, M. Owolabi, G. Patton, J. Pedro, D. Qato, M. Qorbani, K. Rahimi, R.K. Rai, S. Rawaf, A. Ribeiro, S. Safiri, J.A. Salomon, I. Santos, M. Santric Milicevic, B. Sartorius, A. Schutte, S. Sepanlou, M.A. Shaikh, M.J. Shin, M. Shishehbor, H. Shore, D.A.S. Silva, E. Sobngwi, S. Stranges, S. Swaminathan, R. Tabarés-Seisdedos, N. Tadele Atnafu, F. Tesfay, J.S. Thakur, A. Thrift, R. Topor-Madry, T. Truelsen, S. Tyrovolas, K.N. Ukwaja, O. Uthman, T. Vasankari, V. Vlassov, S.E. Vollset, T. Wakayo, D. Watkins, R. Weintraub, A.

Werdecker, R. Westerman, C.S. Wiysonge, C. Wolfe, A. Workicho, G. Xu, Y. Yano, P. Yip, N. Yonemoto, M. Younis, C. Yu, T. Vos, M. Naghavi, C. Murray, Global, Regional, and National Burden of Cardiovascular Diseases for 10 Causes, 1990 to 2015, J. Am. Coll. Cardiol. 70 (2017) 1–25. https://doi.org/10.1016/j.jacc.2017.04.052.

[197] N. Aljefree, F. Ahmed, Prevalence of Cardiovascular Disease and Associated Risk Factors among Adult Population in the Gulf Region: A Systematic Review, Adv. Public Heal. 2015 (2015) 1–23. https://doi.org/10.1155/2015/235101.

[198] WHO, 2021, (n.d.).

[199] O. Bergmann, R.D. Bhardwaj, S. Bernard, S. Zdunek, F. Barnabé-Heider, S. Walsh, J. Zupicich, K. Alkass, B.A. Buchholz, H. Druid, S. Jovinge, J. Frisén, Evidence for Cardiomyocyte Renewal in Humans, Science (80-.). 324 (2009) 98–102. https://doi.org/10.1126/science.1164680.

[200] S. Ahadian, L. Davenport Huyer, M. Estili, B. Yee, N. Smith, Z. Xu, Y. Sun, M. Radisic, Moldable elastomeric polyester-carbon nanotube scaffolds for cardiac tissue engineering, Acta Biomater. 52 (2017) 81–91. https://doi.org/10.1016/j.actbio.2016.12.009.

[201] E. Dattola, E.I. Parrotta, S. Scalise, G. Perozziello, T. Limongi, P. Candeloro, M.L. Coluccio, C. Maletta, L. Bruno, M.T. De Angelis, G. Santamaria, V. Mollace, E. Lamanna, E. Di Fabrizio, G. Cuda, Development of 3D PVA scaffolds for cardiac tissue engineering and cell screening applications, RSC Adv. 9 (2019) 4246–4257. https://doi.org/10.1039/C8RA08187E.

[202] O.S. Kamble, A.S. Sanket, S.K. Samal, S.K. Dubey, P. Kesharwani, R. Dandela, Advances in transdermal delivery of nanomedicine, in: Theory Appl. Nonparenteral Nanomedicines, Elsevier, 2021: pp. 383–408. https://doi.org/10.1016/B978-0-12-820466-5.00016-8.

[203] P.A.J. Kolarsick, M.A. Kolarsick, C. Goodwin, Anatomy and Physiology of the Skin, J. Dermatol. Nurses. Assoc. 3 (2011) 203–213. https://doi.org/10.1097/JDN.0b013e3182274a98.

[204] S. Tang, Z. Wang, P. Li, W. Li, C. Li, Y. Wang, P. Chu, Degradable and Photocatalytic Antibacterial Au-TiO2/Sodium Alginate Nanocomposite Films for Active Food Packaging, Nanomaterials. 8 (2018) 930. https://doi.org/10.3390/nano8110930.

[205] F.-M. Chen, X. Liu, Advancing biomaterials of human origin for tissue engineering, Prog. Polym. Sci. 53 (2016) 86–168. https://doi.org/10.1016/j.progpolymsci.2015.02.004.

[206] K. Vig, A. Chaudhari, S. Tripathi, S. Dixit, R. Sahu, S. Pillai, V. Dennis, S. Singh, Advances in Skin Regeneration Using Tissue Engineering, Int. J. Mol. Sci. 18 (2017) 789. https://doi.org/10.3390/ijms18040789.

[207] A. Przekora, A Concise Review on Tissue Engineered Artificial Skin Grafts for Chronic Wound Treatment: Can We Reconstruct Functional Skin Tissue In Vitro?, Cells. 9 (2020) 1622. https://doi.org/10.3390/cells9071622.

[208] J.R. Yu, J. Navarro, J.C. Coburn, B. Mahadik, J. Molnar, J.H. Holmes, A.J. Nam, J.P. Fisher, Current and Future Perspectives on Skin Tissue Engineering: Key Features of Biomedical Research, Translational Assessment, and Clinical Application., Adv. Healthc. Mater. 8 (2019) e1801471. https://doi.org/10.1002/adhm.201801471.

[209] Y. Wang, R. Xu, G. Luo, Q. Lei, Q. Shu, Z. Yao, H. Li, J. Zhou, J. Tan, S. Yang, R. Zhan, W. He, J. Wu, Biomimetic fibroblast-loaded artificial dermis with “sandwich” structure and designed gradient pore sizes promotes wound healing by favoring granulation tissue formation and wound re-epithelialization, Acta Biomater. 30 (2016) 246–257. https://doi.org/10.1016/j.actbio.2015.11.035.

[210] Y. Zhang, C. Wang, W. Jiang, W. Zuo, G. Han, Influence of Stage Cooling Method on Pore Architecture of Biomimetic Alginate Scaffolds, Sci. Rep. 7 (2017) 16150. https://doi.org/10.1038/s41598-017-16024-x.